LEVEL

ADA065585

INVESTIGATION OF ELECTROMAGNETIC COUPLING THROUGH SINGLE
OR MULTIPLE APERTURES INTO CYLINDRICAL STRUCTURES

Final Report

S. W. Lee

R. Mittra

DDC
RECEIVED
MAR 13 1979
C

79 03 12 090

REPORT DOCUMENTATION PAGE		READ INSTRUCTIONS BEFORE COMPLETING FORM
1. REPORT NUMBER	2. GOVT ACCESSION NO.	3. RECIPIENT'S CATALOG NUMBER
4. TITLE (and Subtitle) INVESTIGATION OF ELECTROMAGNETIC COUPLING THROUGH SINGLE OR MULTIPLE APERTURES INTO CYLINDRICAL STRUCTURES		5. TYPE OF REPORT & PERIOD COVERED Final Report 1 Dec 77 – 28 Feb 79 1 Dec., 77 to 28 Feb., 79
		6. PERFORMING ORG. REPORT NUMBER EM 79-3; UIUL-ENG-79-2542
7. AUTHOR(s) S. W. Lee and R. Mittra		8. CONTRACT OR GRANT NUMBER(s) N00014-75-C-0293
9. PERFORMING ORGANIZATION NAME AND ADDRESS Electromagnetics Laboratory Department of Electrical Engineering University of Illinois, Urbana, IL 61801		10. PROGRAM ELEMENT, PROJECT, TASK AREA & WORK UNIT NUMBERS
11. CONTROLLING OFFICE NAME AND ADDRESS Office of Naval Research Department of the Navy Arlington, Virginia 22217		12. REPORT DATE February 1979
		13. NUMBER OF PAGES 118 127
14. MONITORING AGENCY NAME & ADDRESS(if different from Controlling Office)		15. SECURITY CLASS. (of this report) UNCLASSIFIED
		15a. DECLASSIFICATION/DOWNGRADING SCHEDULE

16. DISTRIBUTION STATEMENT (of this Report)

Distribution Unlimited.   Reproduction in whole or in part is permitted
for any purpose of the United States Government.

17. DISTRIBUTION STATEMENT (of the abstract entered in Block 20, if different from Report)

UIEM-79-3, UILU-ENG-79-2542

18. SUPPLEMENTARY NOTES

19. KEY WORDS (Continue on reverse side if necessary and identify by block number)

Electromagnetic radiation and compatibility problems;   moment method;
ray techniques;   spectral domain approach;   slot on cylinder

20. ABSTRACT (Continue on reverse side if necessary and identify by block number)

    Two topics of interest in the study of high-frequency radiation and
electromagnetic compatibility are described in this report. The first problem
considered is that of penetration of an incident electromagnetic wave through
a slot on a cylinder. This problem is solved via an application of the method
of moments. Next considered was the problem of source radiation from a slot
on the surface of a large cylinder using ray techniques and the spectral
domain approach. New formulas are presented for the radiated fields and a
comparison with the conventional GTD results are included.

Electromagnetics Laboratory Report No. 79-3

INVESTIGATION OF ELECTROMAGNETIC COUPLING THROUGH SINGLE

OR MULTIPLE APERTURES INTO CYLINDRICAL STRUCTURES

Final Report

S. W. Lee
R. Mittra

February 1979

TABLE OF CONTENTS

_____

*Each attachment has its own pagination.

iii

I. INTRODUCTION

The contract entitled, "Investigation Of Electromagnetic Coupling Through Single Or Multiple Apertures Into Cylindrical Structures" (N00014-75-C-0293) was awarded to the University of Illinois for one year, starting December 1, 1977. The contract was later extended to Feb. 28, 1979 at no additional cost. This is the final report of the contract.

II. PERSONNEL

R. Mittra, Professor of Electrical Engineering, Principal Investigator.

S. W. Lee, Professor of Electrical Engineering.

E. K. Yung, Research Associate.

S. Safavi-Naini, Graduate Research Assistant.

III. TECHNICAL RESULTS

During the present contract year, we have studied the following two technical problems:

(a) Penetration of an electromagnetic wave into a cylindrical cavity and the current induced on a wire inside. The technical details of this work are described in Attachment A.

(b) Electromagnetic radiation from a source located on a smooth conducting surface which is detailed in Attachment B.

IV.   PUBLICATIONS AND PRESENTATIONS

[1] E. K. Yung, S. W. Lee, and R. Mittra, "Penetration of an EM wave
     into a cylindrical cavity and the current induced on a wire inside,"
     Electromagnetics Laboratory Technical Report No. 78-9, University
     of Illinois, Urbana, 1978; also to appear in AEU (Germany).

[2] S. Safavi-Naini and R. Mittra, "Source radiation in the presence of
     smooth convex bodies," Electromagnetics Laboratory Technical Report
     No. 78-3, University of Illinois, Urbana, 1978; also to appear as an
     invited paper in Radio Science.

[3] D. C. Chang, S. W. Lee, and L. Rispin, "Simple formula for current
     on a cylindrical receiving antenna, "IEEE Trans. Antenna Propagat.,
     vol. AP-26, pp. 683-690, 1978.

[4] S. Safavi-Naini and R. Mittra, "Effect of surface ray torsion on
     diffraction by a smooth object," Digest of National Radio Science
     Meeting, p. 3, Nov. 1978.

[5] S. Safavi-Naini and R. Mittra, "Source radiation in the presence of
     smooth convex bodies," 1978 International Antenna and Propagation
     Digest, pp. 85-88, 1978.

[6] E. K. Yung, S. W. Lee, and R. Mittra, "EM penetration into a cavity
     and the induced current on a wire inside," ibid, pp. 132-135, also
     to appear in AEU (Germany).

[7] R. Mittra, Y. Rahmat-Samii, and W. L. Ko, "Solution of electromagnetic
     scattering and radiation problems using a spectral domain approach -
     A review," Wave Motion Journal, to appear.

Attachment A

PENETRATION OF AN EM WAVE INTO A CYLINDRICAL
CAVITY AND THE CURRENT INDUCED ON A WIRE INSIDE

by

E. K. Yung

S. W. Lee

R. Mittra

DOCUMENT CONTROL DATA - R&D

(Security classification of title, body of abstract and indexing annotation must be entered when the overall report is classified)

1. ORIGINATING ACTIVITY *(Corporate author)* Electromagnetics Laboratory, Dept. of Elec. Eng. University of Illinois at Urbana-Champaign Urbana, Illinois 61801	2a. REPORT SECURITY CLASSIFICATION 2b. GROUP

3. REPORT TITLE

PENETRATION OF AN EM WAVE INTO A CYLINDRICAL CAVITY AND THE CURRENT INDUCED ON A WIRE INSIDE

4. DESCRIPTIVE NOTES *(Type of report and inclusive dates)*

Technical Report

5. AUTHOR(S) *(Last name, first name, initial)*

E. K. Yung
S. W. Lee
R. Mittra

6. REPORT DATE August, 1978	7a. TOTAL NO. OF PAGES 48	7b. NO. OF REFS 15

8a. CONTRACT OR GRANT NO. N000 14-75-C-0293 b. PROJECT NO. c. d.	9a. ORIGINATOR'S REPORT NUMBER(S) EM 78-9 9b. OTHER REPORT NO(S) *(Any other numbers that may be assigned this report)* UILU-ENG-78-2551

10. AVAILABILITY/LIMITATION NOTICES

Distribution unlimited. Reproduction in whole or in part is permitted for any purpose of the United States Government.

11. SUPPLEMENTARY NOTES	12. SPONSORING MILITARY ACTIVITY Office of Naval Research Department of the Navy Arlington, VA 22217

13. ABSTRACT

This paper addresses the problem of computing the current induced in a thin wire located inside a cylindrical cavity with a circumferential slot when the cavity is illuminated by an incident plane wave. The calculation is carried out in two steps. First, the problem of penetration of the incident field into the cavity is solved by the method of moments under the assumption that the presence of the wire inside the cavity creates little or no perturbation of the interior field. Next, the induced current on the wire is calculated by the following two methods: (i) use of a simple analytical formula derived from the application of the Wiener-Hopf techniques to the finite wire problem; (ii) numerical solution of an integral equation. Extensive numerical results for the induced current are presented. It is found that the current is sensitive to the cylinder radius, the cavity height, the frequency of excitation, and the wire location, but is relatively less sensitive to the variation

(over)

14. KEY WORDS

EM Compatibility
Penetration through Apertures
Cylindrical Structure
Coupling to Wire

PENETRATION OF AN EM WAVE INTO A CYLINDRICAL CAVITY AND THE CURRENT INDUCED ON A WIRE INSIDE

Technical Report

E. K. Yung
S. W. Lee
R. Mittra

August 1978

Electromagnetics Laboratory
Department of Electrical Engineering
Engineering Experiment Station
University of Illinois at Urbana-Champaign
Urbana, Illinois 61801

ABSTRACT

This paper addresses the problem of computing the current induced in a thin wire located inside a cylindrical cavity with a circumferential slot when the cavity is illuminated by an incident plane wave. The calculation is carried out in two steps. First, the problem of penetration of the incident field into the cavity is solved by the method of moments under the assumption that the presence of the wire inside the cavity creates little or no perturbation of the interior field. Next, the induced current on the wire is calculated by the following two methods: (i) use of a simple analytical formula derived from the application of the Wiener-Hopf techniques to the finite wire problem; (ii) numerical solution of an integral equation. Extensive numerical results for the induced current are presented. It is found that the current is sensitive to the cylinder radius, the cavity height, the frequency of excitation, and the wire location, but is relatively less sensitive to the variation in the slot length. In addition, the induced current on a wire inside the cavity can be much larger than its counterpart in free space illuminated by the same incident plane wave at frequencies where the cavity is near resonance.

TABLE OF CONTENTS

LIST OF FIGURES

I. INTRODUCTION

The penetration of an electromagnetic wave through an aperture into a cylindrical structure is of current interest because of its application to EMP, to EMC, and to biological studies. As early as 1949, Sommerfeld [1] studied the problem of an infinitely long circular cylinder with a longitudinal slot, illuminated by a normally incident plane wave. Using a Fourier analysis approach, Sommerfeld reduced the problem to a system of infinitely many linear equations, but declared resignedly, "We can do practically nothing with the problem." Silver and Saunders [2] used the saddle-point integration method for the inversion of Fourier transforms and extracted the far field of Sommerfeld's problem. Hitherto, a number of extensions along this line of work have been reported [3], [4]. With the advent of high-speed digital computers, Sommerfeld's penetration problem can now be solved by numerical means [5], [6]. The penetration of an EM wave into the cylinder through a rectangular aperture was first carried out by Safavi-Naini, Lee and Mittra [7], [8]. Their problem has a more complex geometry than Sommerfeld's in that two conducting plates are introduced inside the cylinder at $z = \pm h$ to form a cavity, as illustrated in Figure 1.

In the present report, and extension of the penetration problem of Safavi-Naini et al. is investigated; in which a thin wire is added inside the cavity and the problem is to determine the current induced on the wire. The wire is oriented parallel to the longitudinal direction of the cylindrical cavity. If the slot in the cavity wall is also longitudinal, there is little induced current on the wire. Hence, we concentrate on

1
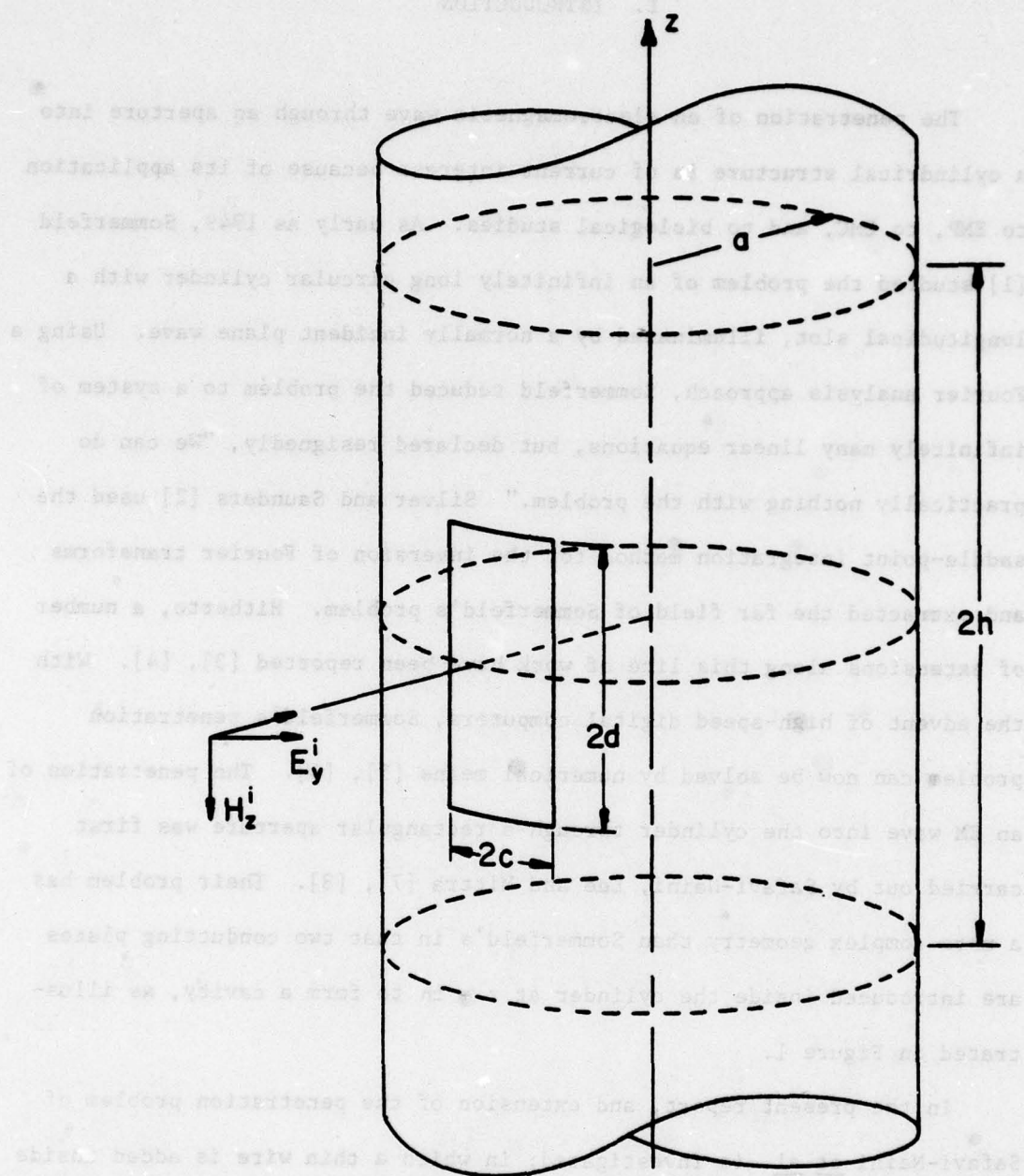
Figure 1. An infinitely long cylinder with a cavity and a longitudinal slot, illuminated by an incident plane wave.

the more interesting case, namely, the slot which is circumferential on the cylindrical cavity wall. The composite geometry of the present problem is sketched in Figure 2.

Due to the thinness of the wire, it appears reasonable to assume that the presence of the wire does not perturb the field generated inside the cavity. Thus, the problem under consideration can be solved in two steps:

(A) Determine the field $\overline{E}$ inside the cavity as if the wire were absent.

(B) Using $\overline{E}$ as an incident field, determine the induced current $I(z)$ as if the wire were situated in the free space.

We emphasize that the above two-step approach is an approximation. The exact degree of approximation will be studied in a separate report.

The plan for the present report is as follows: In Section II, the problem of Part (A) with the wire absent is formulated and a system of infinitely many linear equations derived. The procedures are briefly described below:

1. The unknown electric field across the aperture is represented by a Fourier series.

2. Applying the equivalence principle, the aperture is shorted by a perfect conductor. The effect of the original aperture field is accounted for by introducing equivalent magnetic currents on both sides of the shorted aperture.

3. Inside the cavity, the magnetic field produced by the equivalent magnetic current is determined via a magnetic vector potential. The resultant field is given in the form of a doubly infinite series of eigenfunctions of the cavity.

3
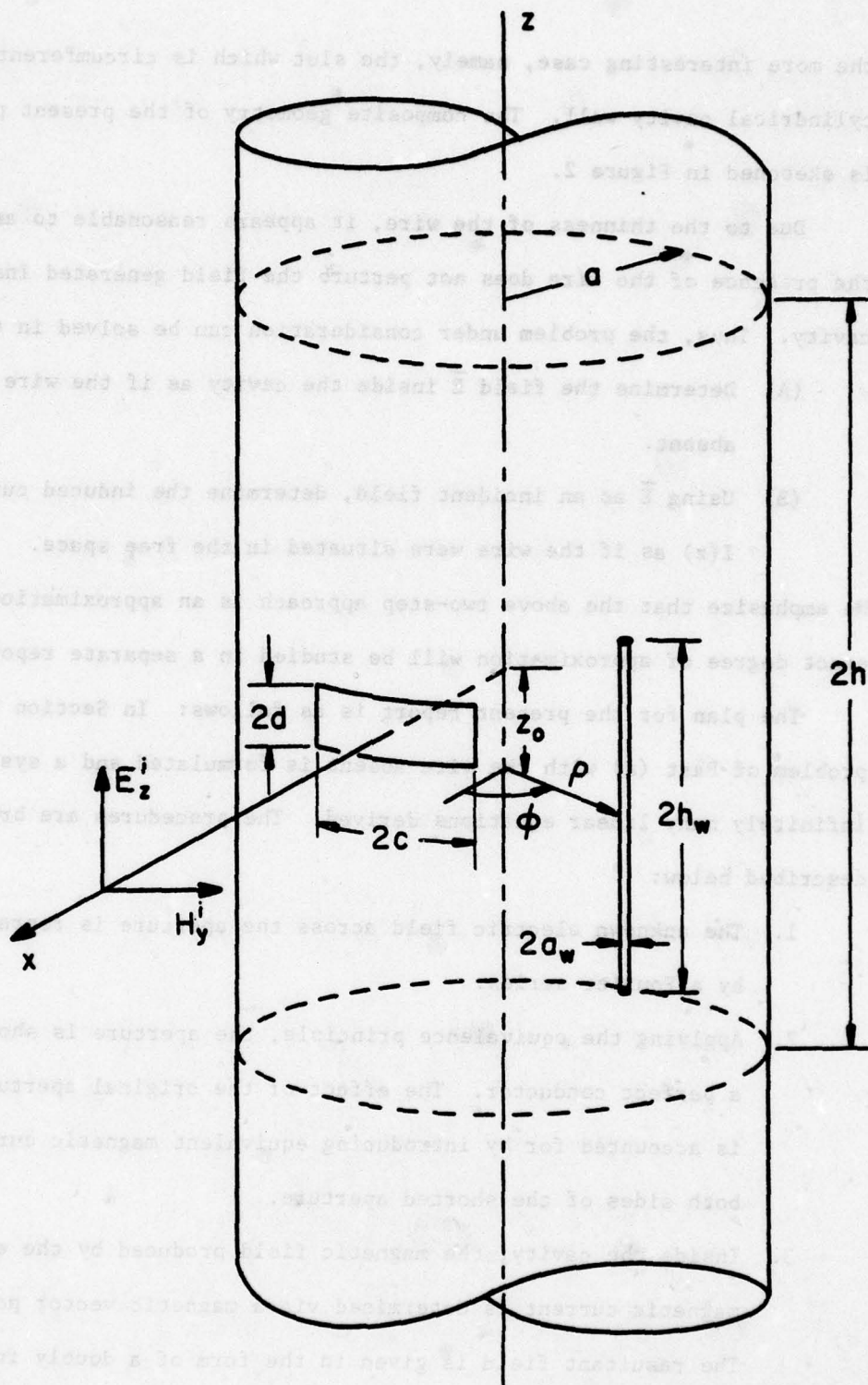
Figure 2. An infinitely long cylinder with a cavity and a wire inside, illuminated by an incident plane wave through a circumferential slot on the cavity wall.

4

4. Exterior to the cavity, the magnetic field is also generated
   via a magnetic vector potential, which is partitioned into three
   components to represent the incident field, the reflected field,
   and that produced by the equivalent magnetic current.

5. The coupled equation from which the unknown aperture electric
   field can be determined is developed by enforcing the continuity
   of the tangential magnetic field across the aperture.

6. The coupled equation is solved numerically by the method of
   moments [9].

In Section III, the current induced on the wire inside the cavity
when it is illuminated by the field $\overline{E}$ computed in Part (A) is derived.
Since $\overline{E}$ is given in terms of a doubly infinite series of eigenfunctions
of the cavity, it can be interpreted as a spectrum of plane waves. As a
result, the induced current $I(z)$ can be determined by superimposing the
currents due to each component of the plane wave spectrum. The current
induced by each component of the spectrum is determined by one of the
following two methods:

1. The standard numerical (moment) method based on an integral
   equation formulation [10], and

2. the simple approximation formula recently developed by Chang,
   Lee, and Rispin [11], [12].

It should be noted that both of the above methods apply only if the incident
plane wave is homogeneous. In the present problem, however, the field $\overline{E}$
inside the cavity consists of both homogeneous and inhomogeneous plane
wave components. Hence, the above two methods have to be extended by
analytical continuation to cover the case of an incident inhomogeneous
plane wave.

5

In Section IV, possible difficulties of numerical computations of the equations derived in Sections II and III are considered. Techniques for improving the convergence rate of the summation procedures are presented in Section IV. Extensive numerical results are presented in Section V.

6

II. FIELD IN THE CAVITY

In this section, the field $\overline{E}$ excited in the cavity with the wire absent is derived. The geometry of the problem under consideration in this section is illustrated in Figure 2, with the wire removed. The conducting circular cylinder is infinitely long and is of radius a. A cylindrical cavity is formed inside the cylinder by two conducting plates located at $z = \pm h$. The cavity is coupled to exterior excitations through a circumferential slot on its cylindrical wall. The rectangular slot is of dimension 2c x 2d and centered at $(x = a, y = 0, z = 0)$. The width of the slot is assumed to be small in terms of wavelength, i.e.,

$$2kd \ll 1 \quad . \tag{2-1}$$

The structure is illuminated by a normally incident plane wave of unit magnitude described by

$$\overline{E}^i = \hat{z} \, e^{ikx} \, , $$
$$\overline{H}^i = \hat{y} \, \frac{1}{\eta} \, e^{ikx} \tag{2-2}$$

where the time harmonic factor $\exp(+j\omega t)$ has been suppressed and $\eta = \sqrt{\mu/\epsilon} = 120 \, \pi$ is the intrinsic impedance of the free space.

The symmetry of the configuration, together with the plane wave excitation given in Eq. 2-2, dictate that the tangential electric field across the aperture be an even function of ϕ. Furthermore, the narrowness of the slot enables us to assume that the aperture field is approximately constant in z and is z-directed. Thus, the tangential electric field across the aperture $\overline{E}_a = E_z \hat{z}$ can be represented by a Fourier-cosine series:

$$E_a = \sum_{\mu=0}^{\infty} E_\mu \cos \Gamma_\mu \phi; \quad |\phi| \leq \phi_0, \ |z| \leq d \quad . \tag{2-3}$$

7

In accordance with the boundary condition that E_a vanishes at $\phi = \pm\phi_0 (\phi_0 = c/a)$, $\{\Gamma_\mu\}$ are found to be

$$\Gamma_\mu = \frac{(2\mu + 1)\pi}{2\phi_0} \quad ; \quad \mu = 0,1,2,\ldots \quad . \tag{2-4}$$

Due to the assumed direction of the aperture electric vector (or the equivalent magnetic current), it can be shown that a field TM with respect to z is sufficient to represent the total field inside the cavity. Such a field can be generated via a z-directed magnetic vector potential $\overline{A} = A_z \hat{z}$. The relations between A_z and the field components are

$$E_\rho = \frac{1}{j\omega\mu\epsilon} \frac{\partial^2 A_z}{\partial\rho\partial z} \quad , \qquad H_\rho = \frac{1}{\mu} \frac{\partial A_z}{\rho\partial\phi} \quad ,$$

$$E_\phi = \frac{1}{j\omega\mu\epsilon} \frac{\partial^2 A_z}{\rho\partial\phi\partial z} \quad , \qquad H_\phi = -\frac{1}{\mu} \frac{\partial A_z}{\partial\rho} \quad ,$$

$$E_z = \frac{1}{j\omega\mu\epsilon}\left[\frac{\partial^2}{\partial z^2} + k^2\right]A_z \quad , \qquad H_z = 0 \quad . \tag{2-5}$$

Inside the cavity, A_z is a linear combination of all possible elementary wave functions that are solutions to the scalar Helmholtz equation [13]. It assumes the form

$$A_z(\rho,\phi,z) = \sum_{m,n=0}^{\infty} A_{mn} J_m(\gamma_n\rho)\cos m\phi \cos \alpha_n z \tag{2-6}$$

where

$$\gamma_n = \begin{cases} \sqrt{k^2 - \alpha_n^2} & k^2 \geq \alpha_n^2 \quad , \\ -j\sqrt{\alpha_n^2 - k^2} & , \quad k^2 < \alpha_n^2 \quad , \end{cases} \tag{2-7}$$

and

$$\alpha_n = \frac{n\pi}{h} \quad , \qquad n = 0,1,2,\ldots \quad . \tag{2-8}$$

8

The constants $\{A_{mn}\}$ are unknowns, and $\{J_m\}$ are the mth order Bessel functions of the first kind. Note that with the choices of the eigenvalues $\{\alpha_n\}$ in Eq. 2-8, the boundary conditions that E_ρ and E_ϕ be zero at $z = \pm h$ are automatically satisfied.

The constants $\{A_{mn}\}$ in Eq. 2-6 are unknown quantities, and by enforcing the conditions that E_z be zero on the cylindrical wall and equal to E_a on the aperture, they can be evaluated in terms of $\{E_\mu\}$, the expansion coefficients of E_a given in Eq. 2-3. First, we evaluate E_z (referring to Eq. 2-5) at $\rho = a$ to obtain

$$\frac{1}{j\omega\mu\varepsilon} \sum_{m,n=0}^{\infty} \gamma_n^2 A_{mn} J_m(\gamma_n a) \cos m\phi \cos \alpha_n z$$

$$= \Omega(\phi,z) \sum_{\mu=0}^{\infty} E_\mu \cos \Gamma_\mu \phi \quad ; \quad |\phi| \le \pi \, , \, |z| \le h \qquad (2-9)$$

where Ω is the characteristic function of the aperture:

$$\Omega(\phi,z) = \begin{cases} 1 \; ; & |\phi| \le \phi_0 \, , \, |z| \le d \, , \\ 0 \; ; & \text{otherwise.} \end{cases} \qquad (2.10)$$

We recognize that Eq. 2-9 is a standard Fourier-Bessel series with unresolved coefficients $\{A_{mn}\}$. Hence, $\{A_{mn}\}$ are determined by standard procedures with the results

$$A_{mn} = \frac{j4\omega\mu\varepsilon \cos m\phi_0 \sin \alpha_n d}{\varepsilon_m \varepsilon_n \pi \alpha_n \gamma_n^2 h J_m(\gamma_n a)} \sum_{\mu=0}^{\infty} E_\mu \frac{(-1)^\mu \Gamma_\mu}{\Gamma_\mu^2 - m^2} \qquad (2-11)$$

$$m,n = 0,1,2,\ldots$$

in which ε_m is the Neumann number, defined by

$$\varepsilon_m = \begin{cases} 2 \, , & m = 0 \\ 1 \, , & m \ne 0 \end{cases} \, .$$

9

In the region exterior to the cylindrical structure, the symmetry of the configuration again leads to a TM field with respect to z. Thus, the exterior field is also determined via a z-directed magnetic vector potential $\overline{A}^+ = \Psi\hat{z}$. For reasons which will be obvious later, Ψ is partitioned into three wave funcitons: $\Psi = \Psi^i + \Psi^r + \Psi^s$. The first of these Ψ^i represents the incident plane wave; it is independent of a and is given by

$$\Psi^i = \frac{j2}{\omega} \sum_{m=0}^{\infty} \frac{j^m}{\varepsilon_m} J_m(k\rho)\cos m\phi \quad . \tag{2-12}$$

The field components of Ψ^i are given in Eq. 2-2. The second wave function Ψ^r represents the reflected wave when the aperture is closed by a perfect conductor; it assumes the form:

$$\Psi^r = \frac{j2}{\omega} \sum_{m=0}^{\infty} \frac{j^m}{\varepsilon_m} \left\{ -\frac{J_m(ka)}{H_m^{(2)}(ka)} \right\} H_m^{(2)}(k\rho)\cos m\phi \tag{2-13}$$

where $\{H_m^{(2)}\}$ are the mth order Hankel functions of the second kind. The third wave function Ψ^s corresponds to the field produced by the equivalent magnetic current. In contrast to both Ψ^i and Ψ^r, Ψ^s depends on a and is represented by a continuous spectrum of cylindrical waves:

$$\Psi^s = \sum_{m=0}^{\infty} \cos m\phi \int_{-\infty}^{\infty} F_m(\alpha) H_m^{(2)}(\gamma\rho) e^{j\alpha z} \, d\alpha \quad , \tag{2-14}$$

where $\{F_m\}$ are unknown functions, and

$$\gamma = \begin{cases} \sqrt{k^2 - \alpha^2} \quad , & k^2 \geq \alpha^2 \\ -j\sqrt{\alpha^2 - k^2} \quad , & k^2 < \alpha^2 \end{cases} \quad . \tag{2-15}$$

To determine $\{F_m\}$, we first evaluate E_z^+ at $\rho = a$ to obtain

10

$$\frac{1}{j\omega\mu\epsilon} \sum_{m=0}^{\infty} \cos m\phi \int_{-\infty}^{\infty} \gamma^2 F_m(\alpha) H_m^{(2)}(\gamma a) e^{j\alpha z} d\alpha$$

$$= \Omega(\phi,z) \sum_{\mu=0}^{\infty} E_\mu \cos \Gamma_\mu \phi \quad , \quad |\phi| \leq \pi \quad , \quad |z| \leq \infty \quad . \quad (2\text{-}16)$$

Then, we multiply both sides of the equation above by $\cos n\phi$, $n = 0,1,2,\ldots$, and after that, integrate the equation over the entire domain of interest. By invoking the orthogonal properties of $\{\cos n\phi\}$, $\{F_m\}$ are determined in terms of $\{E_\mu\}$:

$$F_m(\alpha) = \frac{j2\omega\mu\epsilon \cos m\phi_0 \sin \alpha d}{\epsilon_m \pi^2 \alpha \gamma^2 H_m^{(2)}(\gamma a)} \sum_{\mu=0}^{\infty} E_\mu \frac{(-1)^\mu \Gamma_\mu}{\Gamma_\mu^2 - m^2} \quad ; \quad (2\text{-}17)$$

$$m = 0,1,2,\ldots \quad .$$

With $\{A_{mn}\}$ and $\{F_m\}$ defined by Eqs. 2-11 and 2-17, the requirement that the tangential electric field be continuous across the aperture is automatically satisfied. However, these definitions, of themselves, do not ensure the continuity of the tangential magnetic field across the aperture. To enforce the continuity of the magnetic field, we proceed as follows: In the region exterior to the cylinder, the three partial magnetic fields H_ϕ^i, H_ϕ^r, and H_ϕ^s (H_ρ^+ is immaterial) corresponding respectively to the three wave functions defined in Eqs. 2-12 through 2-14 are

$$H_\phi^i = \frac{2k}{j\omega\mu} \sum_{m=0}^{\infty} \frac{j^m}{\epsilon_m} J_m'(k\rho) \cos m\phi \quad ,$$

$$H_\phi^r = \frac{2k}{j\omega\mu} \sum_{m=0}^{\infty} \frac{j^m}{\epsilon_m} \left[- \frac{J_m(ka)}{H_m^{(2)}(ka)} \right] H_m^{(2)'}(k\rho) \cos m\phi \quad ,$$

$$H_\phi^s = \frac{-1}{\mu} \sum_{m=0}^{\infty} \cos m\phi \int_{-\infty}^{\infty} \gamma F_m(\alpha) H_m^{(2)'}(\gamma\rho) e^{j\alpha z} d\alpha \quad . \quad (2\text{-}18)$$

11

Inside the cavity H_ϕ is given by

$$H_\phi = \frac{-1}{\mu} \sum_{m,n=0}^{\infty} \gamma_n A_{mn} J_m'(\gamma_n \rho) \cos m\phi \cos \alpha_n z \; . \qquad (2\text{-}19)$$

Hence, the desired continuity of the tangential magnetic field across the aperture now reads

$$\frac{2k}{j\omega\mu} \sum_{m=0}^{\infty} \frac{j^m}{\varepsilon_m} \left[J_m'(ka) - \frac{J_m(ka)}{H_m^{(2)}(ka)} H_m^{(2)'}(ka) \right] \cos m\phi$$

$$- \frac{1}{\mu} \sum_{m=0}^{\infty} \cos m\phi \int_{-\infty}^{\infty} \gamma F_m(\alpha) H_m^{(2)'}(\gamma a) e^{j\alpha z} \, d\alpha$$

$$= - \frac{1}{\mu} \sum_{m,n=0}^{\infty} \gamma_n A_{mn} J_m'(\gamma_n a) \cos m\phi \cos \alpha_n z \; ; \qquad (2\text{-}20)$$

$$|\phi| \leq \phi_0, \; |z| \leq d \; .$$

The above equation can be simplified by recognizing that the term in the bracket on the LHS is the Wronskian of Bessel functions:

$$J_m'(ka) - \frac{J_m(ka)}{H_m^{(2)}(ka)} H_m^{(2)'}(ka) = \frac{j2}{\pi k a H_m^{(2)}(ka)} \; .$$

By substituting the above result into Eq. 2-20, it becomes

$$\sum_{m=0}^{\infty} \cos m\phi \int_{-\infty}^{\infty} \gamma F_m(\alpha) H_m^{(2)'}(\gamma a) e^{j\alpha z} \, d\alpha$$

$$- \sum_{m,n=0}^{\infty} \cos m\phi \, \gamma_n A_{mn} J_m'(\gamma_n a) \cos \alpha_n z$$

$$= \frac{4}{\pi\omega a} \sum_{m=0}^{\infty} \frac{j^m \cos m\phi}{\varepsilon_m H_m^{(2)}(ka)} \qquad ; \quad |\phi| \leq \phi_{\hat{0}}, \; |z| \leq d \; . \qquad (2\text{-}21)$$

12

Applying the method of Galerkin [9], the preceding equation can be solved numerically. First, we integrate the equation with respect to z over the aperture; the result is

$$\sum_{m=0}^{\infty} \cos m\phi \int_{-\infty}^{\infty} \frac{2 \sin \alpha d}{\alpha} \gamma F_m(\alpha) H_m^{(2)'}(\gamma a) \, d\alpha$$

$$- \sum_{m,n=0}^{\infty} \cos m\phi \frac{2 \sin \alpha_n d}{\alpha_n} \gamma_n A_{mn} J_m'(\gamma_n a)$$

$$= \frac{4}{\pi \omega a} \sum_{m=0}^{\infty} \frac{j^m \cos m\phi}{\varepsilon_m H_m^{(2)}(ka)} 2d \quad ; \quad |\phi| \leq \phi_0 \, . \tag{2-22}$$

Next we multiply both sides of the equation above by $\cos \nu\phi$, $\nu = 0,1,2,\ldots,$ and the integration of the resultant equation over the entire domain of interest leads to

$$\sum_{m=0}^{\infty} g_{m\nu} \int_{-\infty}^{\infty} \frac{\sin \alpha d}{\alpha} \gamma F_m(\alpha) H_m^{(2)'}(\gamma a) \, d\alpha$$

$$- \sum_{m,n=0}^{\infty} g_{m\nu} \frac{\sin \alpha_n d}{\alpha_n} \gamma_n A_{mn} J_m'(\gamma_n a)$$

$$= \frac{4d}{\pi \omega a} \sum_{m=0}^{\infty} \frac{j^m}{\varepsilon_m} \frac{g_{m\nu}}{H_m^{(2)}(ka)} \quad ; \quad \nu = 0,1,2,\ldots, \tag{2-23}$$

where $g_{m\nu}$ stands for

$$g_{m\nu} = \frac{\sin(m - \nu)\phi_0}{m - \nu} + \frac{\sin(m + \nu)\phi_0}{m + \nu} \, . \tag{2-24}$$

Then, we replace $\{A_{mn}\}$ and $\{F_m\}$ in Eq. 2-23 by their definitions in Eqs. 2-11 and 2-17. After some algebraic manipulations, we arrive at

$$\sum_{\mu=0}^{\infty} E_\mu \left[\Lambda_{\mu\nu}^{(1)} + \Lambda_{\mu\nu}^{(2)} = D_\nu \right]; \nu = 0,1,2,\ldots \tag{2-25}$$

13

where

$$\Lambda_{\mu\nu}^{(1)} = \frac{(-1)^{\mu}\Gamma_{\mu}}{\pi} \sum_{m=0}^{\infty} \frac{g_{m\nu}\cos m\phi_0}{\varepsilon_m(\Gamma_{\mu}^2 - m^2)} \int_0^{\infty} \frac{\sin^2 \alpha_n d\; H_m^{(2)\prime}(\gamma a)}{\alpha^2 \gamma\; H_m^{(2)}(\gamma a)}\; d\alpha \quad ,$$

$$\Lambda_{\mu\nu}^{(2)} = -\frac{(-1)^{\mu}\Gamma_{\mu}}{h} \sum_{m=0}^{\infty} \frac{g_{m\nu}\cos m\phi_0}{\varepsilon_m(\Gamma_{\mu}^2 - m^2)} \sum_{n=0}^{\infty} \frac{\sin^2 \alpha_n d\; J_m'(\gamma_n a)}{\alpha_n^2 \gamma_n\; J_m(\gamma_n a)} \quad ,$$

and

$$D_{\nu} = \frac{-jd}{k^2 a} \sum_{m=0}^{\infty} \frac{j^m g_{m\nu}}{\varepsilon_m H_m^{(2)}(ka)} \quad .$$

Equation 2-25 is the system of infinitely many linear equations that we intended to derive. In general, this system of equations cannot be solved. However, if the series in Eq. 2-3 is truncated at a finite number N, the system would become a system of N x N algebraic equations, with which the unknowns $\{E_{\mu}\}$, $\mu = 0,1,2,...N$, can be determined by solving the equations simultaneously by standard procedures such as the method of Gaussian elimination. After $\{E_{\mu}\}$ are determined, it is a matter of direct substitution of $\{E_{\mu}\}$ into Eq. 2-5 to obtain the field inside the cavity. For example, the z-component of the electric field E_z is given by

$$E_z = \frac{4}{\pi h} \sum_{\mu=0}^{\infty} E_{\mu}(-1)^{\mu}\Gamma_{\mu}$$

$$\times \sum_{n=0}^{\infty} \frac{\sin \alpha_n d \cos \alpha_n z}{\varepsilon_n \alpha_n} \sum_{m=0}^{\infty} \frac{\cos m\phi \cos m\phi_0\; J_m(\gamma_n \rho)}{\varepsilon_m(\Gamma_{\mu}^2 - m^2)\; J_m(\gamma_n a)} \quad ; \qquad (2-26)$$

$$\rho \leq a, \; |\phi| \leq \pi, \; |z| \leq h \quad .$$

This completes our derivation for the field inside the cavity due to the incidence of Eq. 2-2 in the absence of the wire.

14

III. CURRENT INDUCED ON A WIRE IN THE CAVITY

In this section, the current induced on the wire inside the cavity when it is illuminated by the field $\bar{E}$ is derived. We attack the problem by assuming that the presence of the wire does not perturb the field generated inside the cavity. It enables us to use $\bar{E}$ as an incident field and to determine the induced current $I(z)$ as if the wire were situated in the free space.

With reference to Eq. 2-26, we note that the electric field tangential to the wire E_z is given in terms of a doubly infinite series of eigenfunctions of the cavity. The series can be interpreted as a spectrum of plane waves. Explicitly, E_z is rewritten as

$$E_z = \sum_{n=-\infty}^{\infty} f_n(\rho,\phi) \exp(+jk \cos \theta_n z) \quad ; \qquad (3-1)$$

$$\rho \leq a, \ |\phi| \leq \pi, \ |z| \leq h \ ,$$

where

$$\theta_n = \cos^{-1}\left(\frac{n\pi}{kh}\right) \ , \qquad (3-2)$$

and

$$f_n = \frac{2}{\pi h} \sum_{\mu=0}^{\infty} E_\mu \frac{(-1)^\mu \Gamma_\mu \sin \alpha_n d}{\alpha_n} \sum_{m=0}^{\infty} \frac{\cos m\phi \cos m\phi_0 \ J_m(\gamma_n \rho)}{\varepsilon_m (\Gamma_\mu^2 - m^2) \ J_m(\gamma_n a)} \ . \quad (3-3)$$

We interpret each component of the field in Eq. 3-1 as a plane wave in free space propagating in the direction θ_n with respect to the z-axis.

In this report, two methods are used to compute the current induced on the wire due to each component of the plane wave spectrum described in Eq. 3-1. The first of these methods is based on an integral equation formulation:

15

$$\left(\frac{\partial^2}{\partial z^2} + k^2\right) \int_{z_0-h_w}^{z_0+h_w} I_n^{(1)}(z')K(z,z')dz' = -j4\pi\omega f_n e^{jk\cos\theta_n z} \quad . \quad (3-4)$$

The above thin wire scattering problem has been thoroughly studied in recent years, and a number of efficient programs to compute the unknown current $I_n^{(1)}$ have been developed. The program developed by Butler [10], which is based on solving Eq. 3-4 by the method of moments, is adopted here. Applying the principle of superposition, the induced current I is given by

$$I(z) = \sum_{n=-\infty}^{\infty} f_n(\rho,\phi)I_n^{(1)}(z) \quad , \quad (3-5)$$

where ρ is evaluated at the location of the wire.

As is well-known, using moment methods to compute the current on a wire is extremely time-consuming when the wire is of the order of several wavelengths. An alternative method that is suitable for long wires is to use the simple approximation formula developed recently by Chang, Lee and Rispin [11], [12]. The techniques used to derive this simple formula are briefly described below:

1. Using a Wiener-Hopf method, the reflection coefficient from the end of a semi-infinite wire illuminated by a plane wave of unit amplitude is determined.

2. By considering the multiple bounces of the current waves, the current induced on a wire of finite length can be expressed in terms of two Neumann series involving the just mentioned reflection coefficient. The series are then summed up into a closed form to give the desired approximation formula.

16

The induced current due to each component of the plane-wave spectrum is denoted by $I_n^{(2)}$ and is given by

$$I_n^{(2)}(z) = \left[C(\pi-\theta_n) \frac{R(\pi,h_w-z')}{R(\pi,2h_w)} + \Delta(\pi-\theta_n,h_w-z') V(\theta_n,h_w) \right] U(h_w-z')$$

$$+ \left[C(\theta_n) \frac{R(\pi,h_w+z')}{R(\pi,2h_w)} + \Delta(\theta_n,h_w+z') V(\pi-\theta_n,h_w) \right] U(h_w+z')$$

$$+ V(\theta_n,z') \quad , \tag{3-6}$$

where $z' = z - z_0$. In the above formula, V represents the current induced on an infinitely long cylinder by a unit plane wave:

$$V(\theta,z) = -\frac{j4\pi}{\eta} \frac{\exp(-jk\cos\theta_n z')}{\sin\theta_n W(k\cos\theta_n)} \quad , \tag{3-7}$$

in which W stands for

$$W = -j\pi J_0(ka_w \sin\theta_n) H_0^{(2)}(ka_w \sin\theta_n) \quad , \tag{3-8}$$

where J_0 and $H_0^{(2)}$ are, respectively, the zeroth-order Bessel function of the first kind and the Hankel function of the second kind, and a_w is the radius of the cylinder. Another universal function U is found in the simple formula; it represents the current on an infinitely long center-fed antenna generated by a unit voltage impulse. For a thin-wire antenna and for a sufficiently large kz, U can be accurately approximated by

$$U(z) \doteq \frac{2\pi}{\eta} \frac{\exp(-jk|z'|)}{\ln(2k|z'|) - j\pi/2 - 2\ln(ka_w) - \gamma} \quad , \tag{3-9}$$

where $\gamma = 0.57712...$ is the Euler's constant. The reflection coefficient R in Eq. 3-6 is defined by

$$R(\theta,z) = -\frac{\eta}{\pi} \left[\ln(ka_w \sin\frac{\theta_n}{2}) + \gamma + j\frac{\pi}{2} + \frac{e^{jv_0}}{2} E_1(jv_0) \right] \quad , \tag{3-10}$$

17

where

$$V_\theta = kz'(1 - \cos \theta_n) \quad,$$

and E_1 is the exponential integral. Finally, Δ and C are, respectively, shorthand notations for

$$\Delta = R(\theta_n, 2h_w) - R(\theta_n, h_w + z') \quad, \tag{3-11}$$

and

$$C = \frac{R(\pi - \theta_n, 2h_w) V(\theta_n, h_w) R(\pi, 2h_w) U(2h_w) - R(\theta_n, 2h_w) V(\pi - \theta_n, h_w)}{1 - [R(\pi, 2h_w) U(2h_w)]^2} \quad.$$
$$\tag{3-12}$$

Again, the total induced current is obtained by superimposing all $I_n^{(2)}$.

As is illustrated in Figure 3, the electric field of the incident plane wave is in the θ-direction and has an amplitude $f_n / \sin \theta_n$. Therefore, I is related to $I_n^{(2)}$ by

$$I(z) = \sum_{n=-\infty}^{\infty} f_n(\rho, \phi) \frac{I_n^{(2)}(z)}{\sin \theta_n} \quad, \tag{3-13}$$

where ρ is evaluated at the location of the wire.

A careful scrutiny of the techniques in deriving both $I_n^{(1)}$ and $I_n^{(2)}$ reveals that the two methods apply only if the incident plane wave is homogeneous, i.e., $\cos^2 \theta_n \leq 1$ or real incident angle θ_n. In the present problem, however, the field $\bar{E}$ inside the cavity consists of both homogeneous and inhomogeneous components. Hence, both methods have to be extended by analytical continuation to cover the case of an incident inhomogeneous plane wave.

Let us first consider $I_n^{(1)}$ which is obtained by solving Eq. 3-4. Note that Eq. 3-4 is developed by equating the axial component of the

18
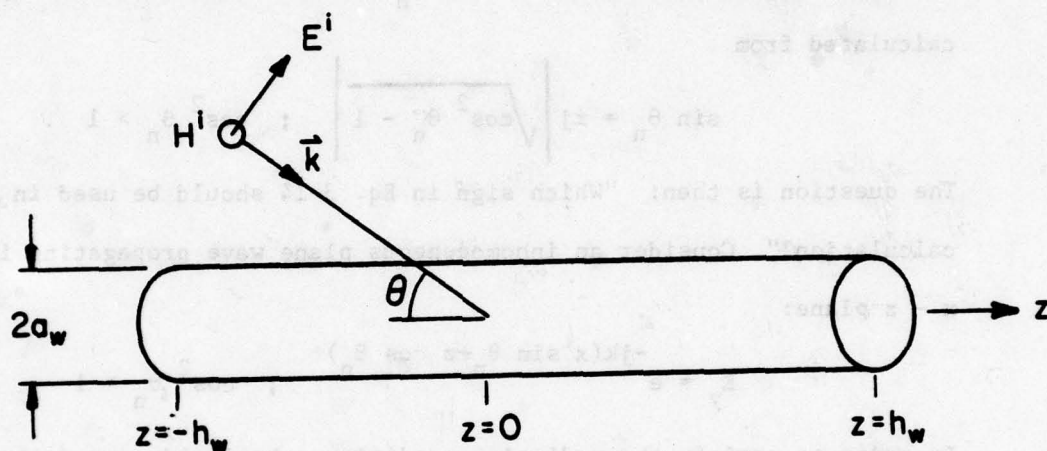
Figure 3. A finite length cylinder illuminated by an incident plane
wave at an oblique angle.

electric field on the wire and that of the incident field. The tangential component of the incident electric field is $f_n \exp(+jk\cos \theta_n z)$ which remains valid even in the case when $\cos^2 \theta_n > 1$. Thus no modification is necessary here, although allowances in the actual computer programming must be made to accommodate the rapidly oscillating nature of $\exp(+jk\cos \theta_n z)$ when $\cos \theta_n$ is large.

Next, we have to extend the formula of $I_n^{(2)}$ in Eq. 3-6. In the case of an inhomogeneous plane wave, $\sin \theta_n$ is pure imaginary, and may be calculated from

$$\sin \theta_n = \pm j \left| \sqrt{\cos^2 \theta_n - 1} \right| \quad ; \quad \cos^2 \theta_n > 1 \quad . \qquad (3\text{-}14)$$

The question is then: "Which sign in Eq. 3-14 should be used in the calculation?" Consider an inhomogeneous plane wave propagating in the $x - z$ plane:

$$E_y = e^{-jk(x \sin \theta_n + z \cos \theta_n)} \quad ; \quad \cos^2 \theta_n > 1 \quad . \qquad (3\text{-}15)$$

In order to satisfy the radiation condition, the field must decay (instead of grow) exponentially as $x \to +\infty$. This imposes a condition on $\sin \theta_n$, viz.,

$$I_m(\sin \theta_n) < 0. \qquad (3\text{-}16)$$

Thus, the lower sign (minus sign) in Eq. (3-14) must be used in the calculation of $I_n^{(2)}$ from Eqs. 3-7, 3-8, 3-10, and 3-13. Furthermore, W in Eq. 3-8 becomes

$$W = 2 I_0(ka_w \sqrt{\cos^2 \theta_n - 1}) K_0(ka_w \sqrt{\cos^2 \theta_n - 1}) \quad , \qquad (3\text{-}17)$$

where I_0 and K_0 are, respectively, the zeroth order modified Bessel functions.

20

IV. NUMERICAL COMPUTATIONS

As it stands, the numerical computation of each element of the system of linear equations in Eq. 2-25 is extremely time-consuming. The summation of the ratio of Bessel functions often presents another problem because both the numerator and the denominator could exceed the range of the computer and yet the quotient is still not small enough to warrant the termination of the summation process. In this section, a technique to circumvent the above difficulty is presented. And, at the same time, it significantly improves the rate of convergence. To best illustrate this technique, the evaluation of $\Lambda_{\mu\nu}^{(1)}$ is discussed in detail.

Besides a multiplying constant, $\Lambda_{\mu\nu}^{(1)}$ is rewritten below with the order of summation and integration interchanged:

$$\Lambda_{\mu\nu}^{(1)} = \int_0^\infty \frac{\sin^2 \alpha d}{\alpha^2 \gamma} \sum_{m=0}^\infty \frac{g_{m\nu} \cos m\phi_0}{\varepsilon_m (\Gamma_\mu^2 - m^2)} \frac{H_m^{(2)\prime}(\gamma a)}{H_m^{(2)}(\gamma a)} \, d\alpha \quad . \qquad (4\text{-}1)$$

Because of the branch point $\alpha = k$, we partition the above integral into two parts:

$$\Lambda_{\mu\nu}^{(1)} = \int_0^k \frac{\sin^2 \alpha d}{\alpha^2 \gamma} \sum_{m=0}^\infty \frac{g_{m\nu} \cos m\phi_0}{\varepsilon_m (\Gamma_\mu^2 - m^2)} \frac{H_m^{(2)\prime}(\gamma a)}{H_m^{(2)}(\gamma a)} \, d\alpha$$

$$- \int_k^\infty \frac{\sin^2 \alpha d}{\alpha^2 \tau} \sum_{m=0}^\infty \frac{g_{m\nu} \cos m\phi_0}{\varepsilon_m (\Gamma_\mu^2 - m^2)} \frac{K_m'(\tau a)}{K_m(\tau a)} \, d\alpha \quad , \qquad (4\text{-}2)$$

where $\{K_m\}$ are the mth order modified Bessel functions and $\tau = \sqrt{\alpha^2 - k^2}$. Note that both integrands above have a non-integrable singularity in the neighborhood of the branch point. Hence, both integrals must be further partitioned such that the integration of a small region around

21

the branch point is deliberately isolated. Each of the partial integrals

would be treated individually in the subsequent paragraphs.

The first integral to be treated is

$$I_1 = \int_0^{k-\delta} \frac{\sin^2 \alpha d}{\alpha^2 \gamma} \sum_H (\gamma a) \, d\alpha \quad , \tag{4-3}$$

where δ is an arbitrarily small number and $\sum_H$ represents the summation of

Hankel functions. By invoking the recurrence relationship between the

Hankel function and its derivative, $\sum_H$ becomes

$$\sum_H (u) = -G_{0\nu} \frac{H_1^{(2)}(u)}{H_0^{(2)}(u)} + \sum_{m=1}^{\infty} G_{m\nu} \left[\frac{H_{m-1}^{(2)}(u)}{H_m^{(2)}(u)} - \frac{m}{u} \right] \quad , \tag{4-4}$$

where $u = \gamma a$ and

$$G_{m\nu} = \frac{g_{m\nu} \cos m\phi_0}{\epsilon_m (\Gamma_\mu^2 - m^2)} \quad ; \quad m = 0,1,2,\ldots \quad . \tag{4-5}$$

Since the real and imaginary parts of $\sum_H$ have different rates of convergence,

they are treated independently as follows: First, by explicitly writing

$H_m^{(2)}$ as $J_m + jY_m$, the real part of $\sum_H$ reads

$$\mathrm{Re}\{\sum_H\} = -G_{0\nu} \frac{J_0(u)J_1(u) + Y_0(u)Y_1(u)}{J_0^2(u) + Y_0^2(u)}$$

$$+ \sum_{m=1}^{\infty} G_{m\nu} \left[\frac{J_m(u)J_{m-1}(u) + Y_m(u)Y_{m-1}(u)}{J_m^2(u) + Y_m^2(u)} \right] . \tag{4-6}$$

Note that for a given u, the large-order approximations of each term of

the sum can be extracted, which are

$$\lim_{m\to\infty} \left[\frac{J_m J_{m-1} + Y_m Y_{m-1}}{J_m^2 + Y_m^2} - \frac{m}{u} \right] = -\frac{m}{u} \tag{4-7}$$

22

and

$$\lim_{m \to \infty} G_{m\nu} = - \cos \nu\phi_0 \frac{\sin 2m\phi_0}{m^3} \quad .$$

(4-8)

By adding and subtracting the large-order approximations from each term of the sum, Eq. 4-6 becomes

$$Re\{\textstyle\sum_H\} = - G_{0\nu} \frac{J_0 J_1 + Y_0 Y_1}{J_0^2 + Y_0^2} + \sum_{m=1}^{\infty} \left\{ G_{m\nu} \left[\frac{J_m J_{m-1} + Y_m Y_{m-1}}{J_m^2 + Y_m^2} - \frac{m}{u} \right] \right.$$

$$\left. - \frac{\cos \nu\phi_0}{u} \frac{\sin 2m\phi_0}{m^2} \right\} + \frac{\cos \nu\phi_0}{u} \sum_{m=1}^{\infty} \frac{\sin 2m\phi_0}{m^2} \quad .$$

(4-9)

The second sum can be evaluated analytically and the result is

$$\sum_{m=1}^{\infty} \frac{\sin 2m\phi_0}{m^2} = - \int_0^{2\phi_0} \ln(2 \sin \frac{t}{2}) \, dt \quad .$$

(4-10)

The integral above is a thoroughly studied special function, known as Clausen's integral [14], whose value can be easily determined. The remaining sum in Eq. 4-9 has to be evaluated numerically. However, as compared with the sum in Eq. 4-6, which converges at a rate of m^{-2}, the modified sum converges at a much faster rate of m^{-4}. Furthermore, in evaluating the mth order Bessel function B_m ($B_m = J_m$ or Y_m), we can apply the following recurrence formula:

$$B_{m+1}(u) = \frac{2m}{u} B_m(u) - B_{m-1}(u) \quad .$$

(4-11)

However, as is well-known, we should use this recurrence formula with *extreme* caution in computing J_m to avoid the so-called "propagation of error" when $2m/u > 1$. In the actual computation, the total sum is broken down into partial sums of 10, e.g., from n to n + 9. We first evaluate J_{n+4} and J_{n+5}; then, we apply the recurrence formula in both the forward and backward directions to obtain the rest of J_m. Moreover, we terminate

23

the summation by comparing the magnitude of the partial sum with the total sum. In doing so, we avoid the danger of terminating the summation prematurely in the case $2n\phi_0$ is a multiple of π (referring to Eq. 4-8). As a final remark, when $ka_w \gg 1$, $\sum_H$ can be approximated by

$$\sum_H(u) \doteq \frac{100}{u} \sum_H(u) \quad ; \quad u > 100 \quad . \tag{4-12}$$

On the other hand, no modification is necessary to sum $\text{Im}\{\sum_H\}$ because its large-order approximation is zero.

The second integral of concern is

$$I_2 = \int_{k+\delta}^{\infty} \frac{\sin^2 \alpha d}{\alpha^2 \tau} \sum_K (\tau a) \, d\alpha \quad , \tag{4-13}$$

where $\sum_K$ represents the summation of the modified Bessel functions $\{K_m\}$. With the derivative of K_m written in terms of K_m and K_{m-1}, $\sum_K$ reads

$$\sum_K(v) = - G_0 v \frac{K_1(v)}{K_0(v)} - \sum_{m=1}^{\infty} G_m v \left[\frac{K_{m-1}(v)}{K_m(v)} + \frac{m}{v} \right] \quad , \tag{4-14}$$

in which $v = \tau a$. Since the large-order approximation of each term of the sum is

$$\lim_{m \to \infty} \left[\frac{K_{m-1}(v)}{K_m(v)} + \frac{m}{v} \right] = \frac{m}{v} \quad , \tag{4-15}$$

we evaluate $\sum_K$ as

$$\sum_K = - G_0 v \frac{K_1(v)}{K_0(v)} + \frac{\cos v \phi_0}{v} \sum_{m=1}^{\infty} \frac{\sin 2m\phi_0}{m^2}$$

$$- \sum_{m=1}^{\infty} \left\{ G_m v \left[\frac{K_{m-1}}{K_m} + \frac{m}{v} \right] + \frac{\cos v \phi_0}{v} \frac{\sin 2m\phi_0}{m^2} \right\} \quad . \tag{4-16}$$

The above formula is similar to Eq. 4-9; therefore, it is evaluated by similar techniques. Furthermore, we extract the large argument approximation

24

of $\sum_K$, which is

$$\sum_K(v) \doteq \sum_K(150) \; ; \quad v \geq 150 \; . \tag{4-17}$$

Substituting the results of Eqs. 4-16 and 4-17 into Eq. 4-13, we arrive at

$$I_2 = \int_{k+\delta}^{\pi/d} \frac{\sin^2 \alpha d}{\alpha^2 \tau} \sum_K(\tau a) \, d\alpha$$

$$+ \sum_{n=1}^{\infty} \int_{n\pi/d}^{(n+1)\pi/d} \frac{\sin^2 \alpha d}{\alpha^2} \left[\frac{1}{\tau} \sum_K(\tau a) - \frac{1}{\alpha} \sum_K(150) \right] d\alpha$$

$$+ \sum_K(150) \int_{\pi/d}^{\infty} \frac{\sin^2 \alpha d}{\alpha^3} \, d\alpha \; . \tag{4-18}$$

By two successive integrations by parts, the last integral above is transformed into

$$\int_{\pi/d}^{\infty} \frac{\sin^2 \alpha d}{\alpha^3} \, d\alpha = d^2 \int_{2\pi}^{\infty} \frac{\cos t}{t} \, dt = - d^2 C_i(2\pi) \; , \tag{4-19}$$

where C_i is the cosine integral [15].

The third integral of concern is

$$I_3 = \int_{k-\delta}^{k} \frac{\sin^2 \alpha d}{\alpha^2 \gamma} \sum_H(\gamma a) \, d\alpha - \int_{k}^{k+\delta} \frac{\sin^2 \alpha d}{\alpha^2 \tau} \sum_K(\tau a) \, d\alpha \; . \tag{4-20}$$

First, we examine the small-argument behaviors of both $\sum_H$ and $\sum_K$; they are

$$\lim_{u \to 0} \text{Re}\{\sum_H\} = - \frac{1}{u} \sum_{m=1}^{\infty} m G_{mv} \; ,$$

$$\lim_{u \to 0} I_m\{\sum_H\} = - \frac{\pi G_{ov}}{2u \, \ell n^2 u} \; ,$$

and

$$\lim_{v \to 0} \sum_K = - \frac{1}{v} \sum_{m=1}^{\infty} m G_{mv} \; . \tag{4-21}$$

25

It can be easily shown that the real part of I_3 tends to zero, and its imaginary part can be approximated by

$$I_m\{I_3\} = \frac{\pi G_{0\nu} \sin^2 kd}{2ak^3 \ell n(a\sqrt{2k\delta})} \quad . \qquad (4\text{-}22)$$

Since the forms of $\Lambda_{\mu\nu}^{(1)}$ and $\Lambda_{\mu\nu}^{(2)}$ are similar, analogous techniques are employed to evaluate $\Lambda_{\mu\nu}^{(2)}$; the result is (besides a multiplying constant)

$$\Lambda_{\mu\nu}^{(2)} = \sum_{n=0}^{N} \frac{\sin^2 \alpha_n d}{\varepsilon_n \alpha_n^2 \gamma_n} \sum\nolimits_J(\gamma_n a) - \sum_{n=N+1}^{\infty} \frac{\sin^2 \alpha_n d}{\alpha_n^2}\left[\frac{1}{\tau_n}\sum\nolimits_I(\tau_n a) - \frac{1}{\alpha_n}\sum\nolimits_I(150)\right]$$

$$- (\frac{h}{\pi})^3 \sum\nolimits_I(150) \sum_{n=N+1}^{\infty} \frac{\sin^2 \alpha_n d}{n^3} \quad , \qquad (4\text{-}23)$$

where N = Integer (kh/π) and

$$\sum\nolimits_J(u) = - G_{0\nu}\frac{J_1(u)}{J_0(u)} - \frac{\cos \nu\phi_0}{u}\sum_{m=1}^{\infty} \frac{\sin 2m\phi_0}{m^2}$$

$$+ \sum_{m=1}^{\infty}\left\{G_{m\nu}\left[\frac{J_{m-1}(u)}{J_m(u)} - \frac{m}{u}\right] + \frac{\cos \nu\phi_0}{u}\frac{\sin 2m\phi_0}{m^2}\right\}, \qquad (4\text{-}24)$$

and

$$\sum\nolimits_I(u) = G_{0\nu}\frac{I_1(u)}{I_0(u)} - \frac{\cos \nu\phi_0}{u}\sum_{m=1}^{\infty} \frac{\sin 2m\phi_0}{m^2}$$

$$+ \sum_{m=1}^{\infty}\left\{G_{m\nu}\left[\frac{I_{m-1}(u)}{I_m(u)} - \frac{m}{u}\right] + \frac{\cos \nu\phi_0}{u}\frac{\sin 2m\phi_0}{m^2}\right\}. \qquad (4\text{-}25)$$

The last sum in Eq. 4-23 can be determined as follows:

$$\sum_{n=N+1}^{\infty} \frac{\sin^2 \alpha_n d}{n^3} = \frac{1}{2}\int_0^{2\pi d/h} f(\theta)d\theta - \sum_{n=1}^{N} \frac{\sin^2 \alpha_n d}{n^3} \quad , \qquad (4\text{-}26$$

where f is the Clausen's integral stated in Eq. 4-10.

26

V. NUMERICAL RESULTS

In determining the field inside the cavity with the wire absent, the series representation of the aperture field in Eq. 2-3 is truncated at n = N (the series contains N + 1 terms). We must first establish the convergence of the aperture field with respect to N. The aperture fields as calculated with N = 0, 1, and 2 are shown in Figure 4. We notice that the aperture fields as computed by N = 1 and that by N = 2 agree reasonably at the main lobe but not so well at the side lobe. For many practical cases, the three-term expansion N = 2 is generally sufficiently accurate for computing the aperture field.

An indication of the accuracy of the field $\overline{E}$ inside the cavity is how well does $\overline{E}$ satisfy the boundary condition on the cavity wall (including the aperture). In Figure 5, E_z as computed from Eq. 2-26 is plotted as a function of ϕ. In the aperture defined by $|\phi| \leq 57.29^o$, the calculated E_z agrees extremely well with the two-term expansion of the aperature field calculated from Eq. 2-3. It drops to less than 0.01% of the aperture field on the wall where E_z should be ideally zero. Also shown in Figure 5 is E_z at points just behind the aperture, $\rho/a = 0.995$. The variations of E_z with respect to z at $\rho/a = 0.0$, 0.5, and 0.8 are sketched in Figure 6. As a function of decreasing (ρ/a), E_z decreases rapidly from its value in the aperture, while it increases at an even faster rate from zero on the cavity wall toward the center of the cavity. These features are illustrated in Figure 7 where E_z is plotted as a function of ρ at z = 0.0 and z/h = 0.3.

Part B of the problem is to compute the current induced on the wire inside the cavity. As mentioned in previous sections, the simple formula

27

Figure 4. E_z in the aperture as a function of ϕ with N as a parameter. The input data are $a = 0.3\lambda$, $c = 0.3\lambda$, $d = 0.015\lambda$, $h = 0.6\lambda$.

Figure 5. E_z inside the cavity as a function of ϕ with (ρ/a) as a parameter. The input data are: $a = 0.3\lambda$, $c = 0.3\lambda$, $d = 0.015\lambda$, $h = 0.6\lambda$, $\phi_0 = 1$.

29

Figure 6. E_z inside the cavity as a function of z with (ρ/a) as a parameter. The input data are $a = 0.3\lambda$, $c = 0.3\lambda$, $d = 0.015\lambda$, $h = 0.6\lambda$, $\phi = 0$.
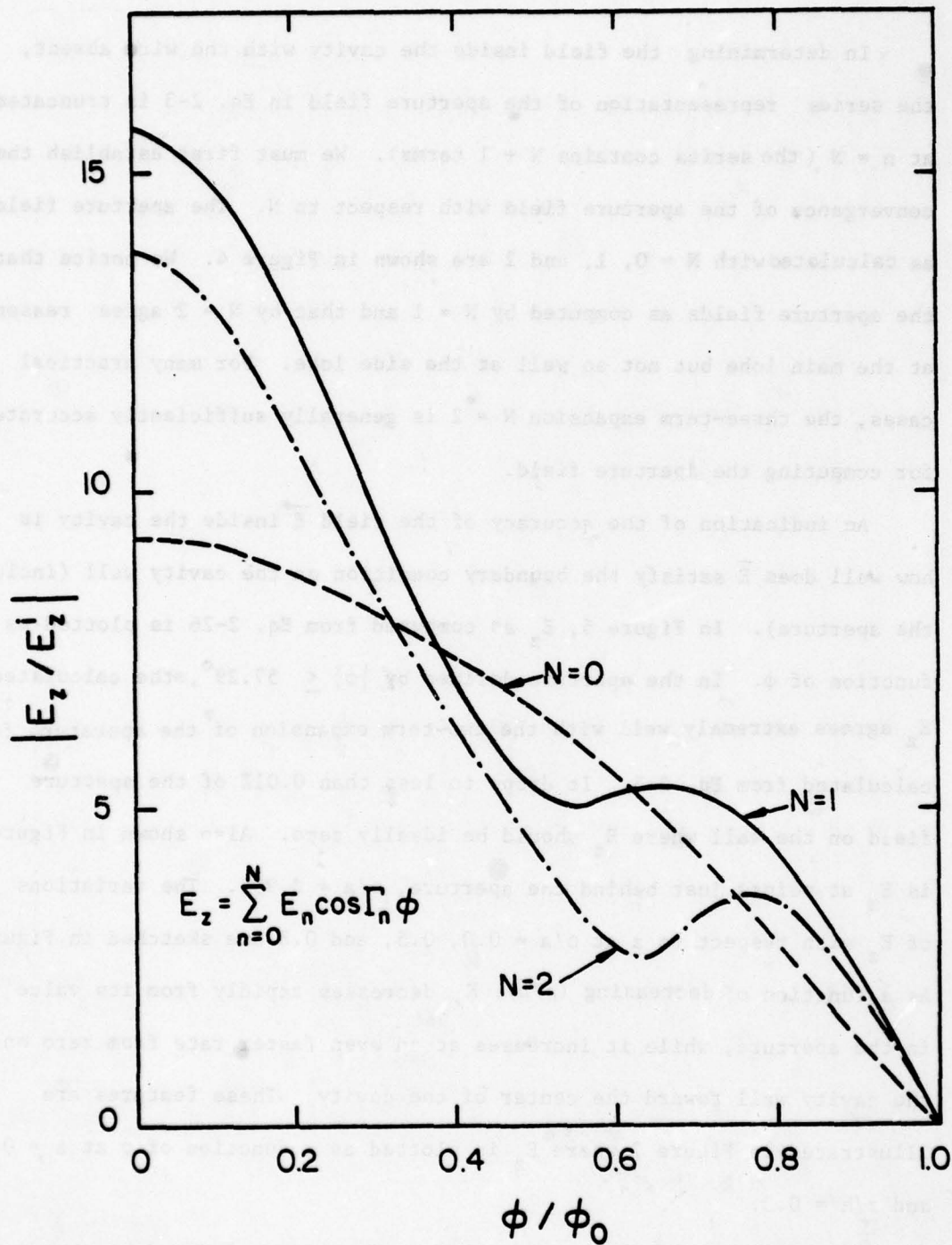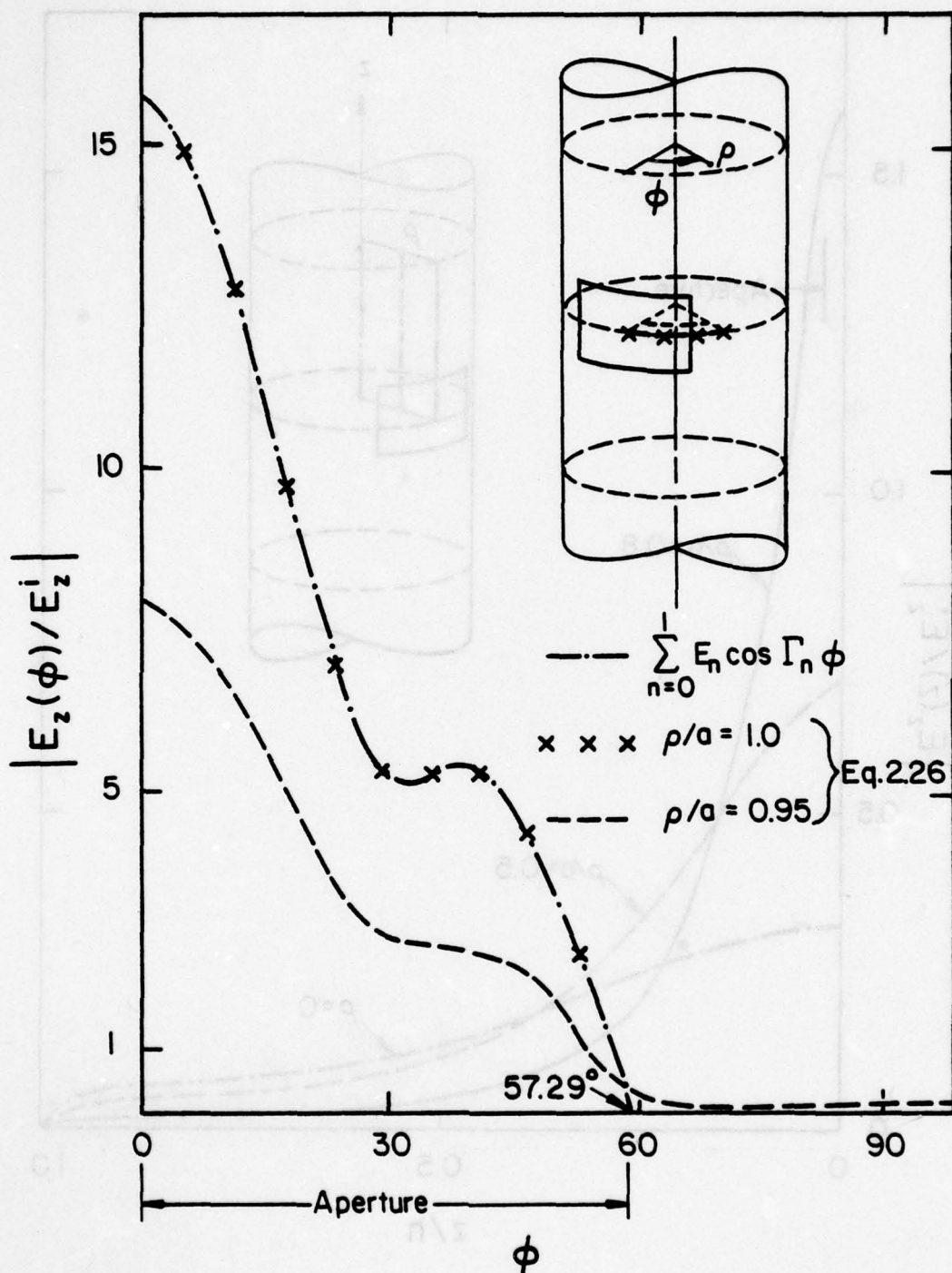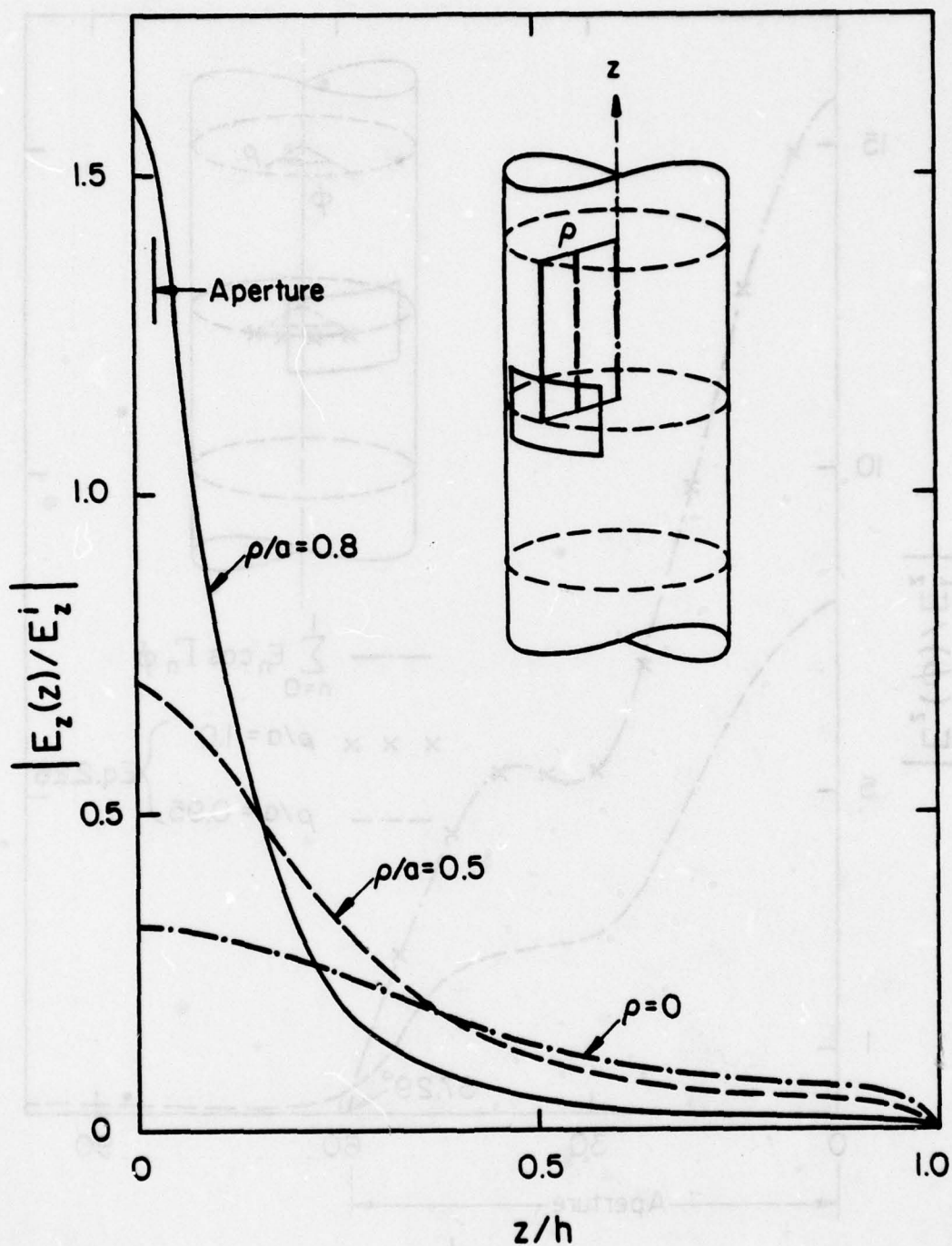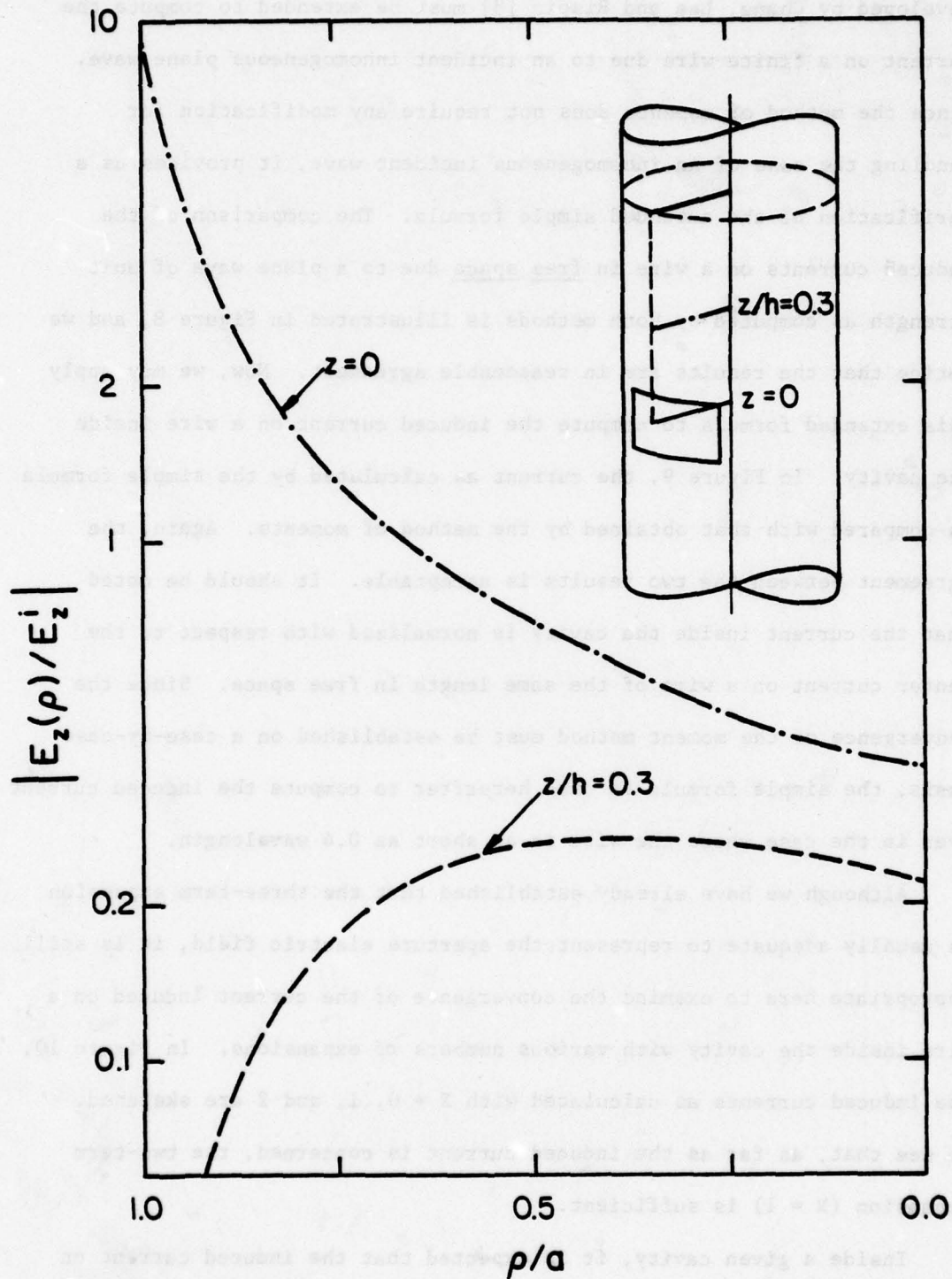
30

Figure 7. E_z inside the cavity as a function of ρ with (z/h) as a parameter. The input data are: $a = 0.3\lambda$, $c = 0.3\lambda$, $d = 0.015\lambda$, $h = 0.6\lambda$.

developed by Chang, Lee and Rispin [3] must be extended to compute the current on a finite wire due to an incident inhomogeneous plane wave. Since the method of moments does not require any modification for handling the case of an inhomogeneous incident wave, it provides us a verification of the extended simple formula. The comparison of the induced currents on a wire in free space due to a plane wave of unit strength as computed by both methods is illustrated in Figure 8, and we notice that the results are in reasonable agreement. Now, we may apply this extended formula to compute the induced current on a wire inside the cavity. In Figure 9, the current as calculated by the simple formula is compared with that obtained by the method of moments. Again, the agreement between the two results is acceptable. It should be noted that the current inside the cavity is normalized with respect to the center current on a wire of the same length in free space. Since the convergence of the moment method must be established on a case-by-case basis, the simple formula is used hereafter to compute the induced current even in the case where the wire is as short as 0.4 wavelength.

Although we have already established that the three-term expansion is usually adequate to represent the aperture electric field, it is still appropriate here to examine the convergence of the current induced on a wire inside the cavity with various numbers of expansions. In Figure 10, the induced currents as calculated with $N = 0$, 1, and 2 are sketched. We see that, as far as the induced current is concerned, the two-term expansion ($N = 1$) is sufficient.

Inside a given cavity, it is expected that the induced current on a given wire with its position fixed would increase with the enlargement

32
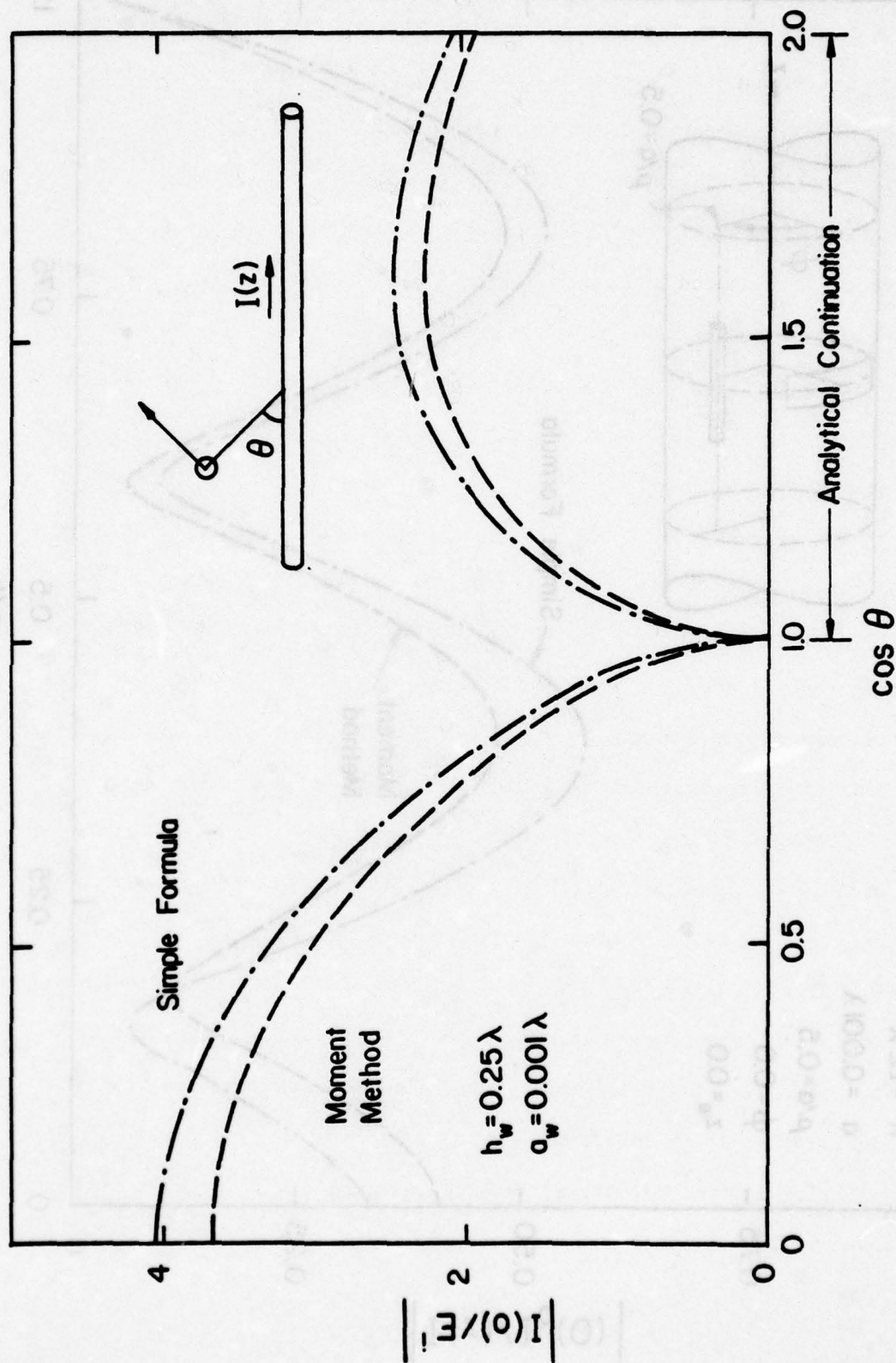
Figure 8. Comparison of the simple formula and the moment method for the determination of the current induced at the center of a cylinder in free space as a function of the angle of incidence θ (real and imaginary).

33
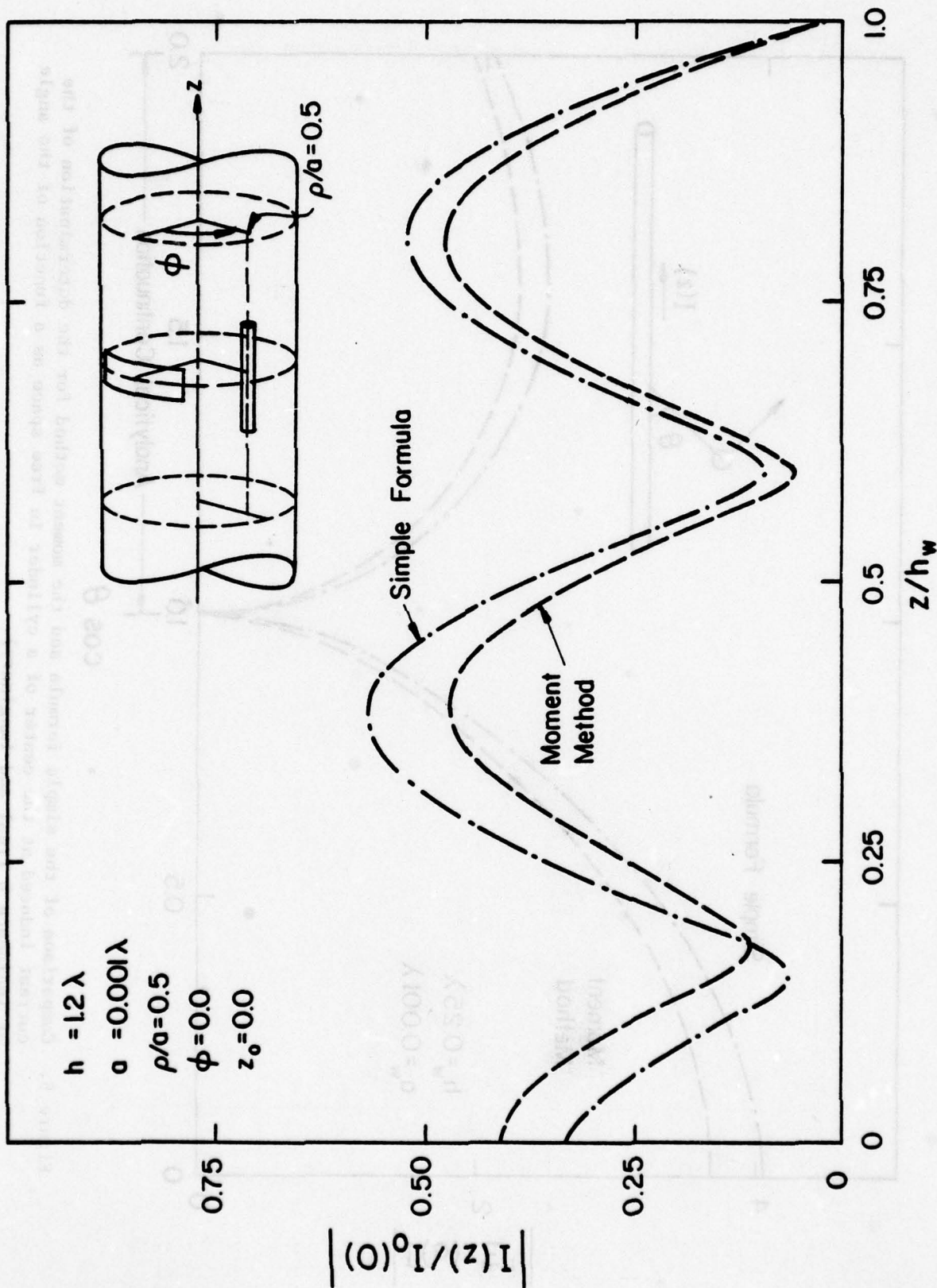
Figure 9. Comparison of the simple formula and the moment method for the determination of the induced current distribution on a wire inside the cavity. The input data are: $a = 0.3\lambda$, $\theta = 0.3\lambda$, $d = 0.015\lambda$, $h = 0.6\lambda$.

34

0.6

0.4

$\left| I(z)/I_0(0) \right|$

0.2

$\rho/a = 1.0$

$2h_w = 1.62$

$E_a = \sum_{n=0}^{N} A_n \cos \Gamma_n \phi$

— — $N=0$
— . — $N=1$
△ △ △ $N=2$

0

0   0.5   1.0

z/h_w

Figure 10.   Induced current on a wire inside the cavity as a
function of z with N as a parameter. The input
data are $a = 1.0\lambda$, $c = 0.6\lambda$, $d = 0.015\lambda$, $h = 2.2\lambda$.

35

of the length of the slot 2c. The induced current at the center of the wire does increase with c when c is relatively small as compared with the radius of the cavity a. The center current acquires its peak value when c/a is about 0.9 and begins to decrease thereafter. These characteristics are demonstrated in Figure 11.

In Figure 12, we show the center current on the wire as a function of a, $0.25 \leq a/\lambda \leq 0.8$, with the other dimensions fixed. We observe that there are three peaks. The first of these peaks corresponds to the resonance at which $J_0(\gamma_0 a) = 0$. The second and third peaks correspond respectively to $J_1(\gamma_0 a) = 0$ and $J_0(\gamma_1 a) = 0$. It should be noted that the resonances would occur more often beyond the range of Figure 12, and numerical solutions for large a would not be reliable.

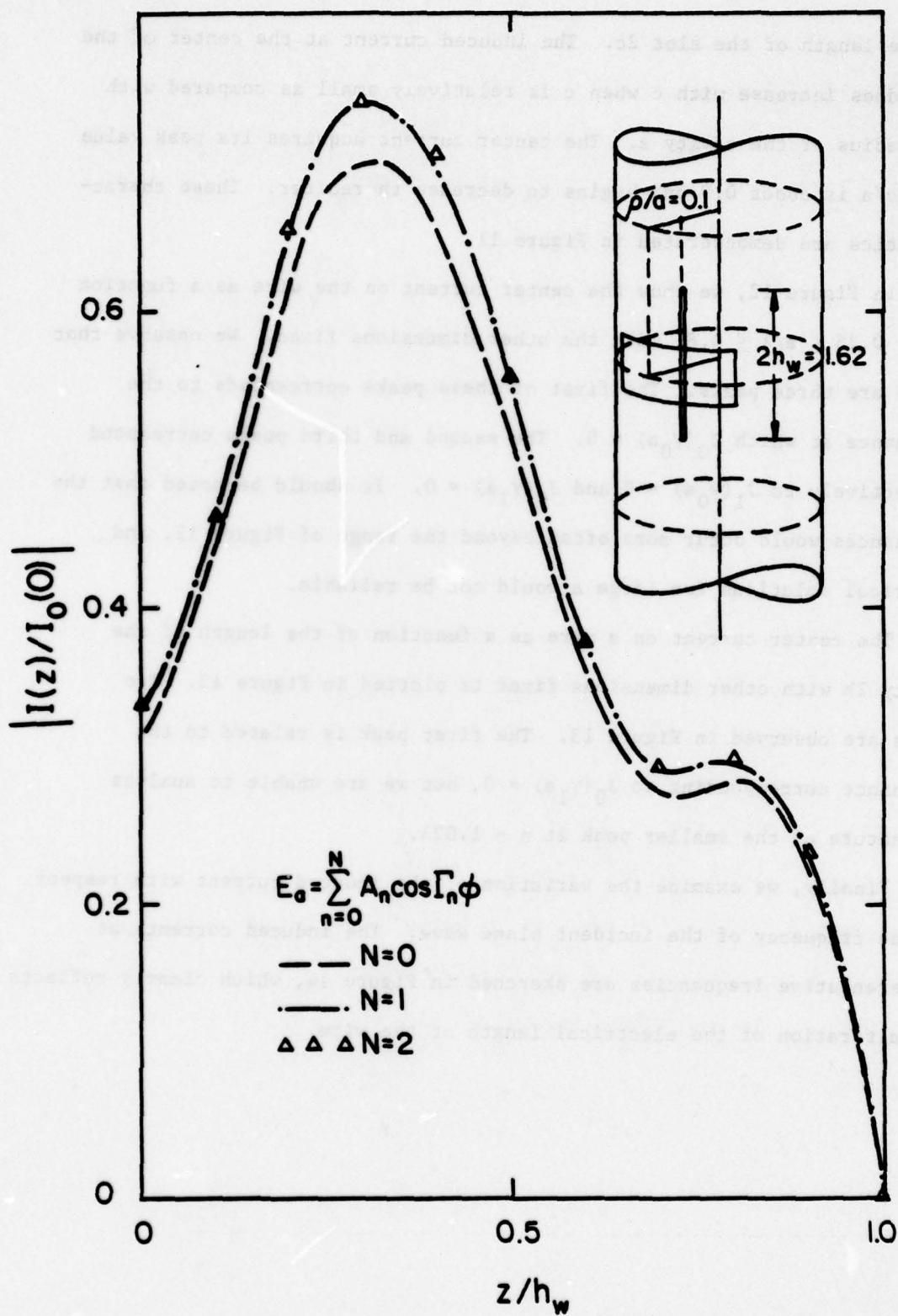The center current on a wire as a function of the length of the cavity 2h with other dimensions fixed is plotted in Figure 13. Two peaks are observed in Figure 13. The first peak is related to the resonance corresponding to $J_0(\gamma_1 a) = 0$, but we are unable to analyze the nature of the smaller peak at $h = 1.02\lambda$.

Finally, we examine the variation of the induced current with respect to the frequency of the incident plane wave. The induced currents at representative frequencies are sketched in Figure 14, which clearly reflects the alteration of the electrical length of the wire.

36
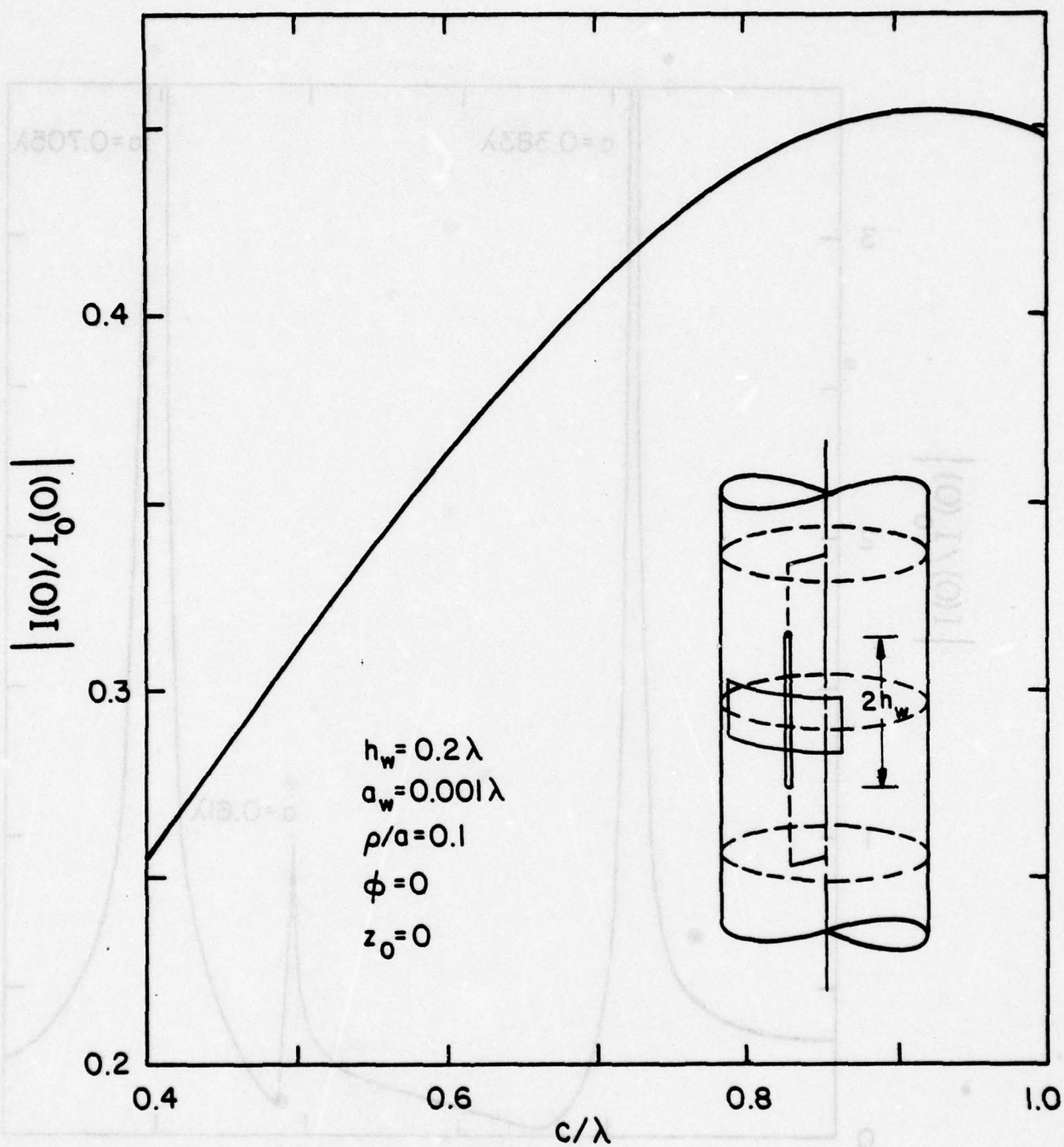
Figure 11. Induced current at the center of the wire inside the cavity as a function of slot length 2c. The input data are: a = 1, d = 0.015, h = 2.2, freq. = 0.3.

37
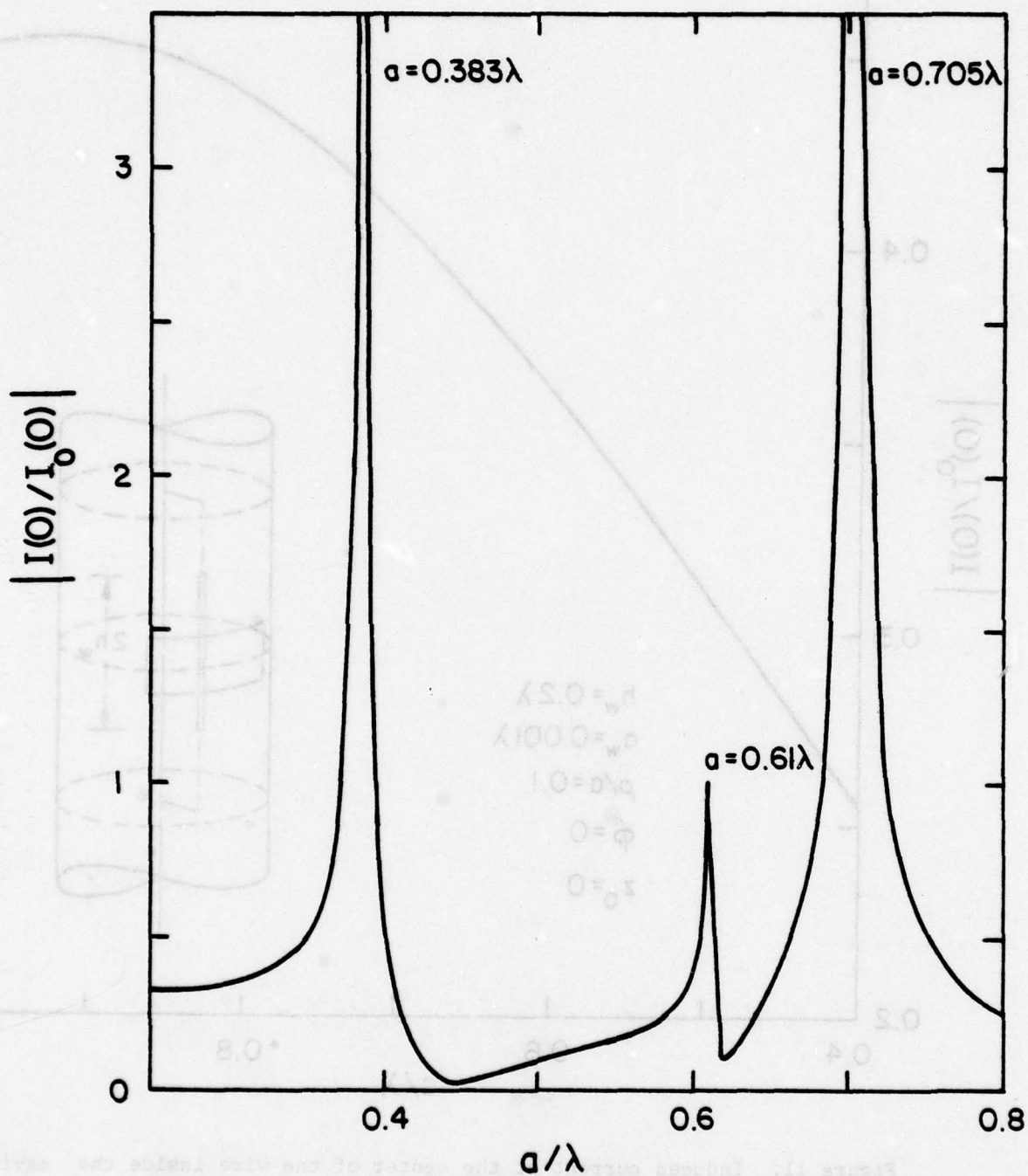
Figure 12. Induced current at the center of the wire inside the cavity as a function of cylinder radius a. The input data are: c = 0.3λ, d = 0.015λ, h = 0.6λ, h_w = 0.2λ, ρ/a = 0.1.

38

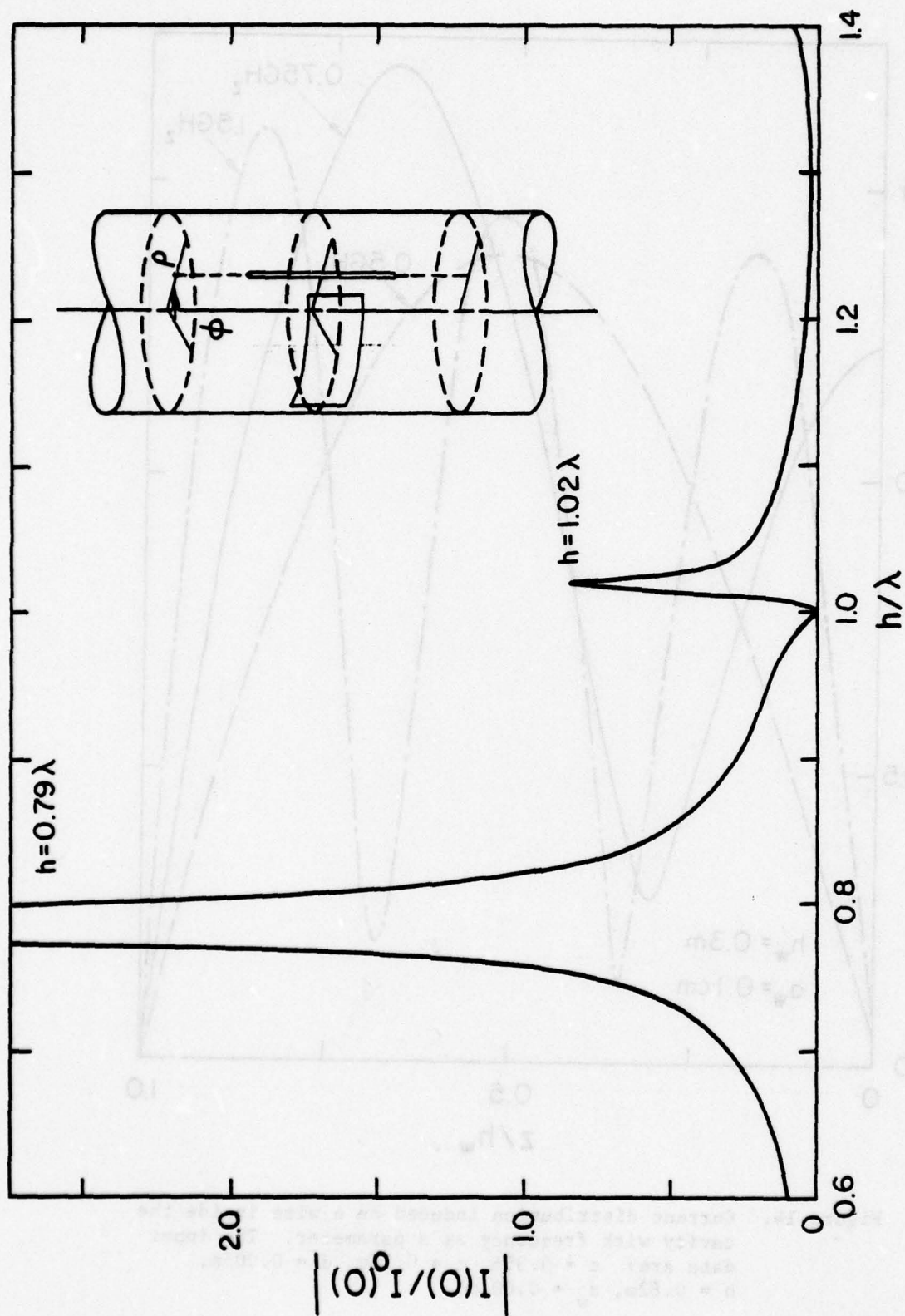Figure 13. Induced current at the center of the wire inside the cavity as a function of cavity length 2h. The input data are: $a = 0.5\lambda$, $c = 0.3\lambda$, $d = 0.015\lambda$, $h_w = 0.2\lambda$, $a_w = 0.001\lambda$, $\rho/a = 0.1$.
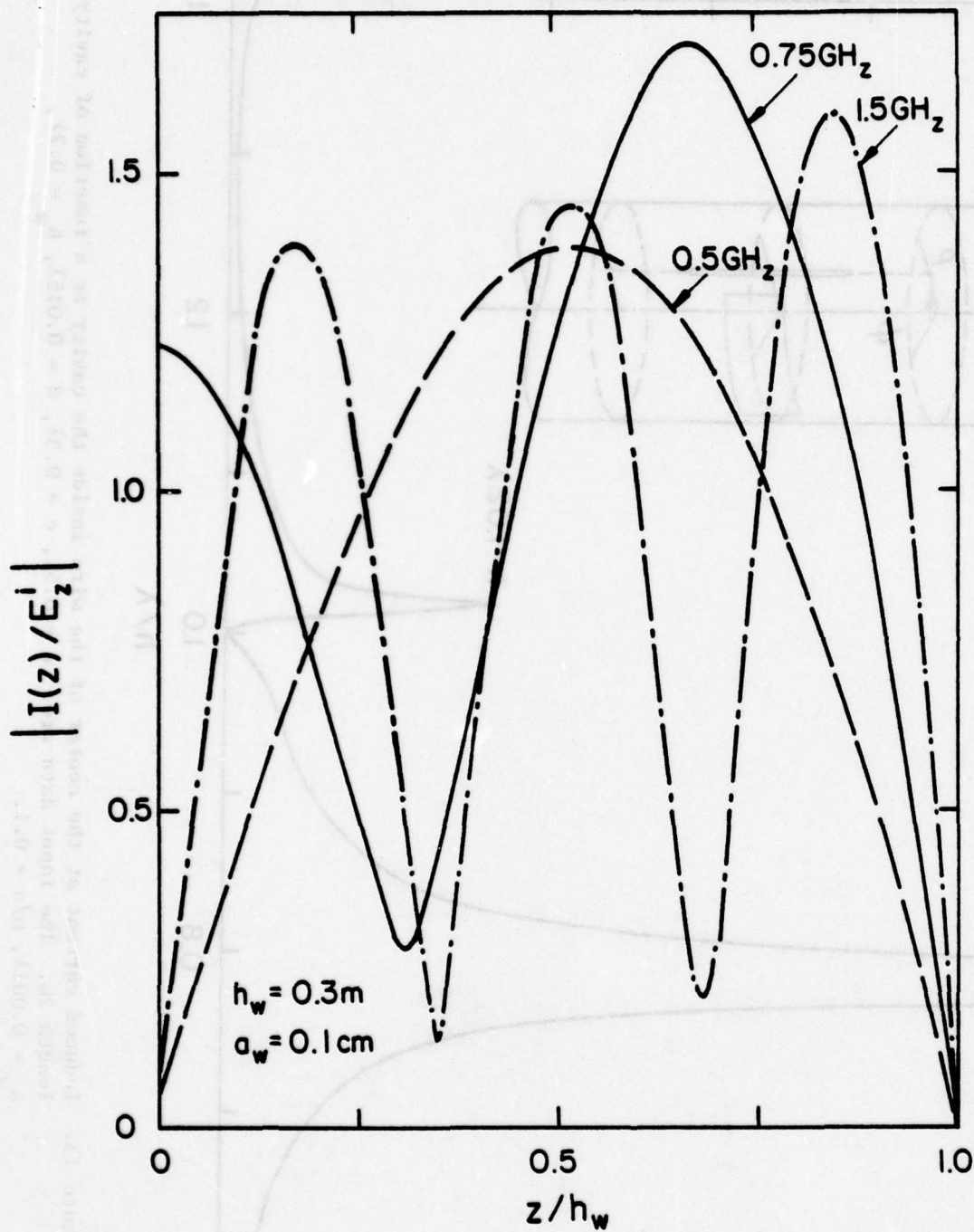
Figure 14. Current distribution induced on a wire inside the cavity with frequency as a parameter. The input data are: a = 0.35m, c = 0.25m, d = 0.005m, h = 0.82m, a_w = 0.001m.

REFERENCES

[1]   A. Sommerfeld, <u>Partial Differential Equations in Physics</u>, New York, Academic Press, 1949, pp. 29, 159.

[2]   Silvers and Saunders, "The External Field Produced by a Slot in an Infinite Circular Cylinder," <u>J. Appl. Phys.</u>, Vol. 21, 5, pp. 153–158, Feb., 1950.

[3]   R. Barakat and E. Levin, "Diffraction of a Plane EM Wave by a Perfectly Conducting Cylindrical Lamina," <u>J. Opt. Soc. Amer.</u>, Vol. 54, 9, pp. 1089–1094, 1964.

[4]   R. F. Wallenberg, "Radiation from Aperture in Conducting Cylinders of Arbitrary Cross Section," <u>IEEE Trans. Antennas Propagat.</u>, Vol. AP-17, No. 1, pp. 56–62, 1974.

[5]   L. L. Bailin and R. J. Spellmire, "Convergent Representations for the Radiation Fields from Slots in Large Circular Cylinders," <u>IRE Trans. Antennas Propagat.</u>, Vol. AP-5, pp. 374–383, 1957.

[6]   S. Safavi-Naini, "Diffraction of Electromagnetic Waves by a Slotted Circular Cylinder," M.S. Thesis, University of Illinois, Urbana, 1976.

[7]   S. Safavi-Naini, S. W. Lee, and R. Mittra, "Transmission of an EM Wave through the Aperture of a Cylindrical Cavity," Electromagnetic Lab. Technical Report No. 76-1, University of Illinois, Urbana, 1976.

[8]   S. Safavi-Naini, S. W. Lee, and R. Mittra, "Transmission of EM Wave through the Aperture of a Cylindrical Cavity," <u>IEEE Trans. Electromagn. Comput.</u>, Vol. EMC-19, pp. 74–81, 1977.

[9]   R. F. Harrington, <u>Field Computation by Moment Methods</u>, Macmillan, New York, 1968, pp. 7, 178.

[10] C. M. Butler, "Evaluation of Potential Integral at Singularity of Exact Kernel in Thin-Wire Calculations," <u>IEEE Trans. Antennas Propagat.</u>, Vol. AP-23, pp. 293–294, March, 1975.

[11] D. C. Chang, S. W. Lee, and L. Rispin, "Simple Expressions for Current on a Thin Cylindrical Receiving Antenna," Scientific Report No. 20, University of Colorado, Dec., 1976.

[12] D. C. Chang, S. W. Lee, and L. Rispin, "Simple Formula for Current on a Cylindrical Receiving Antenna," Electromagnetic Lab. Technical Report No. 77-10, University of Illinois, May, 1977; to appear in <u>IEEE Trans. Antennas Propagat.</u>, 1978.

[13] R. F. Harrington, <u>Time-Harmonic Electromagnetic Fields</u>, McGraw Hill,
      New York, 1961, p. 200.

[14] M. Abramowitz and I. Segun, <u>Handbook of Mathematical Functions</u>, Dover,
      New York, p. 1005.

[15] <u>Ibid</u>, p. 232.

Attachment B

SOURCE RADIATION IN THE PRESENCE

OF SMOOTH CONVEX BODIES

by

S. Safavi-Naini

R. Mittra

SECURITY CLASSIFICATION OF THIS PAGE *(When Data Entered)*

REPORT DOCUMENTATION PAGE		READ INSTRUCTIONS BEFORE COMPLETING FORM
1. REPORT NUMBER	2. GOVT ACCESSION NO.	3. RECIPIENT'S CATALOG NUMBER
4. TITLE *(and Subtitle)* Source Radiation in the Presence of Smooth Convex Bodies		5. TYPE OF REPORT & PERIOD COVERED Technical
		6. PERFORMING ORG. REPORT NUMBER EM 78-3: UILU-ENG-78-2544
7. AUTHOR(s) S. Safavi-Naini R. Mittra		8. CONTRACT OR GRANT NUMBERS(s) N00014-75-C-0293
9. PERFORMING ORGANIZATION NAME AND ADDRESS Electromagnetics Laboratory Department of Electrical Engineering University of Illinois, Urbana, Illinois 61801		10. PROGRAM ELEMENT, PROJECT, TASK AREA & WORK UNIT NUMBERS
11. CONTROLLING OFFICE NAME AND ADDRESS Office of Naval Research Department of the Navy Arlington, Virginia 22217		12. REPORT DATE June 1978
		13. NUMBER OF PAGES 65
14. MONITORING AGENCY NAME & ADDRESS*(If different from Controlling Office)*		15. SECURITY CLASS. *(of this report)* UNCLASSIFIED
		15a. DECLASSIFICATION DOWNGRADING SCHEDULE

16. DISTRIBUTION STATEMENT *(of this Report)*

Distribution unlimited. Reproduction in whole or in part is permitted for any purpose of the United States Government.

17. DISTRIBUTION STATEMENT *(of the abstract entered in Block 20, if different from Report)*

18. SUPPLEMENTARY NOTES

19. KEY WORDS *(Continue on reverse side if necessary and identify by block number)*

Electromagnetic radiation and scattering; geometrical theory of diffraction; spectral domain approach; asymptotic techniques for high frequencies; Fock's theory; stationary phase methods

20. ABSTRACT *(Continue on reverse side if necessary and identify by block number)*

The problem of radiation from sources in the presence of smooth, convex, impenetrable objects is considered, and a brief survey of various high frequency techniques is presented. A generalization of the geometrical theory of diffraction and two new techniques, based on the spectral domain approach and an asymptotic evaluation of the radiation integral for the surface current, are also discussed. Some numerical results derived from the spectral domain formulas are presented

DD FORM 1473 1 JAN 73   EDITION OF 1 NOV 65 IS OBSOLETE   UNCLASSIFIED   (over)

SECURITY CLASSIFICATION OF THIS PAGE *(When Data Entered)*

20. (continued)

and a comparison with available theoretical and experimental data is included.

SOURCE RADIATION IN THE PRESENCE
OF SMOOTH CONVEX BODIES

Technical Report

S. Safavi-Naini and R. Mittra

June 1978

Electromagnetics Laboratory
Department of Electrical Engineering
Engineering Experiment Station
University of Illinois at Urbana-Champaign
Urbana, Illinois 61801

ABSTRACT

The problem of radiation from sources in the presence of smooth, convex, impenetrable objects is considered, and a brief survey of various high frequency techniqes is presented. A generalization of the geometrical theory of diffraction, and two new techniques based on the spectral domain approach and an asymptotic evaluation of the radiation integral for the surface current, also are discussed. Some numerical results derived from the spectral domain formulas are presented and a comparison with available theoretical and experimental data is included.

TABLE OF CONTENTS

LIST OF FIGURES

1. Introduction

The problems of radiation from sources in the presence of impenetrable smooth convex objects and the diffraction of a plane wave by such objects are of great practical interest in the design of antennas on structures, e.g., conformal arrays. Unfortunately, the exact analytical solutions to these problems, based on the methods of "separation of variables" or "function-theoretic" procedures (Wiener-Hopf technique, residue calculus, etc.), exist only for a very limited number of scattering geometries. Furthermore, the exact solutions are typically highly complex in nature; hence, the process of extracting numerical results from them can be very time-consuming and is by no means trivial. This situation has motivated many researchers to explore approaches to the problems of radiation and scattering from smooth convex structures.

In the low and resonant frequency ranges, several reliable numerical procedures, e.g., the moment method, are available for solving the radiation and scattering problems. However, in the high frequency domain, numerical techniques based on matrix methods become unwieldly if not impractical, prompting one to employ asymptotic techniques suitable for large $k(=2\pi/\lambda)$, where λ is the wavelength of the illuminating wave.

In this work, we begin by presenting, in Sec. 2 , a survey of various high frequency asymptotic techniques for the problem stated above. The survey will be necessarily brief, and will cover only the highlights of a number of important approaches to the problem at hand, viz., Fock's theory, the geometrical theory of diffraction (GTD), and the direct integral equation approach. The reader interested in further details may choose to consult the works of Bowman, et al. [1], Uslenghi [2], and Kouyoumjian [3].

1

In Sec. 3, we consider the generalization of GTD and present some new approaches to the curved surface radiation and scattering problems. Some numerical results based on one of these new approaches are presented in Sec. 3 and a comparison with other available methods are included.

2. Survey of Available High-Frequency Asymptotic Techniques

2.1 Watson Transformation

One of the first successful attempts to derive an asymptotic expansion for the far-field generated by a point source located in the proximity of a conducting surface was made by G. N. Watson in 1918 [4]. His method, essentially, consisted of two steps: 1) transforming the original infinite series solution into a contour integral (by Cauchy's residue theorem); 2) deforming the contour of integration so as to capture a set of complex poles of the integrand. The original integral is then expressed in terms of an infinite series which converges very rapidly, provided the observation point is in the shadow region. The first few terms of this series were later interpreted as "creeping waves." The method was first applied to a sphere and circular cylinder, and later to some other geometries as well. The mathematical rigor of the method was the subject of further investigations by other researchers ([5], [6] and [7]). Although Watson transformation can only be applied to a few simple goemetries, e.g., the sphere, cylinder, cone, spheroid,   it is still regarded as one of the cornerstones of the more general high frequency techniques because of its mathematical rigor. Watson transformation is especially powerful in the shadow region of the geometric optics field. In the lit region, the above-mentioned contour integral is evaluated using the "stationary phase" method and yields the reflected field from the surface. In this region, the most significant contribution to the total scattered field typically comes from the surface current induced on the smooth convex part of the object;   the so-called "Physical Optics" approximation can be applied

2

([8], [9], and [10]) to derive the reflected field. The Physical Optics method is based upon approximating the induced surface current in the lit region of the object by the current that would be induced on the local tangent plane, and by assuming that the surface current is zero in the shadow region. The far field is constructed by substituting the above estimate for the induced surface current in the integral representation of the scattered field, and evaluating the same in an asymptotic sense. The dominant term of the asymptotic expansion of this integral can be shown to be identical to the first term of the Luneberg-Kline expansion of the geometrical optics far field ([11] and [12]). However, the higher-order terms derived from the physical optics approach do not provide us with the correct result in the shadow or transition regions where the diffracted field contributes the most.

In the next section, we discuss Fock's theory, which can fill the gap between the Physical Optics in the lit region and the "creeping wave" representation in the shadow region.

2.2 Fock's Theory

The region between the lit and the shadow part on a surface is called "penumbra region." The angular width of this region is approximately given by $(\lambda r_o^2/\pi)^{1/3}$ where λ is the wavelength of the illumination and r_o is the radius of curvature of the surface of the object in this region in the incident plane (Fig. 1). Fock's theory invokes the principle of *local* character of the field in the penumbra region [13] and is based on the conjecture that all bodies with a smoothly varying curvature have the same current distribution in the penumbra region, provided that the curvature and the incident wave are the same near the point under consideration. This principle allows one to locally replace the surface of the object by a portion of a paraboloid of

3
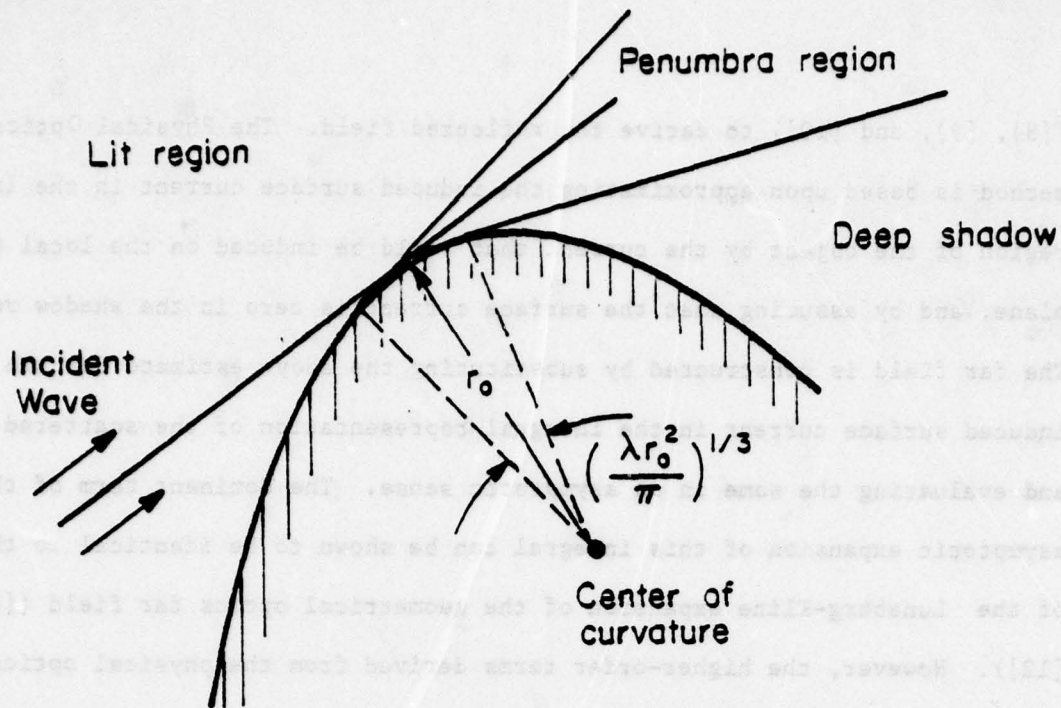
Figure 1: Section of the body in the plane of incidence.
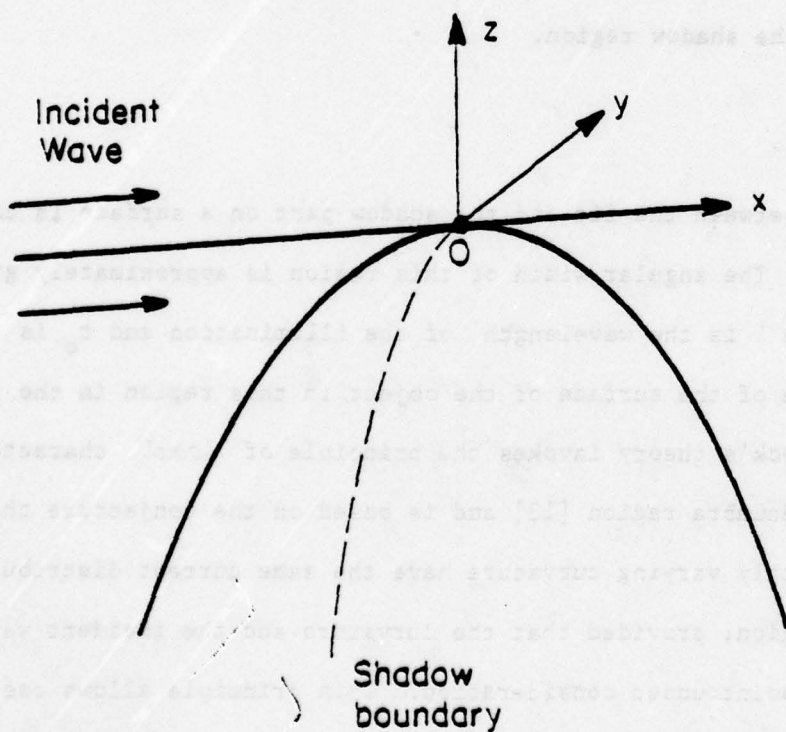
Figure 2: Plane wave incident upon a smooth convex body.

4

revolution. A unique feature of the expressions for Fock currents is that they provide a convenient transformation of the geometric optics currents in the lit region into the creeping wave currents in the shadow region. Fock himself deduced the pertinent formulas for the surface currents by treating a convex body problem [14] described below.

Consider a convex body and a plane wave incident in the direction of the x-axis. If the equation of the surface is

$$f(x,y,z) = 0 \tag{1}$$

then the curve representing the boundary of geometrical shadow is given by

$$f(\vec{r}) = 0 \ , \quad \frac{\partial f}{\partial x} = 0 \tag{2}$$

Consider a point 0 on the boundary of a shadow region where we set up a rectangular coordinate system as shown in Fig. 2 ($\hat{z}$: normal to the surface, $\hat{x}$: in the direction of propagation, and $\hat{y}$ is the tangent to the boundary of shadow). In the vicinity of this point, the surface of the body could be locally replaced by a paraboloid of revolution which is expressed by the equation.

$$z + 1/2 \ (ax^2 + 2bxy + cy^2) = 0 \tag{3}$$

Each of the field components satisfies the Helmholtz   equation

$$(\nabla^2 + k^2)\psi = 0 \tag{4}$$

5

The fact that the incident wave travels along the x-axis, suggests that Ψ be written in the form

$$\Psi = \tilde{\Psi}e^{-jkx} \qquad (5)$$

where an $\exp(j\omega t)$ time dependence has been assumed. Substituting (5) in (4) gives

$$\nabla^2\tilde{\Psi} - 2jk \frac{\partial}{\partial x} \tilde{\Psi} = 0 \qquad (6)$$

At this point, two basic assumptions are introduced in Fock's theory, viz.

i) $\tilde{\Psi}$'s are relatively slowly varying function of coordinates

ii) $\tilde{\Psi}$ varies more rapidly in the z-direction than in x and y,

i.e.,

$$\frac{\partial\tilde{\Psi}}{\partial z} = 0(\frac{k}{m} \tilde{\Psi}), \quad \frac{\partial\tilde{\Psi}}{\partial x} = 0(\frac{k}{m}, \tilde{\Psi}), \quad \frac{\partial\tilde{\Psi}}{\partial y} = 0 \ (\frac{k}{m} \tilde{\Psi}) \qquad (7)$$

Based upon (7), we can write (6) as

$$\frac{\partial^2\tilde{\Psi}}{\partial z^2} - 2jk \frac{\partial\tilde{\Psi}}{\partial x} = 0 \qquad (8)$$

and consequently $m' = m^2$ (m is very large), where the terms of order $1/m^2$ have been omitted.

Inserting these estimates and assumptions into the Maxwell's equation, we can find some simple expressions for all the field components in terms of H_y and H_z. If we write H_y as

6

$$H_y = H_y^0 \, e^{-jkx} \, \tilde{\psi} \qquad (9)$$

where H_y^0 is the magnitude of the incident wave at infinity, then ψ must satisfy

$$\frac{\partial^2 \tilde{\psi}}{\partial z^2} - 2jk \frac{\partial \tilde{\psi}}{\partial x} = 0 \qquad (10)$$

with boundary condition

$$\frac{\partial \tilde{\psi}}{\partial z} - jk \left(ax + by + \frac{1}{\sqrt{\eta}} \right) \tilde{\psi} = 0 \qquad (11)$$

on the surface of the body. Eqn. (11) is the simplified version of the Leontovich boundary condition where

$$\eta = \varepsilon - j \frac{4\pi\sigma}{ek}$$

The final solution for H_y on the surface of the body which satisfies the boundary condition and the condition at infinity, may be written in the form

$$H_y = H_y^{ex} \, G(\xi, q) \qquad (12)$$

where H_y^{ex} = external field

$$G(\xi, q) = e^{-(j/3)\,\xi^3} V_1(\xi, q)$$

$V_1(\xi, q)$ = Fock function defined in the Appendix A.

$\xi = m(ax + by)$ = reduced distance from the shadow boundary = ℓ/d.

d = the width of penumbra region = $(2r_o^2/k)^{1/3}$

ℓ = distance between the observation point and the shadow boundary along the incident ray (Fig. 3).

7
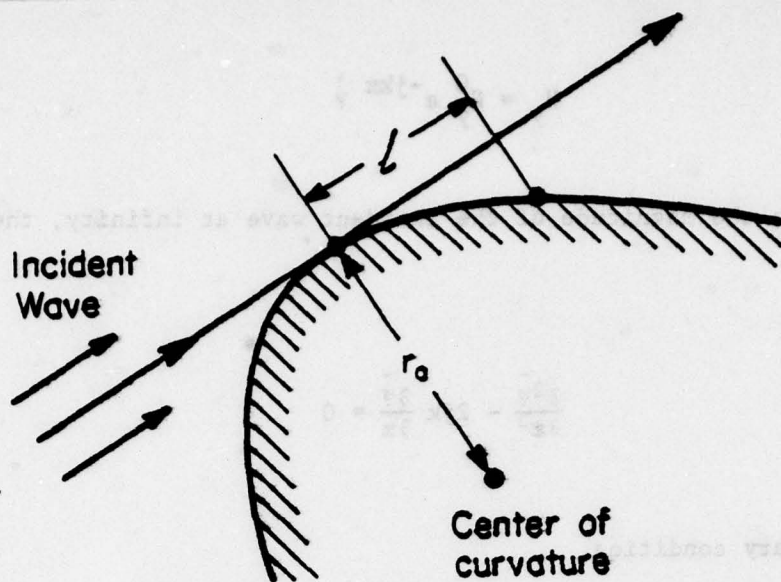
Figure 3: Geometric meaning of the quantity ℓ in (12).
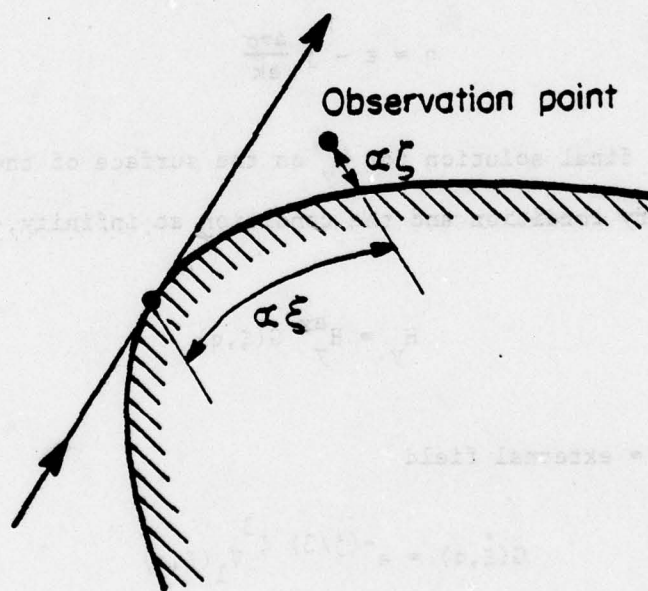
Figure 4: Coordinates of observation point in terms of ξ and ζ.

8

$q = -jm/\sqrt{n} = -(j/n)\ \sqrt[3]{\dfrac{k}{2a}}$ (= 0 for conducting body)

The other tangential component of the magnetic field H_x on the surface of the body can be obtained in a similar manner

$$H_x = H_z^{ex} \left[-\frac{1}{m}\ e^{-(j/3)\xi^3/3}\ f(\xi)\right] \qquad (13)$$

where $f(\xi)$ is another Fock function defined in   Appendix A. Fock's formulas not only give the surface value of the field, but also can be utilized to find the field in the proximity of the object. For a plane wave incidence, the first order, i.e., $O(1/m)$ terms for the scattered field within a certain layer around the object, can be written as

$$H_x = 0, \quad H_y = H_y^0\ e^{-jkx}\ \tilde{\psi}(\xi,\zeta), \quad H_z = H_z^0\ e^{-jkx}\ \tilde{\phi}(\xi,\eta)$$

$$(14)$$

$$E_x = (j/m)H_y^0\ e^{-jkx}\ \partial\tilde{\psi}/\partial\zeta, \quad E_y = H_z, \quad E_z = -H_y$$

where

$\zeta = 2am^2[z + (1/2)(ax^2 + 2bxy + cy^2)]$ = reduced height from the surface of the body (Fig. 4).

$$\tilde{\psi} = -je^{(j\xi\zeta - j/3\ \xi^3)} \int_c e^{-j\xi t}\left[w_1(t-\zeta) - \frac{w_1'(t)-qw_1(t)}{w_2'(t)-qw_2(t)}\ w_2(t-\zeta)\right]dt$$

$$(15)$$

$$\tilde{\phi} = \frac{-je^{j\xi\zeta - (j/3)\xi^3}}{2\sqrt{\pi}} \int_c e^{-j\xi t}\left[w_1(t-\zeta) - \frac{w_1(t)}{w_2(t)}\ w_2(t-\zeta)\right]dt$$

The path of integration for $\tilde{\phi}$ and $\tilde{\psi}$ is shown in Fig. 5 .

9

$Im(t)$

Complex t-plane

$Re(t)$

120°

(C)
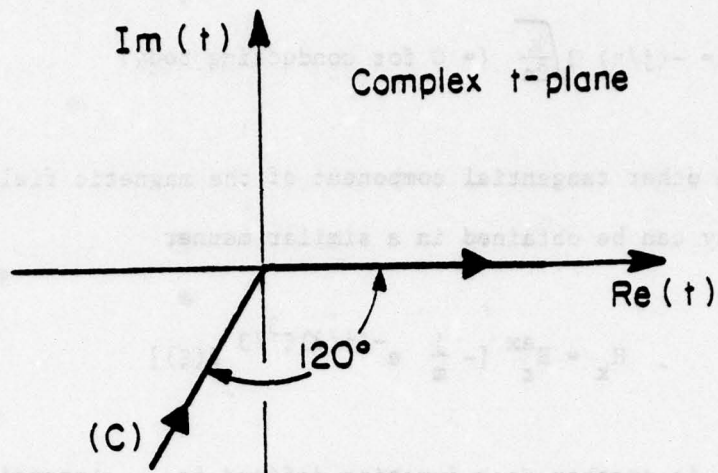
Figure 5: Path of integration for (15) in the complex t-plane.

Incident
Wave

ℓ

s

$\xi^{(Fock)} \propto \ell$

$\xi^{(Goodrich)} \propto s$

a
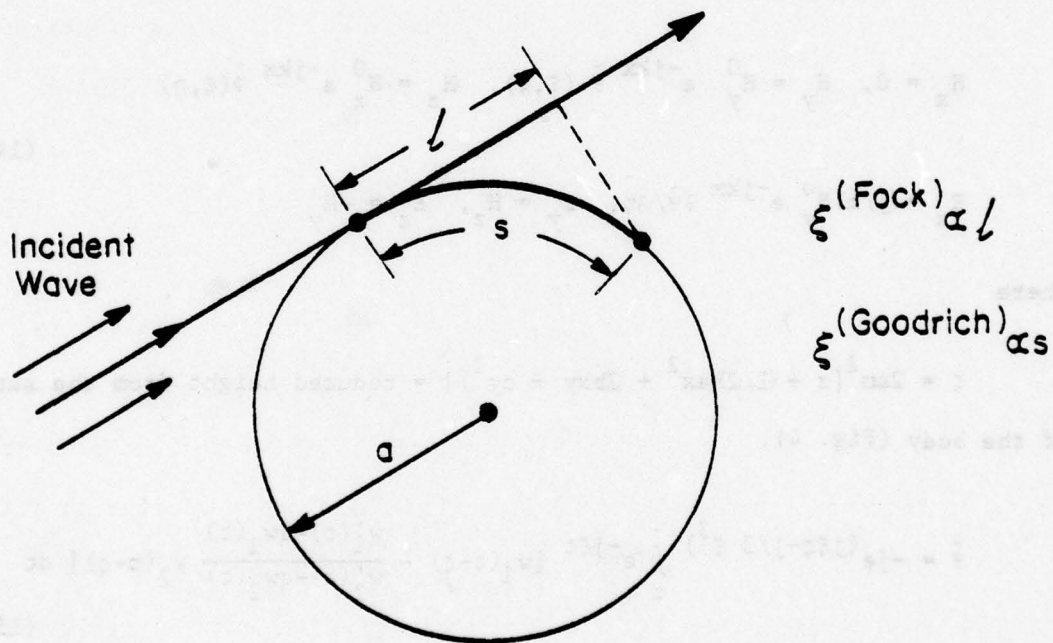
Figure 6: Comparison between the various definitions of parameter ξ for the case of a circular cylinder.

Fock's expressions for the field components in the penumbra region ($\xi \approx 0$) can be extended to the shadow region, by introducing some modifications in the definition of parameter ξ.   Goodrich [15] has generalized the argument used by Fock in the penumbra region to anywhere in the shadow region by introducing a new set of variables, ξ and ζ, for the incremental distances along the path leading into the shadow region. In this generalization, the parameter ξ as defined in (12) is replaced by

$$\xi = \int_0^s (\frac{kR(s)}{2})^{1/3} \frac{ds}{R(s)} \tag{16}$$

where s is the arc length along the geodesics which originate from the shadow boundary and go into the shadow region along the surface, and R(s) is the radius of curvature of the surface along the geodesics. For the case of a circular cylinder of radius a (Fig. 6), the expression ξ simplifies to

$$\xi = (ka/2)^{1/3} \theta = s/d \tag{17}$$

Fock also treated the case where the point source was very close to the surface of the body. He analyzed the radiation of electric dipoles near a spherical model of the earth [16] and derived the formulas for the scattered fields in terms of functions   (attenuation functions) similar to $\bar{\phi}$ and $\bar{\Psi}$, which are valid both in the shadow and transition regions [17]. Fock's assumptions were later proven in a more systematic and mathematically rigorous manner by Cullen [18] and Hong [19] by using a direct integral equation approach. This method is described in the next section.

11

2.3 Direct Integral Equation Approaches

This method, which is closely related to Fock's theory, can be
illustrated by analyzing the diffraction of a plane electromagnetic wave
by an arbitrary conducting body (large compared with λ). Cullen [18] obtained
a first-order asymptotic solution to the integral equation for the induced
surface current

$$\vec{J}(\vec{r}) = 2\vec{n}(\vec{r}) \times \vec{H}^{inc}(\vec{r}) - (1/2\pi)\vec{n}(\vec{r})$$

$$\times \int_S \int ds' \frac{1+jkR}{R^3} \{\vec{J}(\vec{r}') \times \vec{R}r^{-jkR}\}$$

(18)

where $\vec{n}(\vec{r})$ is the outward unit normal to the surface at $\vec{r}$, $\vec{H}^{inc}(\vec{r})$ is
the incident magnetic field on the surface (S) of the body, and $R = \vec{r} - \vec{r}'$
($\vec{r}'$ is a variable point on the surface).

Fock used this integral equation to deduce the important principle
of local character of the field in the penumbra region. Cullen derived a
first-order asymptotic solution to (18) which agreed with Fock's results
given in (12) and (13). Cullen's method consists of transferring the two-
dimensional integral equation (18), in the penumbra region, to a one-dimensional,
Volterra-type   equation. This is accomplished by applying the stationary
phase technique to the original integral while integrating with respect to
one of the variables. The resulting one-dimensional Volterra equation is then
solved in Cullen's method by the Fourier transform technique. A similar
procedure was used by Hong [19] to analyze, asymptotically, the diffraction
of electromagnetic and acoustic plane waves by smooth convex bodies. We will
now proceed to explain Hong's method in a little more detail by referring
back, once again, to the integral equation (18). The surface is parametrized by

12

the geodesic coordinate system (σ, v) such that the shadow boundary for the incident plane wave traveling along the tangent $\hat{\sigma}(0,v)$ to the $v = 0$ curve is the $\sigma = 0$ curve. The quantities $\hat{\sigma}(\sigma,v)$, $\hat{b}(\sigma,v)$ and $\hat{n}(\sigma,v)$ form a right-hand local orthonormal basis $(\hat{n} = \hat{\sigma} \times \hat{b})$ (Fig. 7).

Since the incident field has a phase factor $e^{-jk\hat{\sigma}(0,0)\cdot\vec{r}(\sigma,0)}$, we write the surface current in the form

$$\vec{J}(\vec{r}) = [I_\sigma(\vec{r}) \; \hat{\sigma}(\vec{r}) + I_b(\vec{r}) \; \hat{b}(\vec{r})] \; e^{-jk\sigma} \qquad (19)$$

where σ is the arc length along the geodesic. Substituting (19) back into (18) and restricting the resulting equation to the points on the geodesic $v=0$, we obtain two coupled, two-dimensional integral equations for $I_\sigma(\sigma,0)$ and $I_b(\sigma,0)$. It can be shown that these integrals have saddle points at $v=0$ (for the v-integration). Applying the "steepest descent path" method to v-integration, and keeping the terms up to the order $1/M_0^2$, where $M_0 = (k\rho_\sigma(\sigma,0))^{1/3}$, we obtain the following decoupled one-dimensional, Volterra-type integral equations for $I_b(\xi,0)$ and $I_\sigma(\xi,0)$

$$I_\sigma(\xi,0) = 2 \; I_\sigma^{inc}(\xi,0) - \int_{-\infty}^{\xi} d\tau \; I_\sigma(\xi,0) \; K_\sigma(\xi-\tau) + 0 \, (M_0^{-3})$$

$$\qquad (20)$$

$$I_b(\xi,0) = 2 \; I_b^{inc}(\xi,0) - \int_{-\infty}^{\xi} d\tau \; I_b(\xi,0) \; K_b(\xi-\tau) + 0(M_0^{-3})$$

$\rho_\sigma(\sigma,v)$ is the radius of curvature of the surface along geodesics (v = constant curves) at point (σ,v).

Solving (20) by Fourier transforms, we obtain the expression for the induced currents in the penumbra and shadow regions, and the first-order solutions

13

Figure 7: Geodetic coordinate system on a smooth convex body.

are found to be the same as those of Fock and GTD [20]. One of the important conclusions drawn from Hong's solution is that the leading term in the asymptotic expansion, which is the same for the acoustic and electromagnetic problems, is independent of curvature in the direction transverse to the geodesic, provided the divergence factor is suppressed. However, we should bear in mind that Hong's method was designed for the case of axial incidence on symmetric objects, and in this case, the geodesics are torsionless. The above conclusion does not seem to be valid in the cases where the rays have nonzero torsion ([21], [22]). In Hong's expressions for the surface current, the transverse curvature has only a second-order effect. It was also shown that up to the terms of order $(k\rho_\sigma)^{-2/3}$ in the asymptotic expansion, the tangential and binormal components of the creeping waves are not coupled.

Both Fock's theory and the "direct integral equation approach" give the induced surface current, or the scattered field in the neighborhood of the surface of the scatterer, due to an incident plane wave. These expressions can also be used to derive the radiated field via the use of the reciprocity theorem.

The methods which have been discussed thus far are mathematically rigorous. However, they are limited in the scope of their application to geometries satisfying some special smoothness and symmetry criteria. "Geometrical theory of diffraction" (GTD), which we discuss in the next section, has a broader scope, although it does lack the mathematical rigor of approaches described until now.

2.4 Geometrical Theory of Diffraction (GTD)

Geometrical theory of diffraction (GTD), developed by J. B. Keller ([20], [23], [24], [25], and [26]), is a generalization of geometrical optics.

It is based upon the assumption that fields propagate along rays. Keller's major contribution was to introduce the new kinds of rays called the "diffracted rays," which together with the geometrical optics rays, constitute the total field. In our problem, viz., source radiating in the proximity of the smooth object, the diffracted rays travel along the curves on the surface of the scatterer. By applying Fermat's principle to these surface rays, we conclude that the above-mentioned curves should be geodesics on the surface of the body. In the GTD procedure, one assigns a value to the field along each ray of these surfaces. The total field at any point in the space is the sum of the fields due to various rays (incident, reflected and diffracted) passing through that point. An important advantage of the GTD approach is that it can be applied to both scalar (acoustic) and vector (electromagnetic) problems and to smooth convex objects of an arbitrary shape.

Consider the problem of determining the radiated field of a scalar point source located on the surface of a smooth convex opaque body. If the observation point is in the shadow region, the ray paths originating at Q and reaching P (observation point) are comprised of two sections. One of these sections follows the straight line path P_1P, while the other travels along a geodesic on the surface (Fig. 8). Let us consider the propagation of the field along each section separately.

a) Rays in free space: Behavior of the fields along these rays can be determined by obtaining a high-frequency asymptotic solution to Maxwell's equation in a source-free homogeneous isotropic medium. We begin with the Luneberg-Kline asymptotic expansion of the electric field ([11] and [12]):

$$\vec{E}(\vec{r}) \sim k^{\tau} e^{-jk_o S(\vec{r})} \sum_{m=0}^{\infty} (jk)^{-m} \vec{e}_m(\vec{r}) \qquad (21)$$

16
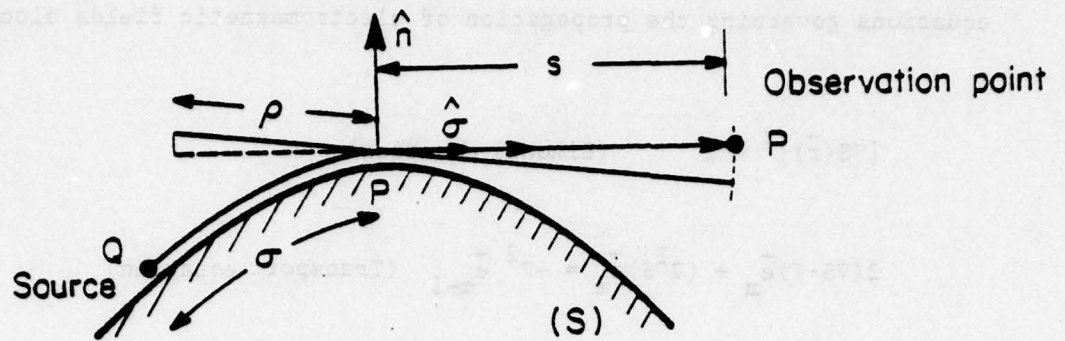
Figure 8: Diffraction by a smooth convex body when the observation point is in the shadow region of the source Q.
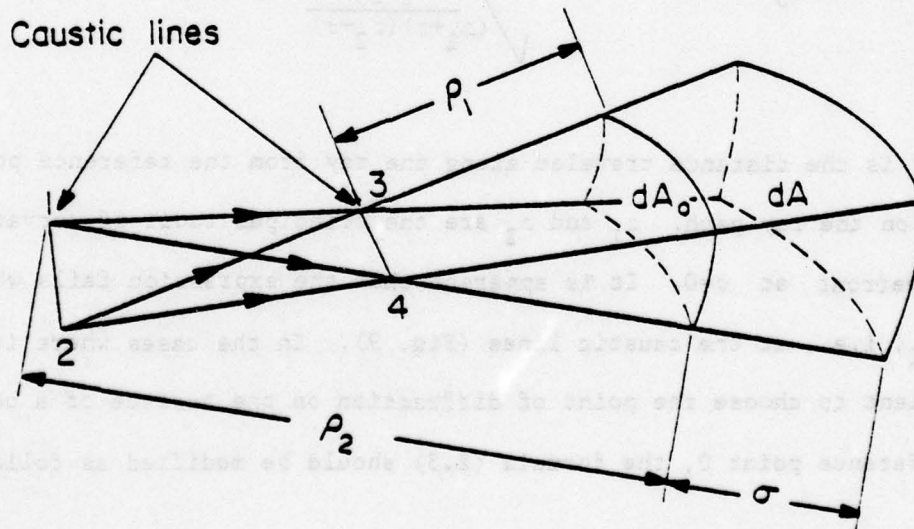
Figure 9: Diverging pencil of rays in free space.

and insert it into the Maxwell's equations. This results in the following
equations governing the propagation of electromagnetic fields along the rays.

$$[\nabla S(\vec{r})]^2 = 1 \qquad \text{(Eikonal equation)} \tag{22}$$

$$2(\nabla S \cdot \nabla)\vec{e}_m + (\nabla^2 S)\vec{e}_m = -\nabla^2 \vec{e}_{m-1} \qquad \text{(Transport equation)} \tag{23}$$

$$\nabla S \cdot \vec{e}_m = -\nabla \cdot \vec{e}_{m-1} \qquad \text{(Gauss's Law)} \tag{24}$$

$$e_{-1} = 0, \qquad m = 0, 1, 2, \ldots$$

The zeroth-order solution to the above system of equations, which turns out
to be in agreement with what one would obtain by geometric optics, may be
written as

$$E(\sigma) = E_0(0)e^{-jk_0 S(0)} \cdot \sqrt{\frac{\rho_1 \rho_2}{(\rho_1 + \sigma)(\rho_2 + \sigma)}} \; e^{-jk_0 \sigma} \tag{25}$$

where σ is the distance traveled along the ray from the reference point
$0(\sigma=0)$ on the ray path. ρ_1 and ρ_2 are the principal radii of curvature of
the wavefront at $\sigma=0$. It is apparent that the expression fails when $\sigma=-\rho_1$ or
$\sigma = -\rho_2$, i.e., at the caustic lines (Fig. 9). In the cases where it is
convenient to choose the point of diffraction on the surface of a body as
the reference point 0, the formula (2.5) should be modified as follows

$$E(\sigma) = \vec{\delta}_0 \cdot \sqrt{\frac{\rho}{\sigma(\rho + \sigma)}} \; e^{-jk\sigma} \tag{26}$$

18

In these cases, the point of diffraction itself is a caustic, and σ is the distance between this point and the second caustic.

b) Surface Rays: These rays follow the surface S along the geodesics into the shadow region, and shed off energy tangentially as they propagate. In order to study the behavior of the field along these rays, we introduce a special ray-fixed coordinate system, $\hat{\sigma}, \hat{n}, \hat{b}$.

$\hat{\sigma}$: Unit vector tangent to the ray; $\hat{n}$: outward unit normal to the surface; and $\hat{b} = \hat{t} \times \hat{n}$ or binormal direction; a vector field can be decomposed into its components along these unit vectors as

$$\vec{E} = E_\sigma \hat{\sigma} + E_n \hat{n} + E_b \hat{b} \tag{27}$$

At this point, several important assumptions are introduced in the GTD approach [20]:

i) $\vec{E}$ and $\vec{H}$ are orthogonal to each other and to the ray.

ii) Variation of the phase of the field along the ray is the same for both fields.

iii) E_n and E_b propagate independently, and $E_\sigma = 0$.

iv) E_b satisfies the scalar wave equation $(\nabla^2 + k^2)\,u = 0$ with the boundary condition $u = 0$ on the surface S, while E_n satisfies the same equation with the boundary condition $\dfrac{\partial u}{\partial n} = 0$.

The next step in the GTD approach is to conjecture, on the basis of the solution to some canonical problems, that the surface field propagating along each ray is comprised of an infinite set of "modes." Along a ray-fixed path GTD assigns a complex value to each component of the field associated with the individual modes. The propagation of these modal field is described by the equation

19

$$a(\sigma) = A(\sigma) \, e^{j(\phi_0 - k\sigma)} \tag{28}$$

when σ is the distance between an arbitrary point along the ray and the source Q and ϕ_0 is the phase of the field at the source point. Next, invoking the principle of conservation of energy between two adjacent rays, and using the fact that the surface rays shed energy off tangentially, we can arrive at the following expression for $a(\sigma)$

$$a(\sigma) = K \sqrt{\frac{d\Psi_1}{\rho d\Psi_2}} \; \exp[-jk\sigma - \int_0^\sigma \alpha \, (\sigma') d\sigma'] \tag{29}$$

where $\alpha(\sigma)$ is the "attenuation constant," K is proportional to the strength of the source, and $d\Psi_1$, $d\Psi_2$ and ρ are shown in Figure 10. The quantity $[d\Psi_1/(\rho d\Psi_2)]^{1/2}$ indicates the spreading of the surface ray tube" as it travels along the surface. Equations (26) and (29) describe the laws of propagation for the rays which originate from the source point Q, are diffracted at P_1, and reach the observation point P. To complete the solution, we need to determine the actual values of the fields from these equations. These require the knowledge of δ_0 and K, which, in turn, are related to the initial values of the rays QP_1 and P_1P as well as the attenuation constant $\alpha(\sigma)$. The initial value of the field at Q is related to the strength of the source by L(Q), the so-called "launching coefficient," while the initial value of the field at P_1 is related to the actual field on the surface at P_1 through the "diffraction coefficient" $D(P_1)$. If we now sum up the contributions of all the modes, we obtain the final solution [25] for the field radiated in the shadow region by an infinitesimal magnetic dipole of strength $\vec{M}$ located on a smooth convex conducting body

20
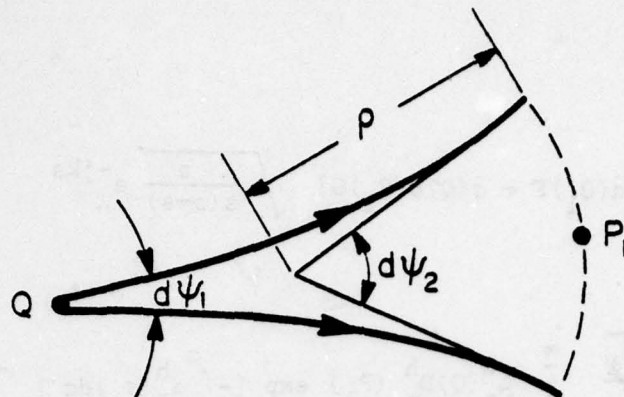
Figure 10: Divergence of surface rays.
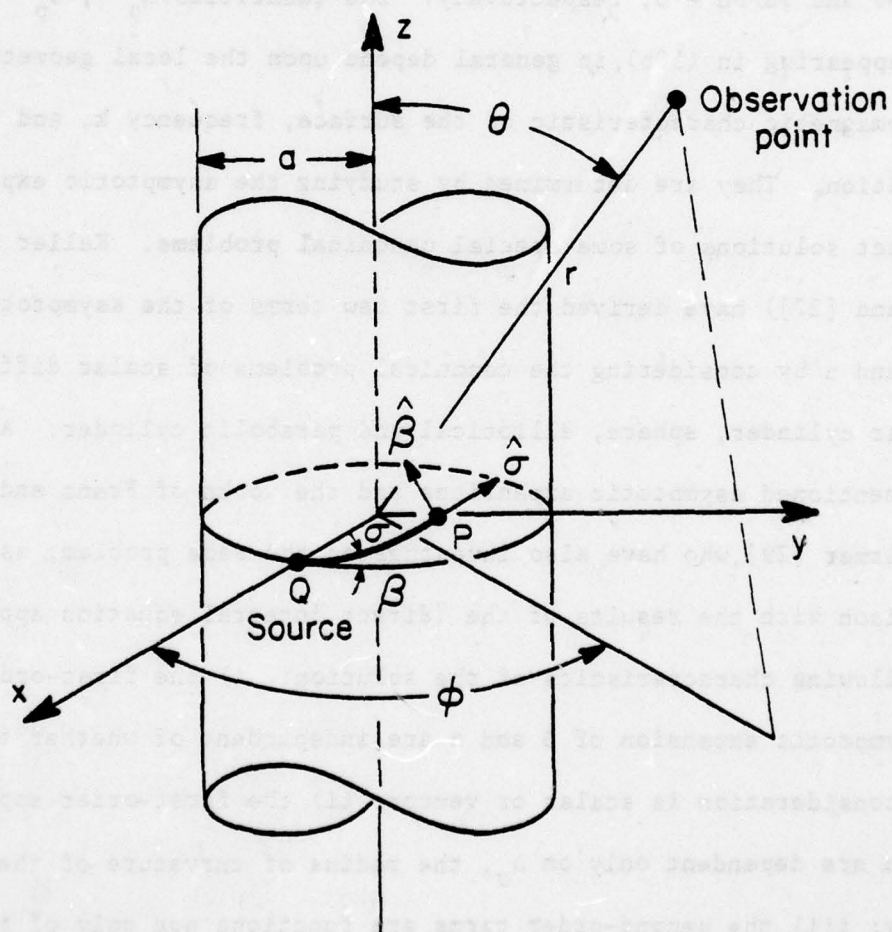
Figure 11: Geometry of the cylinder problem.

21

$$\vec{E}^d(P) = \vec{M} \cdot [\hat{\delta}(Q)\hat{n}(Q_1)F + \hat{\sigma}(Q)\hat{\sigma}(P_1)G] \sqrt{\frac{\rho}{s(\rho+s)}} \; e^{-jks} \qquad (30a)$$

where

$$F = \frac{-jke}{4\pi}^{-jk\sigma} \sqrt{\frac{d\Psi_1}{\partial\Psi_2}} \; \sum_{p=1}^{\infty} L_p^h(Q)D_p^h(P_1) \; \exp\left[-\int_0^\sigma \alpha_p^h(\sigma')d\sigma'\right] \qquad (30b)$$

and the expression for G is obtained by replacing the superscript "h" by "s" in (30b), where h and s stand for hard and soft boundary conditions, viz., u=0 and $\partial u/\partial n = 0$, respectively. The quantities $L_p^{h,s}$, $D_p^{h,s}$ and $\alpha_p^{h,s}$, appearing in (30b), in general depend upon the local geometry and the electromagnetic characteristic of the surface, frequency k, and the mode of propagation. They are determined by studying the asymptotic expansions of the exact solutions of some special canonical problems. Keller and Levy ([20] and [27]) have derived the first few terms of the asymptotic expansions for D and α by considering the canonical problems of scalar diffraction by a circular cylinder, sphere, elliptical and parabolic cylinder. A study of the above-mentioned asymptotic expansions and the works of Franz and Klante [28] and Voltmer [29], who have also investigated the same problem, as well as a comparison with the results of the "direct integral equation approach," reveals the following characteristics of the solution: i) the first-order terms in the asymptotic expansion of D and α are independent of whether the problem under consideration is scalar or vector; ii) the first-order approximation of D and α are dependent only on ρ_σ, the radius of curvature of the surface along the ray; iii) the second-order terms are functions not only of ρ_σ, but also of $\frac{d\rho_\sigma}{d\sigma}$, $\frac{d^2\rho_\sigma}{d\sigma^2}$, and $\rho_{\sigma n}$ (the radius of the curvature of the surface transverse to the ray). Finally, the higher-order terms are different for scalar and vector problems.

22

The leading terms in the asymptotic expansion of "diffraction coefficient" D, "attentuation constant" α and "launching coefficient" L are presented below:

"Soft" polarization:

$$[D_p^s]^2 = \frac{\pi^{1/2} \cdot 2^{-5/6} \cdot \rho_\sigma^{1/3} \cdot e^{-j\pi/12}}{k^{1/6} \cdot [Ai'(-r_p)]^2} \tag{31}$$

$$\alpha_p^s = \frac{r_p \cdot e^{j\pi/6}}{\rho_\sigma} \left(\frac{k\rho_\sigma}{2}\right)^{1/3} \tag{32}$$

$$L_p^s = e^{-j\pi/12} (2\pi k)^{1/2} \left(\frac{2}{k\rho_\sigma}\right)^{2/3} \cdot Ai'(-r_p) \cdot D_p^s \tag{33}$$

"Hard" polarization:

$$[D_p^h]^2 = \frac{\pi^{1/2} \cdot 2^{-5/6} \cdot \rho_\sigma^{1/3} \cdot e^{-j\pi/12}}{k^{1/6} \cdot r_p' \cdot [Ai(-r'_p)]^2} \tag{34}$$

$$\alpha_p^h = \frac{r_p' \cdot e^{j\pi/6}}{\rho_\sigma} \left(\frac{k\rho_\sigma}{2}\right)^{1/3} \tag{35}$$

$$L_p^h = e^{j\pi/12} \cdot (2\pi k)^{1/2} \left(\frac{2}{k\rho_\sigma}\right)^{1/3} \cdot Ai(-r'_p) \cdot D_p^h \tag{36}$$

where Ai(x) is the Airy function:

$$Ai(x) = \frac{1}{\pi} \int_0^\infty \cos\left(\frac{t^3}{3} + xt\right) dt \quad (x \text{ real}) \tag{37}$$

23

and $Ai(-r_p) = 0$, $Ai'(-r_p') = 0$, (Ai' is the derivative of Ai with respect to its argument). Higher-order terms in the expansion of D, α and L have been given in [25] and [30] and in some of the other works on GTD mentioned earlier.

The expression (30) is convenient to use in the lit region. In the shadow part of the transition region, since the exponential decay of the terms in (30) is weak. The convergence of the series representation is very slow. Furthermore, the series diverges in the lit part of the transition region. Consequently, in these regions, it is more reasonable to use an integral representation for the surface ray field, which, in our case, can be expressed in terms of Fock functions [25].

Attempts have been made to establish the mathematical validity of GTD and to minimize its "nondeductive parts" (parts which are based upon physical intuition or the study of the asymptotic solution of some simple problem geometrical concepts of different kinds of rays, diffraction coefficients, attenuation constants, etc.). Kravtsov [31] and Ludwig [32] have analyzed the field near the caustic surface (smooth envelope of a family of ray), and have developed a "uniform asymptotic solution" in the sense that it is finite at the caustic and reduces to geometrical optics away from the caustic.

3. Generalization of GTD and Investigation of Alternate Methods

3.1 Generalization of GTD to Arbitrary Surfaces

Keller's generalization of GTD for the analysis of the field diffracted from a smooth convex object is closely related to what is known as the "boundary layer technique" in the theory of differential equations [43]. On the other hand, the "uniform asymptotic theory" is analogous to the method used by R. E. Langer and F. J. Oliver to find the asymptotic solutions of the

24

second-order differential equations near their "turning points," which are counterparts of the transition regions in our case [33], [34], and [35].

The procedure is based upon the generalization of the geometric optical interpretation of the circular cylinder problem. The solution obtained by this method involves some functions with unknown phase and amplitude, similar to Bessel and Hankel functions. Since the surface of a smooth object is actually the caustic surface of diffracted rays, the above-mentioned formulation is applicable in this case, too. Lewis, et al. [36] have modified this solution to make it satisfy the boundary condition on a convex body. Using ray formalism, they have obtained an asymptotic solution in a complicated form, which they call "creeping wave" and satisfies the boundary condition on and is uniformly valid near and away from the surface. It should be mentioned that the method has been developed primarily for scalar diffraction problems.

Creeping waves that are traveling on the surface of the body generate other kinds of diffracted rays in the presence of the irregularities in the geometric or electromagnetic characteristics of the surface. The effects of discontinuity in the surface curvature, its higher-order derivatives, or the surface impedance have been studied by many authors [37], [38], [39] or [40]. An exhaustive study of various diffraction mechanisms and corresponding diffraction coefficients, and constants associated with the propagation of creeping waves, has been carried out by Albertsen [41].

At this point, let us examine one of the most important features of GTD and its various modifications. GTD formulation is essentially scalar in nature and is heuristic in some parts. Thus, when GTD is applied to a vector problem, it is not surprising that the coupling between various components of the fields

25

are neglected, and each one of them is treated as an uncoupled scalar wave. The other assumptions in GTD are concerned with the directions of these field components and the kind of boundary conditions they satisfy (see Sec. 2.4). As mentioned earlier, non-deductive parts of GTD are based on asymptotic expansions of known solutions to some selected "canonical" problems. Quite often these canonical problems are not general enough to fully and accurately describe the local behavior of the field for an arbitrary structure. Finally, most of the canonical problems investigated are two-dimensional in nature. The only exception to this is the sphere. However, in so far as the geometric properties of the surface are concerned, the sphere is a very special case since its radius of curvature is the same in all directions and, consequently, the surface rays are torsionless. Finally, GTD fails when the observation point is located in the transition regions, shadow boundaries or in the neighborhood of a caustic. In each of these regions, one needs to carefully modify the GTD formulas and often such a modification is not too simple. Nevertheless, in spite of these difficulties, GTD is recognized to be a powerful high-frequency technique for computing the leading terms of the asymptotic solution. Two of the principal attributes of GTD are its simplicity and wide scope of application.

3.2 Spectral Domain Approach

We now examine an approach different from GTD which uses the spectrum of the induced current, or the expression for the radiated field, as a starting point. In order to gain a better insight into the curved-surface radiation and scattering problem and to verify the basic assumption of GTD, it is worthwhile to consider such alternative approaches, particularly if they apply to canonical problems which are more general in nature than those employed to derive the GTD results. An example of such a study would be to consider the

26

case of surface ray propagation with non-zero torsion, a situation that occurs when a magnetic dipole source radiates from a location on the surface of a circular cylinder.

The geometry of the problem is shown in Fig. 11 (p. 21). The radius of the cylinder is a and the source, which is an infinitesimal magnetic dipole with density $\vec{M}$, is located at the point Q described by the spherical polar coordinates $(r=a, \theta=90°, \phi=0°)$. Each point P on the surface of the cylinder is defined by a "geodetical polar coordinate" system (σ, β), where σ is the arclength of the geodesic connecting Q to P and β is the angle between $\hat{\phi}$ (at point Q) and geodesic QP. The local orthonormal basis vectors $(\hat{\sigma}, \hat{\beta})$ are also associated with these two parameters. The observation point in the far field is specified by its spherical polar coordinates (r, θ, ϕ). The radiated field at an arbitrary point can be expressed in terms of two potentials, Φ and Ψ, which, in cylindrical coordinates, can be written as:

$$\Phi = \frac{1}{2\pi} \sum_{n=-\infty}^{\infty} e^{-jn\phi} \int_{-\infty}^{\infty} f_n(k_z) \cdot H_n^{(2)}(k_t\rho) \, e^{-jk_z z} \, dk_z \qquad (37)$$

$$\Psi = \frac{1}{2\pi} \sum_{n=-\infty}^{\infty} e^{-jn\phi} \int_{-\infty}^{\infty} g_n(k_z) \cdot H_n^{(2)}(k_t\rho) \cdot e^{-jk_z z} \, dk_z \qquad (38)$$

For the problem under consideration, we can express the spectral weight coefficients as

$$f_n(k_z) = \frac{j\omega\epsilon M_\phi}{2\pi k_t^2 H_n^{(2)}(k_t a)} \qquad (39)$$

$$g_n(k_z) = \frac{1}{k_t H_n^{(2)'}(k_t a)} \left[\frac{-M_z}{2\pi} + \frac{nk_z M_\phi}{2\pi k_t^2 a} \right] \qquad (40)$$

27

where

$$k_t = \begin{cases} \sqrt{k^2 - k_z^2} & , \quad k > k_z \\ -j\sqrt{k_z^2 - k^2} & , \quad k < k_z \end{cases} \tag{41}$$

In order to derive an asymptotic expansion of (37) and (38), we proceed as follows. As a first step, we apply Watson's transformation to the infinite summation with respect to n and employ appropriate asymptotic formulas for Hankel functions with large order and argument to derive the following expressions for (37) and (38) under the conditions that ka is large and ϕ small compared to π:

$$\phi \sim \frac{\omega \varepsilon M_\phi}{(2\pi)^2} \sqrt{\frac{2\pi}{\rho}} \, e^{j\pi/4} \int_{-\infty}^{\infty} dk_z \, e^{-j\Omega} \cdot \frac{m^2}{k^{5/2}} \cdot f_0(\xi_1) \tag{42}$$

$$\psi \sim \frac{jM_\phi}{(2\pi)^2} \sqrt{\frac{2\pi}{\rho}} \cdot \frac{e^{j\pi/4}}{2} \cdot \int_{-\infty}^{\infty} dk_z \cdot e^{-j\Omega} \cdot \frac{k_z}{k_t^{5/2}} [jm \, g_1(\xi_1) + 2m^3 g_0(\xi_1)]$$

$$-j \frac{M_z}{(2\pi)^2} \cdot a \sqrt{\frac{2\pi}{\rho}} \cdot \frac{e^{j\pi/4}}{2} \cdot \int_{-\infty}^{\infty} dk_z \cdot \frac{e^{-j\Omega}}{k_t^{1/2}} \cdot g_0(\xi_1) \tag{43}$$

where

$$\Omega = k_z z + k_t [\rho + a(\phi - \pi/2)]$$

$$m = (k_t a/2)^{1/3}$$

$$\xi_1 = m(\phi - \pi/2)$$

f_0, g_0, g_1 = Fock's functions defined in Appendix A.

M_ϕ and M_z = components of $\vec{M}$, $(\vec{M} \cdot \hat{n} = 0)$

Next, applying the "saddle-point" technique to (42) and (43) and keeping only the first-order terms, the far field can be written in terms of its components along the normal and tangent to the surface at the "stationary point" P_1 as

$$E_{n_2} = (\vec{M} \cdot \hat{\beta}_1) \left(\frac{jke^{-jk\sigma}}{4\pi} \right) \cdot g_0(\xi_{1s}) \cdot \frac{e^{-jkR}}{R}$$

$$+ \frac{(\vec{M} \cdot \hat{\phi}_1)(\hat{\phi}_1 \cdot \hat{\beta}_1)}{4\pi} \cdot e^{-jk\sigma} \cdot \left(\frac{k\sigma}{2} \right)^{1/3} \cdot g_1(\xi_{1s}) \cdot \frac{e^{-jkR}}{R} \qquad (44)$$

$$E_{3_2} = - \frac{(\vec{M} \cdot \hat{\phi}_1)(\hat{\phi}_1 \cdot \hat{\sigma}_1)}{2\pi} \cdot \left(\frac{k\sigma}{2} \right)^{2/3} \cdot e^{-jk\sigma} \cdot f_0(\xi_{1s}) \cdot \frac{e^{-jkR}}{R} \qquad (45)$$

29

where

P_1: is the stationary point of Ω which turns out to be the
same as the point of diffraction predicted by GTD.

$$\xi_{1s} = (\frac{ka}{2})^{1/3} (\phi - \pi/2) \cdot \sin^{1/3} \theta$$

ρ_g = radius of curvature of geodesic QP_1

σ = arc length QP_1

R = the distance between the point of diffraction P_1 and
the observation point

$n_2 = \hat{\sigma}_2 \times \hat{\beta}_2$; normal to the surface at P_1

The details of the derivations of (44) and (45) are given in Appendix B.

Fig. 12 illustrates the geometric meaning of some of the parameters
appearing in (44) and (45), for the observation point is located in the shadow
region. In this case, ξ_{1s}, which is identical to ξ given in (16), is the
reduced distance traveled by the surface ray before leaving the surface
tangentially.

In the lit region, the geometric interpretations of σ and ξ are shown
in Fig. 13. The rays, like QP_1P, that do not obey the generalized Fermat's
principle are called "psuedo-rays" [25]. The ray QP_1P appears to travel along
the surface up to the point P_1 and then leaves the surface at P_1 tangentially
in the opposite direction, to reach the observation point P. It should be
noted that formulas (44) and (45) give us the contribution of the ray which

30
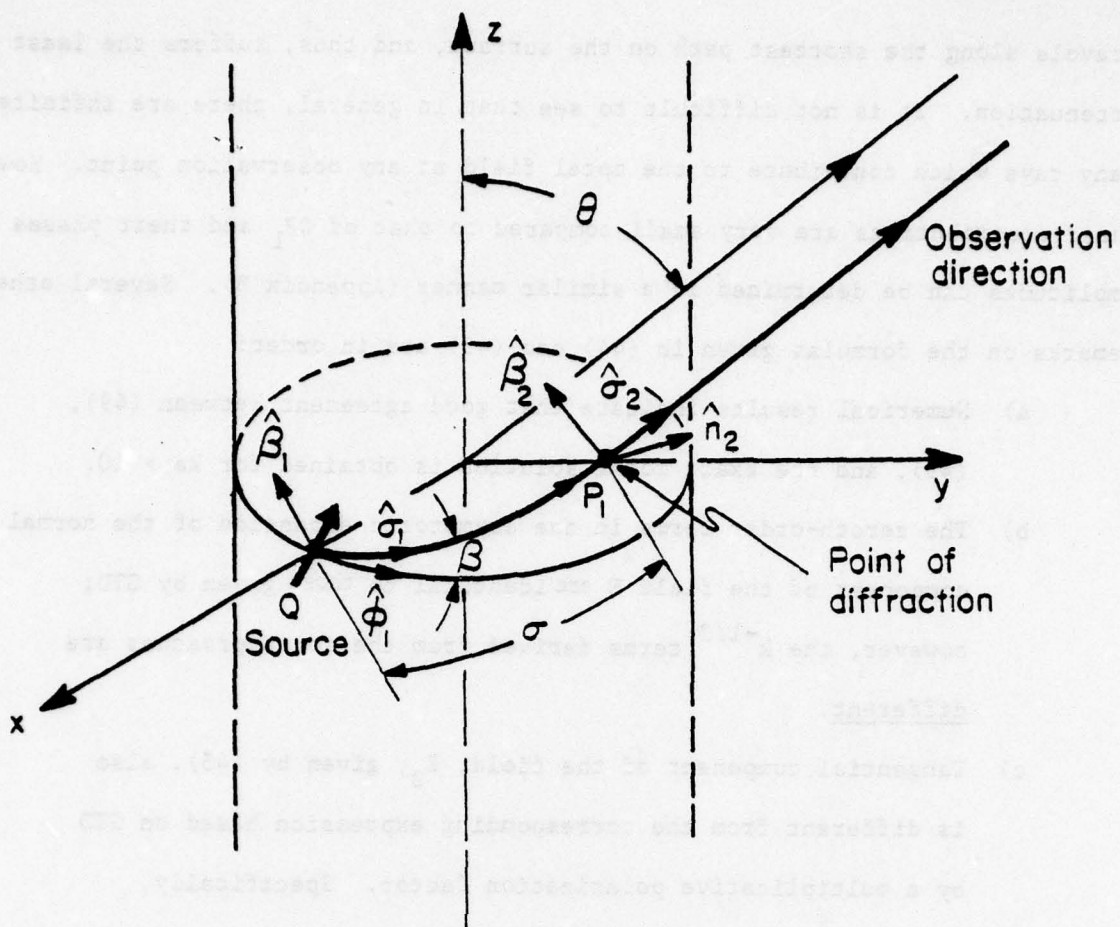
Figure 12: Diffraction of rays by a cylindrical body.
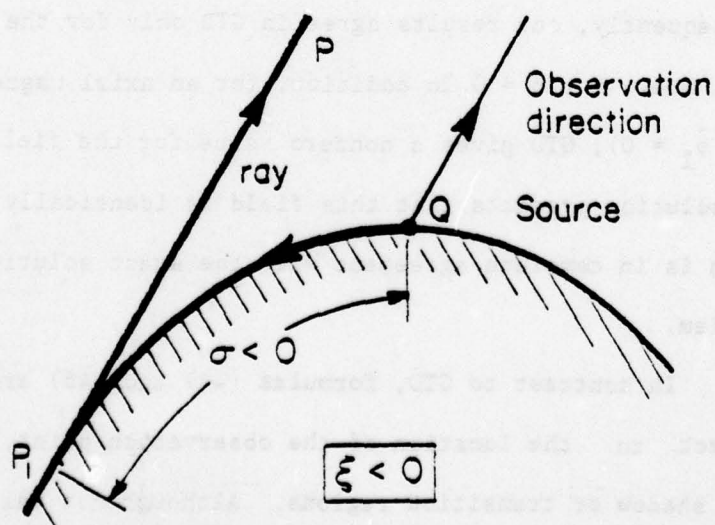
Figure 13: Diffraction of "psuedo-rays."

31

travels along the shortest path on the surface, and thus, suffers the least attenuation. It is not difficult to see that, in general, there are infinitely many rays which contribute to the total field at any observation point. However, their contributions are very small compared to that of QP_1 and their phases and amplitudes can be determined in a similar manner (Appendix B). Several other remarks on the formulas given in (44) and (45) are in order:

a) Numerical results indicate that good agreement between (49), (45), and the exact modal solution is obtained for ka > 10.

b) The zeroth-order terms in the asymptotic expansion of the normal component of the field E are identical to those given by GTD; however, the $k^{-1/3}$ terms derived from the two approaches are different.

c) Tangential component of the field, E_β, given by (45), also is different from the corresponding expression based on GTD by a multiplicative polarization factor. Specifically,

$$(45) = [\frac{(\vec{M}\cdot\hat{\phi}_1)}{(\cos\beta)\cdot(\vec{M}\cdot\hat{\sigma}_1)}] \ (GTD) \qquad\qquad (46)$$

Consequently, our results agree in GTD only for the circumferential ray, i.e., for $\beta = 0$. In addition, for an axial magnetic dipole $(\vec{M}\cdot\hat{\phi}_1 = 0)$, GTD gives a nonzero value for the field in the $\hat{\beta}_2$ direction our solution predicts that this field is identically zero, a result which is in complete agreement with the exact solution for the problem.

In contrast to GTD, formulas (44) and (45) are valid in respect to the location of the observation point, be it in the lit, shadow or transition regions. Although not valid in the paraxial region ($\beta \approx 90°$), they can be generalized to work along this direction.

32

Finally, let us consider the possibility of the generalization of
(44) and (45) to other convex surfaces of more general nature.
By "more general surfaces," we mean those surfaces which are not substantially
different from cylinders, some examples being cylinders with noncircular
(elliptical, hyperbolic and parabolic) cross sections and conical
surfaces with small apex angles. The key step in a systematic approach to
generalizing (44) and (45) is to use the generalized definition of ξ given
in (16).

Fig. 14 exhibits some initial results of the generalization of these
formulas to the case of a cone. It is evident that results obtained from
the present approach agree quite well with the series solution which is rather
tedious and time-consuming. We also observe from Fig. 14c that there is a
noticeable discrepancy between the analytical solution and the experiment. Thus,
within   the range of experimental error, our results agree quite well with
those published in the literature.

3.3 Approach Based on an Asymptotic Evaluation of the Radiation Integral
     of the Surface Current

As a final topic, we consider an approach based on the asymptotic
evaluation of the radiation integral expressed in terms of the induced surface
current which is itself derived in an asymptotic manner for surfaces with
large radius of curvature.

It was shown in Sec. 2 that Fock's theory can provide us with an
expression for the scattered field in the neighborhood of a smooth convex
body illuminated by a plane wave. Using this solution in conjunction with
the reciprocity principle, we can find the far field radiated by a point source
located on the surface of the body. By generalizing the definition of ξ in

33
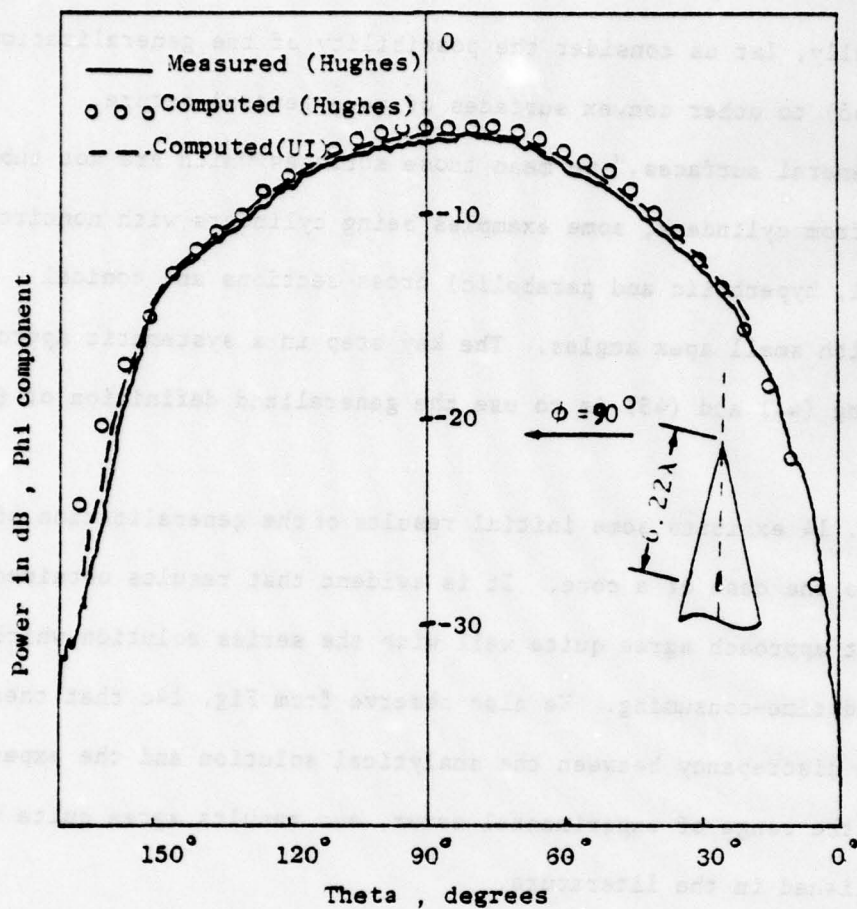
(a) $\phi = 90°$ cut;

Figure 14: Comparison between spectral domain results (UI),
modal approach (Hughes), and experimental measure-
ments (Hughes). The UI results are derived from a
generalized version of (44) and (45) for a cone.
The Hughes' results have been reproduced from [63]
and are based on a modal series of 13 terms. All
results are for $\lambda/2$ radial slot on a cone of
half-angle 10°.

END
DATE
FILMED

5 -- 79
DDC

(b) φ = 220° cut

35

Measured (Hughes)

O O O O Computed (Hughes)

$\phi = 40°$

Power in dB , Phi component

6.22λ

--10

--20

--30

150°   120°   90°   60°   30°   0°

Theta , degrees
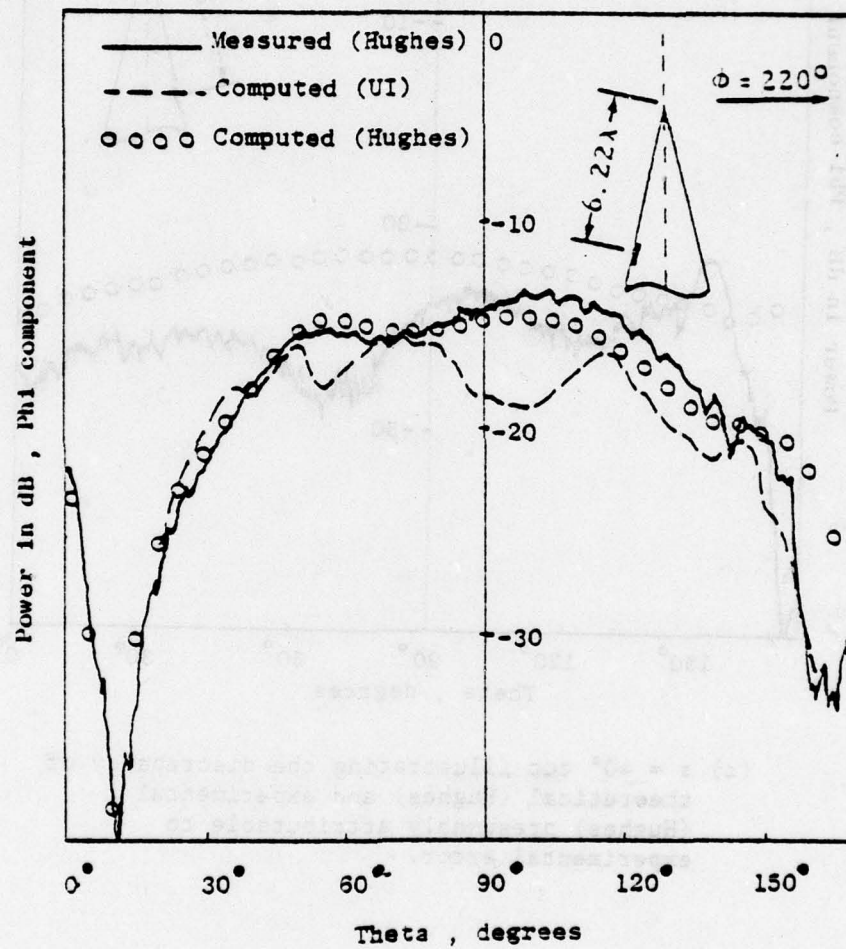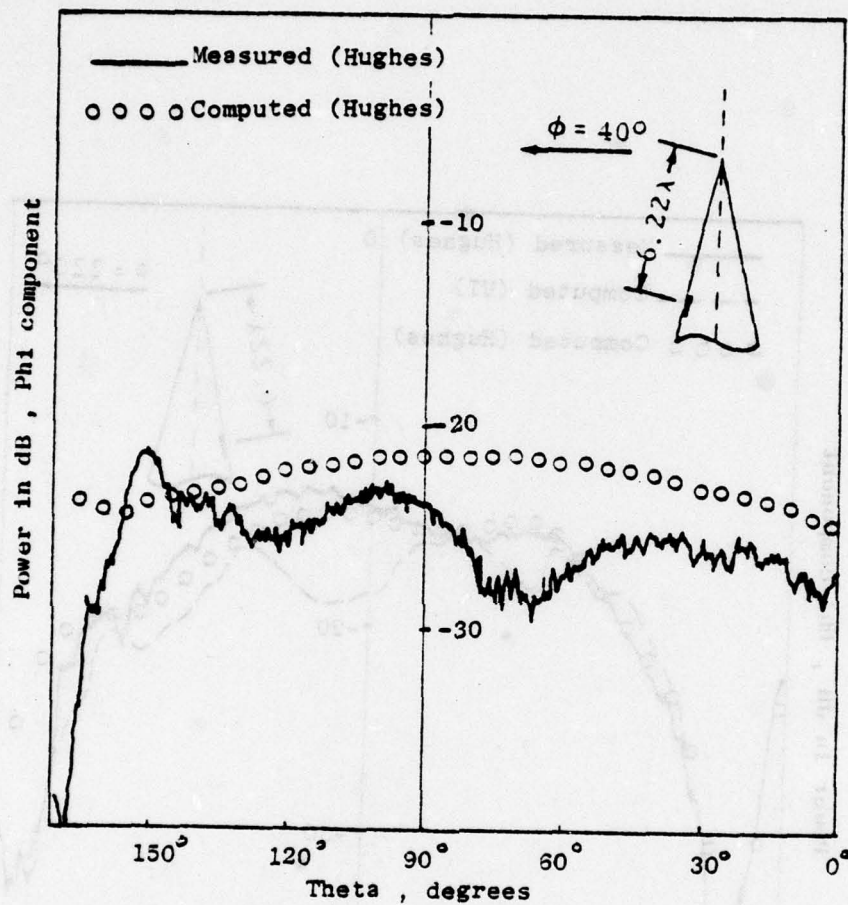
(c) $\phi = 40°$ cut illustrating the discrepancy of
theoretical (Hughes) and experimental
(Hughes) presumably attributable to
experimental error.

Fock's theory, we can also write the final result in a GTD format and represent it as a surface ray. The total field at a point on the surface is obtained by adding all the possible rays which reach the observation point P. Various techniques can be used to determine the field propagation along these rays. For instance, when the source is located on the surface, and the surface is a conical one, the field at each point can be decomposed into two parts.

$$F = F_1 + F_2 \tag{47}$$

where F_1 is the geometrical optics field when the observation point is directly illuminated by the source, and is the creeping-wave contribution derivable via an extension of Fock's theory when the point is in the shadow region. The other term, F_2, is the so-called tip contribution, and can be obtained by physical optics or GTD. Goodrich et al. [42] have applied this procedure to find the radiation pattern of slot arrays on cones.

The approximate induced surface current distribution can be obtained by Fock's theory, GTD [13], [14], [16] and [25] or some other appropriate high frequency technique. The induced surface current due to a magnetic dipole on a perfectly conducting circular cylinder and cone has been calculated by Chang et al. [44], and Chan et. al [45] whose procedure is based upon an asymptotic expansion of the exact modal solution to the above-mentioned problems. Lee, et al. [46] and [22] have treated the same problem by a method based on Fock's asymptotic solution of the problem of a sphere [47]. These expressions for the current distribution can be used in the radiation integral representation of the far field.

The numerical evaluation of this integral is a formidable task, especially when the frequency is very high. Thus, it is highly desirable to have an analytical and explicit formula for the far field expressed in terms of the

surface current. We now discuss an approach for accomplishing this task and examine the problem of deriving an asymptotic expansion of the far field radiated due to a point source located on the surface of a smooth, conducting, and convex body of an arbitrary shape.

Consider an arbitrary smooth convex surface S shown in Fig. 15. Let a magnetic dipole source be located at a point Q on S. We parametrize the surface S introducing a "geodetical polar coordinate" system with the pole located at Q such that an arbitrary point P_1 on the surface is defined by a pair of numbers (σ, β), where is the arc length of the geodesic QP_1 and is the angle between QP_1 and some reference direction at Q. Unit vectors along the constant parameter curves $\hat{\sigma}$ and $\hat{\beta}$ are locally orthogonal. The unit normal to the surface, $\hat{n}$, is given by $\hat{n} = \hat{\sigma} \times \hat{\beta}$. An element of length in this coordinate system may be written as

$$ds^2 = d\sigma^2 + G \, d\beta^2$$

(48)

The radiation integral for the scattered far field can be written

$$\vec{E} = \frac{-j\omega\mu}{4\pi} \int\int_S \vec{J}(1-\hat{R}\hat{R}) \cdot \frac{\exp(-jkR)}{R} \, dS$$

(49)

where R is the distance between any point on the surface and the observation point. In the geodetical polar coordinate system, we can rewrite a scalar component of (49), say M, in terms of a double integral of the following general form

$$M = \int\int_D F(\sigma, \beta, P) \frac{\exp[-jk(R+\sigma)]}{R} \sqrt{G} \, d\sigma \, d\beta$$

(50)

38
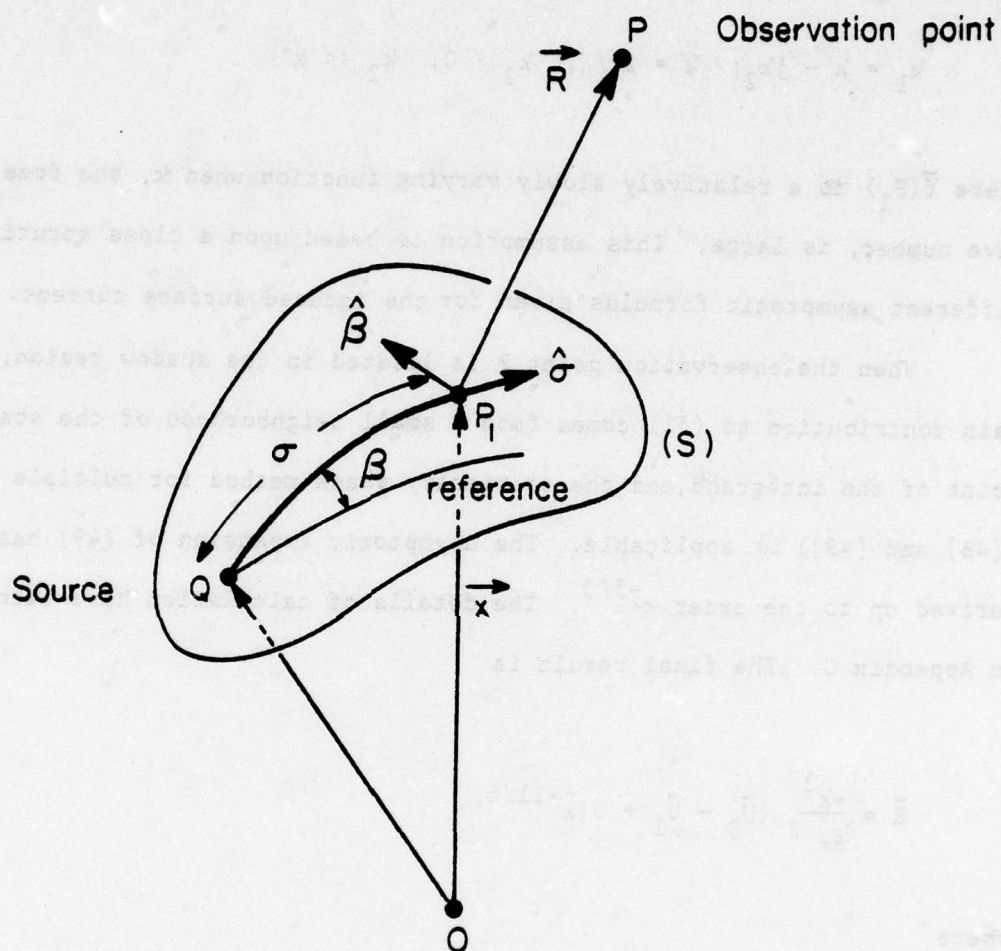
Figure 15: Source radiation in the presence of a smooth convex surface, parametrized by geodetical polar coordinate system.

where we have assumed the following form for the surface current:

$$\vec{J}(P_1) = \vec{f}(P_1) \exp(-jk_1\sigma) = J_\sigma\hat{\sigma} + J_\beta\hat{\beta}$$

(51)

$$k_1 = k - jk_2; \quad k = 2\pi/\lambda, \quad k_2 > 0, \quad k_2 << k$$

where $\vec{f}(P_1)$ is a relatively slowly varying function when k, the free-space wave number, is large. This assumption is based upon a close scrutiny of different asymptotic formulas given for the induced surface current.

When the observation point P is located in the shadow region, the main contribution to (51) comes from a small neighborhood of the stationary point of the integrand, and the stationary phase method for multiple integrals ([48] and [49]) is applicable. The asymptotic expansion of (49) has been derived up to the order $k^{-5/3}$. The details of calculation have been presented in Appendix C. The final result is

$$\vec{E} = \frac{-k^2}{8\pi}2 \left(\vec{U}_0 + \vec{U}_1 + O(k^{-11/6})\right)$$

(52)

where

$$U_0 = \hat{\beta} J_\beta \cdot \frac{D_0}{k^{5/6}}\sqrt{\frac{\rho_g}{R(R+\rho_g)}} \cdot e^{-jkR}$$

(53)

$$U_1 = [(AJ_\beta + \frac{\partial}{\partial\sigma}(J_\beta e^{jk\sigma})e^{-jk\sigma})\hat{\beta} + (BJ_\beta + CJ_\sigma)\hat{n}]$$

(54)

$$\cdot \frac{D_1}{k^{7/6}} \sqrt{\frac{\rho_g}{(R+\rho_g)R}} \cdot e^{-jkR}$$

40

$$D_0 = e^{-j\pi/4} \cdot 6^{5/6} \cdot \Gamma(1/2) \cdot \Gamma(1/3) \cdot \rho_\sigma^{2/3} \tag{55}$$

$$D_1 = \frac{-je^{-j\pi/4}}{3} \cdot 6^{7/6} \cdot \Gamma(2/3) \cdot \Gamma(1/2) \cdot \rho_\sigma^{4/3} \tag{56}$$

A, B, and C are dependent upon geometric properties of the surface at the stationary point which turns out to be exactly the same as the "point of diffraction" of surface rays. The quantities A, B, and C are given by

$$A = \frac{1}{2G} \frac{\partial}{\partial\sigma}G - \frac{\rho_\sigma}{2} \cdot \frac{\partial}{\partial\sigma}\left(\frac{1}{\rho_\sigma}\right) + \frac{\rho_g}{2G}\left[\frac{L^{\beta\beta}}{\rho_\sigma}\right.$$
$$\left. + (L^{\beta\sigma})^2 - (1/2)\frac{\partial^2 G}{\partial\sigma^2}\right] + 0\left(\frac{1}{R}\right) \tag{57}$$

$$B = L^{\beta\sigma}/G^{1/2}, \quad C = -1/\rho_\sigma \tag{58}$$

where

ρ_σ = radius of curvature of the geodesic

ρ_g = geodetic radius of curvature

$L^{\beta\beta}$, $L^{\beta\sigma}$ = coefficients of the second fundamental form of the surface (S)

A geometric interpretation of these parameters has been illustrated in Fig. 16. It is evident from this figure that $\left[\frac{\rho_g}{R(R+\rho_g)}\right]^{1/2}$ is simply the divergence factor of the rays leaving the surface tangentially at the point of diffraction. In using formula (56), we should bear in mind that the various terms in U_0 and U_1 are not of the same order. For example, in the deep shadow, J_σ is exponentially larger than J_3.

41
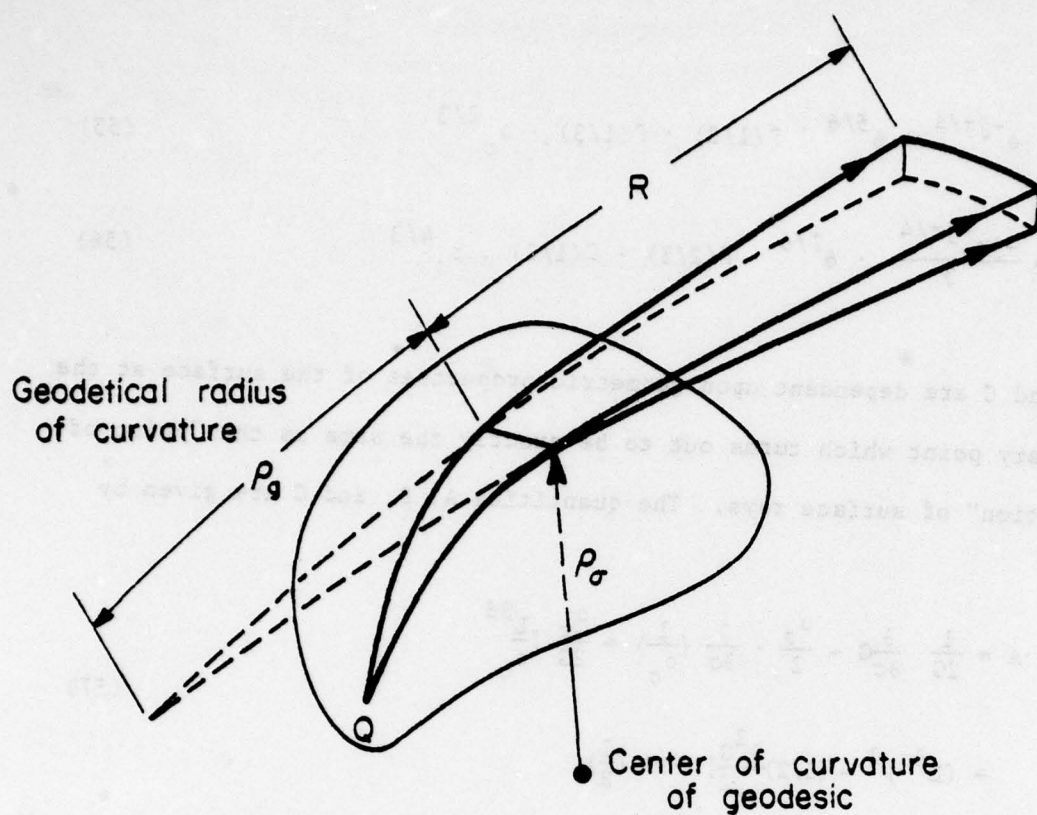
Figure 16: Diffraction of rays by a smooth convex body and geometric meaning of quantities ρ_g, ρ_σ and R.
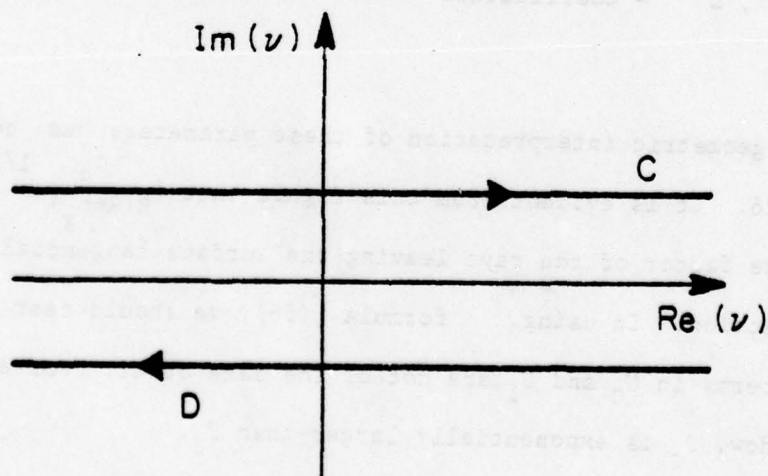
Figure 17: Paths C and D in Watson transformation.

The formulas given in (56) have been tested and compared with other available solutions. An important conclusion derived from this comparison is that although the method of radiation integral is based on less restrictive assumptions, it is perhaps not as useful as the spectral domain approach because the stationary point of the phase of the integrand in (50) is of the second order, and hence, the asymptotic expansion of this integral converges rather slowly except when $k\rho_\sigma$ is very large (≈ 40 or more).

ACKNOWLEDGEMENT

APPENDIX A: FOCK FUNCTIONS

In studies of radio-wave propagation around the earth by Van der Pol, Bremmer, Pryce, Fock, and others, and also the later studies of diffraction of electromagnetic waves by certain bodies of revolution ([51],[52],[53], [54],[55],[48],[56],[57],[58],[59],[60] and [50]), a class of universal functions was introduced which can be used to predict the amplitude and the phase of the reflected or diffracted field by smooth convex surfaces [17]. An exhaustive treatment of these functions which, in general, are defined as Fourier integrals having combinations of Airy integrals in their integrands, has been carried out by N. A. Logan [61]. (See also Bowman, et al. [1] and Logan and Yee [17]).

Since the first extensive application of these functions to diffraction theory was done by Fock, many authors named them after him. Here we list only the most important formulas and expressions for these functions without going through the details of their derivations. We have followed Logan's set of notations for these functions [61]. However, since his time dependence factor, $\exp(-i\omega t)$, is different from one we have used throughout this paper, namely $\exp(+j\omega t)$, our expressions, listed below, are conjugates of what have been presented in [61].

First we start with general definitions. Fock's most general form of the "Van der Pol-Bremmer diffraction formula" is

$$V(x,y_1,y_2,q) = \exp(j\pi/4) \cdot \sqrt{\frac{x}{\pi}} \cdot \int_{-\infty}^{\infty} \cdot e^{-jxt} \cdot w_2(t - y_>) \cdot \left\{ v(t - y_<) \right.$$

$$\left. - \frac{v'(t) - qv(t)}{w_2'(t) - qw_2(t)} \cdot w_2(t - y_>) \right\} dt \qquad (A.1)$$

44

where $w_1(t)$, $w_2(t)$, $u(t)$ and $v(t)$ are Fock-type Airy functions, defined as

$$u(t) = \sqrt{\pi}\; Bi(t) \qquad , \qquad v(t) = \sqrt{\pi}\; Ai(t)$$

$$w_1(t) = u(t) + jv(t) \qquad , \qquad w_2(t) = w_1(t)^*$$

We note that w_1 and w_2 can also be defined as in Sec. 2. $y_>$ and $y_<$ are the larger and smaller of the two numbers y_1 and y_2. $V(x,y_1,y_2,q)$ is proportional to the attenuation suffered by an electromagnetic wave generated by a source located at reduced height y_1 above the surface of a smooth convex body, when it reaches the observation point located at reduced height y_2 above the same surface. x is the reduced distance between the source and the observation point along the surface, and q is dependent upon the impedance of the surface. Let us consider some useful limiting cases.

When $y_1 = y_2 = 0$, then $V(x,0,0,q)$ is denoted by V_0, where

$$V_0(x,q) = \frac{e^{j\pi/4}}{2} \cdot \sqrt{\frac{x}{\pi}} \cdot \int_{-\infty}^{\infty} \frac{e^{-jxt}\, w_2(t)}{w_2'(t) - qw_2(t)} \cdot dt \qquad (A.2)$$

We also have

$$v(x) = V_0(x,0) = \frac{e^{j\pi/4}}{2} \sqrt{\frac{x}{\pi}} \int_{-\infty}^{\infty} \frac{e^{-jxt}\, w_2(t)}{w_2'(t)}\, dt \qquad (A.3)$$

$$u(x) = \lim_{q\to\infty}\left[-2jxq^2 V_0(x,q)\right] = \frac{e^{j3\pi/4}}{\sqrt{\pi}} \cdot x^{3/2} \int_{-\infty}^{\infty} \frac{e^{-jxt}\, w_2'(t)}{w_2(t)}$$

$$\qquad (A.4)$$

When $y_1 = 0$ and $y_2 \to \infty$, then $V \to V_1(x,q)$:

$$V_1(x,q) = \frac{1}{\sqrt{\pi}} \cdot \int_{-\infty}^{\infty} \frac{e^{-jxt}}{w_2'(t) - qw_2(t)} \cdot dt \qquad (A.5)$$

and also

$$g(x) = V_1(x,0) = \frac{1}{\sqrt{\pi}} \cdot \int_{-\infty}^{\infty} \frac{e^{-jxt}}{w_2'(t)}\, dt \qquad (A.6)$$

45

$$f(x) = \lim_{q \to \infty} \left[- q V_1(x,q) \right] = \frac{1}{\sqrt{\pi}} \cdot \int_{-\infty}^{\infty} \frac{e^{-jxt}}{w_2(t)} \, dt \qquad (A.7)$$

Based on Equations (A.6) and (A.7), a class of functions can be defined:

$$f^{(n)}(x) = \frac{(-j)^n}{\sqrt{\pi}} \cdot \int_{\Gamma} \frac{t^n \cdot e^{-jxt}}{w_2(t)} \cdot dt = \frac{d^n f(x)}{dx^n} \qquad (A.8)$$

$$g^{(n)}(x) = \frac{(-j)^n}{\sqrt{\pi}} \cdot \int_{\Gamma} \frac{t^n \, e^{-jxt}}{w_2'(t)} \cdot dt = \frac{d^n g(x)}{dx^n} \qquad (A.9)$$

where Γ is any path in the complex t-plane which comes from $-\infty$ in a sector defined by $-\tau \le \arg(t) < -\frac{\pi}{3}$ and goes to $+\infty$ in the sector $-\frac{\pi}{3} < \arg(t) < \frac{\pi}{3}$. In what follows, we will give the suitable formulas for $f(x)$ and $g(x)$ in different ranges. Tabulated values and graphs of these functions can be found in [57],[54] and [61].

When x is very large and negative, the following asymptotic expansions for $f(x)$ and $g(x)$ can be used [61]:

$$f(x) \sim -2jxe^{jx^3/3}\left\{ 1 + \frac{j}{4x^3} + \frac{1}{2x^6} - \frac{j175}{64x^9} - \frac{395}{16x^{12}} + \frac{j318175}{1024x^{15}} + \ldots \right\} \qquad (A.10)$$

$$g(x) \sim 2e^{jx^3/3}\left\{ 1 - \frac{j}{4x^3} - \frac{1}{x^6} + \frac{j469}{64x^9} + \frac{5005}{64x^{12}} - \frac{j1122121}{1024x^{15}} - \ldots \right\} \qquad (A.11)$$

The above formulas are valid and accurate for $x \ll -1$. For moderate values of x, namely, $-1 \le x \le 1$, it is difficult to find an appropriate expression. Although there are some analytical techniques like "stationary phase method" or "Poisson summation formula" which may be used to evaluate $f^{(n)}$ and $g^{(n)}$ for these values, another possible way which is probably easier and more efficient is to interpolate the tabulated values of these functions in this range.

46

In the vicinity of zero ($|x| \approx 0$), the Taylor expansion can be used to calculate f and g. The coefficients are given by

$$f^{(n)}(0) = e^{-j(5n\pi/6-\pi/3)} \cdot \sqrt{\pi} \cdot \left(\frac{3\pi}{2}\right)^{(2/3)(n-1/4)} \cdot \sum_{m=0}^{\infty} A_m(n) \cdot \left(\frac{2}{3\pi}\right)^{2m}$$

$$\cdot \tau\left(2m - \frac{4n-1}{6} , \frac{3}{4}\right) \tag{A.12}$$

$$g^{(n)}(0) = e^{-j5n\pi/6} \cdot \sqrt{\pi} \cdot \left(\frac{3\pi}{2}\right)^{(2/3)(n-3/4)} \cdot \sum_{m=0}^{\infty} B_m(n) \cdot \left(\frac{2}{3\pi}\right)^{2m}$$

$$\cdot \tau\left(2m - \frac{4n-3}{6} , \frac{1}{4}\right) \tag{A.13}$$

where $\tau(\lambda,\mu)$ is the generalized "tau" function:

$$\tau(\lambda,\mu) = \sum_{n=0}^{\infty} \frac{(-1)^n}{(n+\mu)^{\lambda}} , \quad \lambda > 1 \tag{A.14}$$

$$A_0(n) = 1 , \quad A_1(n) = \frac{5}{48}(n-1)$$

$$A_2(n) = 5\left(5n^2 - 143n + \frac{26385}{16}\right)/(2^9 \cdot 3^2)$$

$$B_0(n) = 1 , \quad B_1(n) = -7(n-3/2)/48$$

$$B_2(n) = (49n^2 + 364n + 39849/16)/(2^9 \cdot 3^2)$$

When x is large, and positive, residue series can be used to compute $f^{(n)}$ and $g^{(n)}$:

$$f^{(n)}(x) = e^{j(2+7n)\pi/6} \sum_{p=1}^{\infty} \frac{(r_p)^n \exp(r_p \cdot x \cdot e^{-j5\pi/6})}{Ai'(-r_p)} \tag{A.15}$$

47

$$g^{(n)}(x) = e^{j7\pi n/6} \sum_{p=1}^{\infty} \frac{(r_p')^{n-1} \exp(r_p' \cdot x \cdot e^{-j5\pi/6})}{\text{Ai}(-r_p')} \tag{A.16}$$

where $\text{Ai}(-r_p) = 0$ and $\text{Ai}'(-r_p') = 0$ for $p = 1,2,3,\ldots$.

APPENDIX B: DERIVATION OF FORMULAS (44) and (45)

Here, we consider only the derivation of the asymptotic expansion of Φ for a circumferential magnetic dipole. In this case, Φ may be written as:

$$\Phi = \frac{-j\omega\epsilon M_\phi}{(2\pi)^2} \int_{-\infty}^{\infty} dk_z \cdot \frac{e^{-jk_z z} \cdot S(k_t)}{k_t^2} \tag{B.1}$$

where

$$S(k_t) = \sum_{n=-\infty}^{\infty} e^{-jn\phi} \cdot \frac{H_n^{(2)}(k_t \rho)}{H_n^{(2)}(k_t a)} \tag{B.2}$$

Applying the Watson transformation to (B.2),

$$S(k_t) = \frac{j}{2} \cdot \int_{C+D} \frac{H_\nu^{(2)}(k_t \rho)}{H_\nu^{(2)}(k_t a)} \cdot \frac{e^{-j\nu(\phi-\pi)}}{\sin \nu\pi} \cdot d\nu \tag{B.3}$$

where C and D are shown in Figure 17. Or,

$$S(k_t) = j \cdot \int_{-\infty}^{\infty} \frac{\cos \nu(\pi - \phi)}{\sin \nu\pi} \cdot \frac{H_\nu^{(2)}(k_t \rho)}{H_\nu^{(2)}(k_t a)} \cdot d\nu \tag{B.4}$$

Substituting the expansion

$$\frac{\cos \nu(\pi - \phi)}{\sin \nu\pi} = j \sum_{i=1}^{2} \sum_{l=0}^{\infty} e^{-j\nu(\phi_i + 2\pi l)} \tag{B.5}$$

where $\phi_1 = \phi$ and $\phi_2 = 2\pi - \phi$, in (B.4), the result will be:

$$S(k_t) = -\sum_{i=1}^{2} \sum_{l=0}^{\infty} \int_{-\infty}^{\infty} \frac{H_\nu^{(2)}(k_t \rho)}{H_\nu^{(2)}(k_t a)} \cdot e^{-j\nu(\phi_i + 2\pi l)} \cdot d\nu \tag{B.6}$$

Each term of the above expansion is associated with a "creeping wave" travelling in a counterclockwise (i = 1) or clockwise (i = 2) direction around the cylinder. Following the ray concept, each creeping wave

49

appears to be travelling along a specific surface ray. Now, as $\rho \to \infty$ (far zone) for each fixed ν, we have [62]

$$H_\nu^{(2)}(k_t\rho) \sim \sqrt{\frac{2}{\pi k_t\rho}} \cdot e^{-j(k_t\rho - \nu\pi/2 - \pi/4)} \tag{B.7}$$

On the other hand, it can be shown that the significant contribution to $S(k_t)$ comes from a small neighborhood of $k_t a$. In this neighborhood, where $k_t a$ and ν are large and close to each other ($|k_t a - \nu| \leq |\nu|^{1/3}$), the Hankel's asymptotic expansion (B.7) is not valid any longer. In this case, it is necessary to expand Bessel's functions in terms of Fock-type, Airy functions, $w_1(t)$ and $w_2(t)$, and their derivatives [16]:

$$H_\nu^{(2)}(x) \sim \frac{i}{m\sqrt{\pi}}\left\{w_2(t) - \frac{1}{60m^2}\left[4t\, w_2(t) + t^2\, w_2'(t)\right] + \ldots\right\} \tag{B.8}$$

$$H^{(2)'}(x) \sim \frac{-i}{m^2\sqrt{\pi}}\left\{w_2'(t) + \frac{1}{60m^2}\left[4t\, w_2'(t) + (6 - t^3)\, w_2(t)\right] + \ldots\right\} \tag{B.9}$$

where

$$m = \left(\frac{x}{2}\right)^{1/3} \quad , \quad t = \frac{\nu - x}{m} \quad \text{(m is very large)}$$

Inserting (B.7) and the first-order terms of (B.8) and (B.9) into (B.6) and (B.1), we obtain

$$\phi \sim \frac{\omega\epsilon M_\phi}{(2\pi)^2} \cdot \sqrt{\frac{2\pi}{\rho}} \cdot e^{j\pi/4} \cdot \sum_{i=1}^{2} \sum_{1=0}^{\infty} \int_{-\infty}^{\infty} dk_z \cdot e^{-j\Omega_{i1}} \cdot f_0(\xi_{i1}) \cdot \frac{m^2}{k_t^{5/2}} \tag{B.10}$$

where

$$m = (k_t a/2)^{1/3}$$

$$\Omega_{i1} = k_z z + k_t[\rho + a(\rho_i + 2\pi 1 - \pi/2)]$$

$$\xi_{i1} = m(\rho_i + 2\pi 1 - \pi/2)$$

50

Introducing a new integration variable α:

$$k_z = k \sin \alpha \qquad (B.11)$$

$$k_t = k \cos \alpha \qquad (B.12)$$

$$\beta_{il} = \tan^{-1}\{z/[\rho + a(\phi_i + 2\pi l - \pi/2)]\} \qquad (B.13)$$

we have:

$$\Omega_{il} = kR_{il} \cos(\beta_{il} - \alpha) \qquad (B.14)$$

where

$$R_{il} = \left\{z^2 + [\rho + a(\phi_i + 2\pi l - \pi/2)]\right\}^{1/2}$$

Now (B.10) takes the following form:

$$\phi \sim -\frac{\omega\epsilon M_\phi}{(2\pi)^2} \cdot \sqrt{\frac{2\pi}{\rho}} \cdot \frac{m_0^2}{k^{3/2}} \cdot e^{j\pi/4} \cdot \sum_{i=1}^{2} \sum_{l=0}^{\infty} \int_\gamma d\alpha \cdot e^{-jkR_{il}\cos(\alpha-\beta_{il})}$$

$$\cdot \cos^{-5/6}\alpha \cdot f_0(\xi_{il}) \qquad (B.15)$$

γ is the path of integration in the complex α-plane, which is shown in Figure 18.

Now we deform the path of integration into the "steepest descent path," SDP, passing through the saddle point of the phase of the integrand. Performing the "saddle-point integration," we can derive the asymptotic expansion of (B.15) for large kR_{il}. The first order term is:

$$\phi \sim -\frac{\omega\epsilon M_\phi}{2\pi k^2} \cdot e^{j\pi/2} \cdot \left(\frac{ka}{2}\right)^{1/3} \cdot \sum_{i=1}^{2} \sum_{l=0}^{\infty} (\cos \beta_{il})^{-4/3} \cdot \frac{e^{-jkR_{ils}}}{R_{ils}} \cdot f_0(\xi_{ils})$$

$$(B.16)$$

where R_{ils} and ξ_{ils} are the values of these parameters at the stationary point specified by $\alpha = \beta_{il}$.

51

Im(α)

$-\pi/2$

$45°$

$\pi/2$ Re(α)

SDP

(γ)
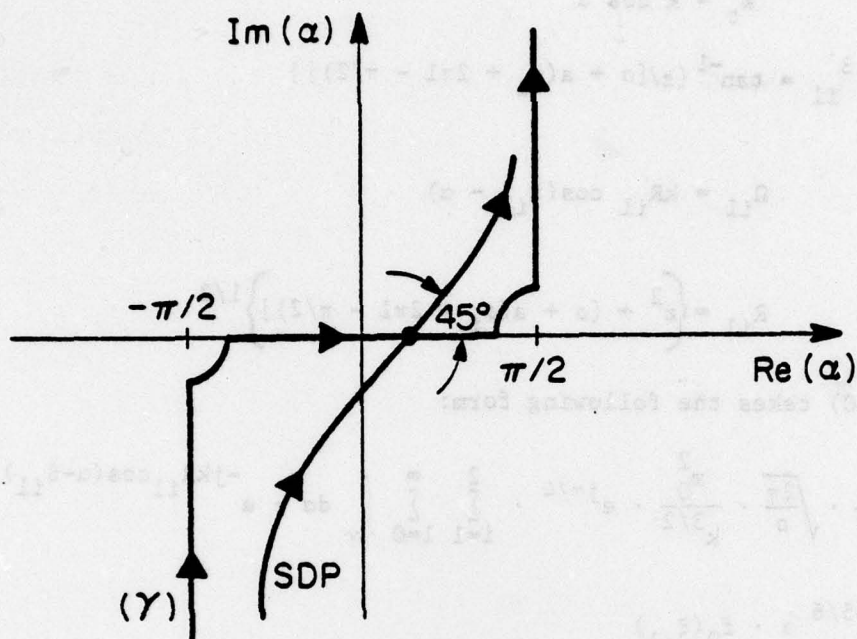
Figure 18: Steepest descent path (SDP) for integral (B.15).

52

Eqn. (B.16) is the creeping-wave representation of the far field. If the cylinder is large (ka >> 1) and $|\phi|$ is not very close to π, then only the first term ($i = 0$, $1 = 1$) has the most important contribution to the total infinite sum, and the other terms are not significant. Neglecting the other terms, we obtain the result given in (44 and 45). It should be emphasized that (44) and (45) are not valid when $|\beta|$ is close to $\pi/2$ (paraxial region), because in this case, $k_t a$ is very small, and (B.7), (B.8) and (3.9) no longer apply.

The other formulas can be derived in a similar manner.

53

APPENDIX C: ASYMPTOTIC EVALUATION OF THE RADIATION INTEGRAL

Consider the following double integral:

$$U(k) = \int\!\!\int_D g(x,y) \cdot e^{jk\phi(x,y)} \, dxdy \qquad (C.1)$$

where $g(x,y)$ is rather slowly varying, and $\phi(x,y)$ has a stationary point (x_s, y_s) inside domain D. The objective is to derive an asymptotic expansion for (C.1) when k is large.

Suppose g and ϕ have the following forms around (x_s, y_s):

$$\begin{cases} g(x,y) = (x - x_s)^{\lambda_0 - 1}(y - y_s)^{\mu_0 - 1} g_1(x,y), \quad \lambda_0, \mu_0, > 1 \\ \phi(x,y) = \phi(x_s, y_s) + a_{\delta,0}(x - x_s)^{\delta}[1 + P(x,y)] + b_{0,\tau}(y - y_s)^{\tau}[1 + Q(x,y)] \end{cases} \qquad (C.2)$$

N. Chako [48] has derived the following asymptotic series for U:

$$U(k) \sim B_0 \cdot \sum_{p,q=0}^{\infty} A_{pq}(\alpha_1 + \alpha_2)(\beta_1 + \beta_2) \cdot \Gamma\left(\frac{\lambda_0 + p}{\delta}\right) \cdot \Gamma\left(\frac{\mu_0 + q}{\tau}\right)$$

$$\frac{1}{(ka_{\delta 0})^{\lambda_0/\delta}} \cdot \frac{1}{(kb_{0,\tau})^{q/\tau}} \qquad (C.3)$$

where

$$B_0 = \frac{1}{(ka_{\delta,0})^{\lambda_0/\delta}} \cdot \frac{1}{(kb_{0,\tau})^{\mu_0/\tau}} \cdot \frac{1}{(\delta\tau)} \cdot e^{jk\phi(x_s,y_s)}$$

$$\alpha_1 = \exp[j\pi(\lambda_0 + p)/(2\delta)], \quad \alpha_2 = \exp\left\{[j\pi/(2\delta)]\left[(\lambda_0 + p)(2\delta + e^{j\pi\delta}) - 2\delta\right]\right\}$$

$$\beta_1 = \exp[j\pi(\mu_0 + q)/(2\tau)], \quad \beta_2 = \exp\left\{[j\pi/(2\tau)]\left[(\mu_0 + q)(2\tau + e^{j\pi\tau}) - 2\tau\right]\right\}$$

$$g_1(x,y) = \sum_{k,l=0}^{\infty} g_{k,l}(x - x_s)^k (y - y_s)^l$$

$$P(x,y) = \sum_{m+n \geq 1} a_{mn}(x - x_s)^m (y - y_s)^n$$

$$Q(x,y) = \sum_{m+n \geq 1} b_{mn}(x - x_s)^m (y - y_s)^n$$

$$A_{00} = g_{00} \; , \quad A_{10} = g_{10} - g_{00}\left[(\lambda_0 + 1)\frac{a_{10}}{\delta} + \frac{b_{10}}{\tau}\right]$$

$$A_{01} = g_{01} - g_{00}\left[\frac{a_{01}}{\delta} + (\mu_0 + 1) \cdot \frac{b_{01}}{\tau}\right]$$

In order to apply this procedure to the integrals of the type (5.4) for which

$$\phi(x,y) = -\Omega(\sigma,\beta) = -(R + \sigma) \tag{C.4}$$

$$g(x,y) = F(\sigma,\beta,P) \frac{\sqrt{G}}{R} \tag{C.5}$$

When F is one of the components of $\vec{J}(1 - \hat{R}\hat{R})$, one should first determine the stationary point of Ω, wherein its first-order derivatives vanish. The second step is to compute the various order derivatives of Ω, J, $\hat{R}$, ...,at this point, and then insert them into (C.3). We just give the main formulas needed for these derivations.

Suppose the surface of the body, $\vec{x}(\sigma,\beta)$, is parametrized by a geodetical polar coordinate system. As discussed previously,in this system, σ is the arclength of the surface geodesic connecting the pole Q to $\vec{x}(\sigma,\beta)$, and β is the angle between the geodesic and some fixed reference geodesic at Q (Fig. 15).

The element of length in this system is given by

$$ds^2 = d\sigma^2 + G(\sigma,\beta)\, d\beta^2 \tag{C.6}$$

55

Let us denote $d\vec{x}(u)/du$ by $\vec{x}_u$; then we have the following set of relations

$$\vec{x}_{\beta\beta} = \frac{-\partial G/\partial\sigma}{2} \cdot \vec{x}_\sigma + \frac{\partial G/\partial\rho}{2G} \vec{x}_\beta + L^{\beta\beta} \vec{x}_3 \qquad (C.7)$$

$$\vec{x}_{\beta\sigma} = \vec{x}_{\sigma\beta} = \frac{\partial G/\partial\sigma}{2G} \vec{x}_\beta + L^{\beta\sigma} \vec{x}_3 \qquad \cdot (C.8)$$

$$\vec{x}_\sigma = \frac{-\vec{x}_3}{\rho_\sigma} \qquad (C.9)$$

where $\vec{x}_\sigma = \hat{\sigma}$, and $\vec{x}_\beta/\sqrt{G} = \hat{\beta}$ are unit vectors along $\beta =$ const. and $\sigma =$ const. curves, and

$$\vec{x}_3 = \hat{n} = \frac{\vec{x}_\sigma \times \vec{x}_\beta}{\sqrt{G}} \qquad (C.10)$$

is the outward unit normal to the surface. Another quantity of interest is the "geodetical curvature" κ_g given by

$$\kappa_g = \frac{\partial G/\partial\sigma}{2G} \qquad (C.11)$$

Using the above relations, we can derive the following expressions which holds true at the stationary point:

$$\frac{\partial\Omega}{\partial\sigma} = 1 - \hat{R} \cdot \vec{X}_\sigma = 0 \qquad (C.12)$$

$$\frac{\partial\Omega}{\partial\beta} = -\hat{R} \cdot \vec{x}_\beta = 0 \qquad (C.13)$$

$$\frac{\partial^2\Omega}{\partial\sigma^2} = 0 \quad , \quad \frac{\partial^2\Omega}{\partial\sigma\partial\beta} = 0 \quad , \quad \frac{\partial^2\Omega}{\partial\beta^2} = G\left(\frac{1}{R} + \frac{1}{\rho_3}\right) \qquad (C.14)$$

where $\rho_\beta = 1/\kappa_g$, and

$$\frac{\partial^3\Omega}{\partial\sigma^3} = \frac{1}{\rho_\sigma^2} \quad , \quad \frac{\partial^3\Omega}{\partial\sigma^2\partial\beta} = -L^{\beta\sigma}/\rho_\sigma \qquad (C.15)$$

56

$$\frac{\partial^3 \Omega}{\partial \beta^2 \partial \sigma} = \frac{G}{R^2} + \frac{\partial G/\partial \sigma}{R} + \frac{\partial^2 G/\partial \sigma^2}{2} - \frac{L^{\beta\beta}}{\rho_\sigma} \qquad (C.16)$$

$$\frac{\partial^3 \Omega}{\partial \beta^3} = \frac{3\partial G/\partial \beta}{2R} + \frac{\partial G}{\partial \beta} \cdot \frac{\partial G}{\partial \sigma} \cdot \frac{1}{4G} + L^{\beta\sigma} \cdot L^{\beta\beta} + \frac{1}{2} \cdot \frac{\partial^2 G}{\partial \sigma \partial \beta} \qquad (C.17)$$

where ρ_σ is the radius of curvature of the geodesic.

Equations (C.12) and (C.13) determine the location of the stationary point. At this point $\hat{R} = \vec{x}_\sigma$, which, if we introduce the ray concept, tells us that the surface rays leave the surface at the "point of diffraction" tangentially. Equation (C.14) indicates that the stationary point is of second order, so that we need higher-order derivities of the phase. $L^{\sigma\sigma}$, $L^{\beta\sigma}$ and $L^{\beta\beta}$ are coefficients of the second fundamental form of the surface evaluated at the stationary point. They are defined as

$$L^{\sigma\sigma} = \vec{x}_{\sigma\sigma} \cdot \vec{x}_3 \quad , \quad L^{\sigma\beta} = \vec{x}_{\sigma\beta} \cdot \vec{x}_3 \quad , \quad L^{\beta\beta} = \vec{x}_{\beta\beta} \cdot \vec{x}_3$$

Using the relationships given above, one can find the expansion co-efficients g_{kl}, a_{mn}, b_{mn} and A_{pq} in (C.3). Zeroth and first-order terms in (C.3) give us formulas (5.6).

A few remarks should be made concerning the expansion presented in (C.3). First of all, (C.3) is a doubly infinite series; therefore, for each fixed power of k^{-1} a finite number of terms should be summed up. The coefficients of various terms in these finite sums, namely A_{pq}'s, become very complicated when p and q are greater than 0 or 1. Another difficulty with this series is that when the stationary point of the phase is of an order higher than 1, the difference between the order of the successive terms (when they are ordered according to the descending power of k) becomes very

57

small, and consequently the infinite series converges very slowly. For instance, in our problem where $\delta = 3$ and $\tau = 2$ (stationary point is of second order), sometimes the difference between the orders of successive terms is $k^{-1/6}$, which indicates the weak convergence (in an asymptotic sense) of the expansion in the cases where the frequency is not very large.

REFERENCES

[1] J.J. Bowman, T.B.A. Senior and P.L.E. Uslenghi, _Electromagnetic and Acoustic Scattering by Simple Shapes_, North-Holland Publishing Co., Amsterdam (1969).

[2] P.L.E. Uslenghi, _Lectures on High-Frequency Scattering Methods_, Sorrento, Italy. Sept. 5-8, (1972).

[3] R.G. Kouyoumjian, "Asymptotic high-frequency methods", Proc. IEEE, 53, 1965, pp. 364-876.

[4] G.N. Watson, "The diffraction of electric waves by the earth", Proc. Roy. Soc., A95, pp. 83-99, 1918.

[5] E. Pflumm, "Expansion problems arising from the Watson transformation", Research Report No. BR-35, New York University, New York (1960).

[6] E. Fischer, "On the Watson transformation", Comm. Pure Appl. Math., 19, pp. 287-297 (1966).

[7] D.S. Cohen, "New eigenfunction expansions and alternative representations for the reduced wave equations", J. Math. Mech., 14, pp. 403-412 (1965).

[8] J.W. Crispin, Jr. and A.L. Maffett, "Radar cross-section estimation for simple shapes", Proc. IEEE, 53, pp. 833-843 (1965).

[9] K.M. Siegel, "Far field scattering from bodies of revolution", Appl. Sci. Res., B7, pp. 293-328, (1958).

[10] K.M. Siegel, R.F. Goodrich and V.H. Weston, "Comments on far field scattering from bodies of revolution", Appl. Sci. Res., B8, pp. 8-12,)1959).

[11] R.K. Luneburg, _Mathematical Theory of Optics_, Brown University Notes, Providence, 1944.

[12] M. Kline and I. Kay, <u>Electromagnetic Theory and Geometrical</u>
      <u>Optics</u>, Interscience Publishers, New York, 1965.

[13] V.A. Fock, "The distribution of currents induced by a plane
      wave on the surface of a conductor", J. Phys. USSR, <u>10</u>, pp. 130-
      136, 1946.

[14] V.A. Fock, "The field of a plane wave near the surface of a
      conducting body", J. Phys. Ussr, <u>10</u>. pp. 399-409, 1946.

[15] R.F. Goodrich, "Fock Theory--An Appraisal and Exposition",
      IRE Trans. Antennas Propagation, <u>AP-7</u>, Special supplement,
      pp. 28-36, 1959.

[16] V.A. Fock, "Diffraction of radio waves around the earth's
      surface", J. Phys., Vol.9, pp. 225-266, 1945.

[17] N.A. Logan, K.S. Yee, "A mathematical model for diffraction
      by convex surfaces", <u>Electromagnetic Waves</u>, edited by R.E. Langer,
      <i>The University of Wisconsin Press</i>, Madison, pp. 139-180, 1962.

[18] J.A. Cullen, "Surface Current Induced by Short-Wavelength
      Radiation", Physc, Rev., 2nd series, Vol. 9, No. 6, pp. 1863-1867,
      1958.

[19] S. Hong, "Asymptotic Theory of Electromagnetic and Acoustic
      Diffraction by Smooth Convex Surfaces of Variable Curvature",
      J. Math. Phys., Vol. 8, No. 6, 1967, pp. 1223-1232.

[20] B.R. Levy and J.B. Keller, "Diffraction by a Smooth Object",
      Comm. Pure Appl. Math., vol. XII, pp. 159-209, 1959.

[21] S.W. Lee and S. Safavi-Naini, "Asymptotic solution of surface
      field due to a magnetic dipole on a cylinder", Electromagnetics
      Laboratory Technical Report No. 76-11, University of Illinois at
      Urbana-Champaign, Nov. 1976.

[22] S.W. Lee and S. Safavi-Naini, "Asymptotic solution of surface

field due to a magnetic dipole on a cylinder", to be published

in IEEE Trans. on Antennas and Propagation (1978).

[23] J.B. Keller, "Diffraction by a convex cylinder", IRE Trans.,

Vol. AP-4, pp. 312-321, 1956.

[24] J.B. Keller, "Diffraction by an aperture I, II", J. Appl. Phys.,

Vol. 28, pp. 426-444 and 570-579, 1957.

[25] R.G. Kouyoumjian, "The GTD and its application", chapter 6 of

Numerical and Asymptotic Techniques in Electromagnetics, edited

by R. Mittra, Springer-Verlag, 1975.

[26] P.H. Pathak and R.G. Kouyoumjian, "The radiation from apertures

in curved surfaces", ElectroScience Lab, Department of Electrical

Engineering, Ohio State University. Report 3001-2, Dec. 1972.

[27] J.B. Keller and B.R. Levy, "Decay exponents and diffraction

coefficients for surface waves on surfaces of nonconstant curvature',

IRE Trans. Antennas Propagation, AP-7, pp. S52-S61, 1959.

[28] W. Franz and K. Klante, "Diffraction by surfaces of variable

curvature", IRE Trans. Antennas Propagation, AP-7, pp. S63-S70,

1959.

[29] D.R. Voltmer, "Diffraction by doubly curved convex surfaces",

Ph.D. dissertation, Ohio State University, Columbus, Ohio, 1970.

[30] P.H. Pathak and R.G. Kouyoumjian, "An analysis of the radiation

from apertures in curved surfaces", Proc. IEEE, Vol. 62, pp. 1438-

1447, 1974.

[31] Yu. A. Kravtsov, "A modification of the geometrical optics method",

Radiofizika, Vol. 7, pp. 664-673, 1964.

[32] D. Ludwig, "Uniform asymptotic expansions at a caustic", Comm.

Pure Appl. Math., Vol. 19, pp. 215-250, 1966.

[33] E. Zauderer. "Uniform asymptotic solutions of the reduced wave equation", J. Math. Anal. Appl., Vol. 30, pp. 157-171, 1970.

[34] R.E. Langer, "Turning Point in Linear Asymptotic Theory", Res. Rept. No. 127, University of Wisconsin, 1960.

[35] F.W.J. Olver, "Asymptotic solution of linear differential equation of second order in a domain containing one transition point", Phil. Trans. Roy. Soc. London, Ser. A, Vol. 249, p. 65, 1956.

[36] R.M. Lewis, N. Bleistein and D. Ludwig, "Uniform asymptotic theory of creeping waves", Comm. Pure and Appl. Math., Vol. XX, pp. 295-328, 1967.

[37] V.H. Weston, "The effect of a discontinuity in curvature in high frequency", IRE Trans. Antennas Propagation, AP-10, pp. 775-730, 1962.

[38] J.B. Keller and Kaminetzky, "Diffraction coefficients for higher order edges and vertices", SIAM J. Appl. Math., Vol. 22, pp. 109-134, 1972.

[39] Thompson, "Radio propagation over a sectionally cylindrical surface", Proc. Roy. Soc., Ser. A, Vol. 267, pp. 183-196, 1962.

[40] P.L. Christiensen, "Diffraction of creeping wave by discontinuity in the surface impedance of a smooth body", URSI spring meeting, Washington, D.C., USA, 1966.

[41] N. Chr. Albertsen, "Diffraction of creeping waves", Tech, Rept., Technical University of Denmark, Lyngby, Dec. 1974.

[42] R.F. Goodrich, R.E. Kleinman, A.L. Maffett, C.E. Schonsted, K.M. Siegel, M.G. Chernin, H.E. Shank and R.E. Plummers, "Radiation from slot arrays and cones", IRE Trans. Antennas Propagation, pp. 213-222, 1959.

[43] R.N. Buchal and J.B. Keller, "Boundary layer problems in diffraction theory", Comm. Pure Appl. Math., Vol. 13, pp. 85-114, 1960.

[44] Z.W. Chang, L.B. Felsen and A. Hessel, "Surface ray methods for mutual coupling in conformal arrays on cylindrical surfaces", Final Report, Department of Electrical Engineering and Electrophysics, Polytechnic Institute of New York, Feb. 1976.

[45] K.K. Chan, L.B. Felsen, A. Hessel and J. Shmoys, "Creeping waves on a perfectly conducting cone", IEEE Trans. Antennas Propagation, Vol. AP-25, No. 5, pp. 661-671, 1977.

[46] S.W. Lee and R. Mittra, "Mutual admittance between slots on a cylinder or cone", Tech, Rept. No. 77-24, Electromagnetic Laboratory, Department of Electrical Engineering, University of Illinois at Urbana-Champaign, 1977.

[47] V.A. Fock, "The field from a vertical and a horizontal dipole raised above the earth's surface", J. Expt. and Theor. Phys. (JETP), 19, No. 10, p. 916, 1949 (in Russian). English translation can be found in Electromagnetic Diffraction and Propagation Problems, Pergamon Press, 1965.

[48] N. Chako, "Asymptotic expansion of double and multiple integrals occuring in diffraction theory", J. Inst. Math. Applic., Vol. 1, pp. 372-422, 1965.

[49] D.S. Jones and M. Kline, "Asymptotic expansion of multiple integrals and the method of stationary phase", J. Math. Physc., Vol. 37, pp. 7-28, 1958.

63

[50] J.W. Nicholson, "On the bending of electric waves around the earth", Phil. Mag., Vol. 18, pp. 757-760, 1910.

[51] B. Van der Pol, "On the propagation of electromagnetic waves around the earth", Phil. Mag., Vol. 38, pp. 365-380, 1919.

[52] B. Van der Pol and H. Bremmer, "Diffraction of electromagnetic waves from an electrical point source around a finitely conducting sphere with applications to radio-telegraphy and the theory of the rainbow", Part I: Phil. Mag., Vol. 24, pp. 141-176, 1937; Part II: Phil. Mag. Vol. 24, pp. 825-864, 1937.

[53] M.H.L. Pryce, "The diffraction of radiowave by the curvature of the earth", Advance in Physics, Vol. 2, pp. 67-95, 1953.

[54] V.A. Fock, Tables of the Airy Function, Moscow, 1946.

[55] J.R. Wait and A.M. Conda, "Diffraction of electromagnetic waves by smooth obstacles for grazing angles", Journal of Research NBS D. Radio Propagation, Vol. 63D, 1959.

[56] J.R. Wait, Electromagnetic Radiation from Cylindrical Structures, Pergamon Press, New York, 1959.

[57] M.G. Belkina, Tables to Calculate the Electromagnetic Field in the Shadow Region for Various Soils, Soviet Radio Press, Moscow, 1949 (translated by M.D. Friedman, ASTIA Document No. AD110298, 1956).

[58] A.S. Goriainov, "An asymptotic solution of the problem of diff-raction of a plane wave by a conducting cylinder", Radiotekh i Elektron., Vol. 3, pp. 603-614, 1958.

[59] V.A. Fock, L.A. Vainshtein and M.G. Belkina, Diffraction of Electromagnetic Waves by Certain Bodies of Revolution, Soviet Radio.

[60] S.O. Rice, "Diffraction of plane radio waves by a parabolic cylinder--Calculation of shadows behind the hills", Bell System

J., Vol. 33, pp. 417-504, March 1954.

[61] N.A. Logan, <u>General Research on Diffraction Theory</u>, Vols. 1 and 2,
Lockheed Missiles and Space Division Technical Reports LMSD-288087
and LMSD-288088 (ASTIA Nos. AD241228 and AD243182), Sunnyvale,
California, 1959.

[62] M. Abramowitz and I.A. Stegun, <u>Handbook of Mathematical Functions</u>,
Chapter 9, Dover Pub., Inc., New York, 1970.

[63] P.C. Bargeliotes, A.T. Villeneuve and W.H. Kummer, "Pattern Synthesis
of Conformal Arrays", prepared for Department of the Navy, Washington,
D.C. by Radar Microwave Laboratory, Aerospace groups, Hughes Aircraft
Company - Culver City, California, Jan, 1975.